

Victoria University

A method of characterisation of the nonlinear vibration transmissibility of cushioning materials

Anthony James Parker

*A thesis submitted in fulfilment of the requirements for the degree of
Doctor of Philosophy*

School of Architectural, Civil and Mechanical Engineering
VICTORIA UNIVERSITY
Melbourne, Australia
2007

Supervisors: M. A. Søk
: V. Rouillard

Doctor of Philosophy Declaration

I, Anthony James Parker, declare that the PhD thesis entitled, A method of characterisation of the nonlinear vibration transmissibility of cushioning materials, is no more than 100,000 words in length, exclusive of tables, figures, appendices, references and footnotes. This thesis contains no material that has been submitted previously, in whole or part, for the award of any other academic degree or diploma. Except where otherwise indicated, this thesis is my own work.

Signature:

Date:

Acknowledgements

I would like to thank my supervisors, Dr. Michael Søk for his continued encouragement and support throughout the progression of this work, and Mr. Vincent Rouillard who has been a great source of energy and enthusiasm for me.

Technical support from Laszlo Kovacs was greatly valued.

I would also like to express my appreciation to Victoria University Australia, for the continuing opportunity to study.

Finally, to Connie, thank you.

Abstract

The majority of mechanical damage to packages or products in shipment can be ascribed to shocks and vibrations experienced during transportation. Vibrations can cause resonance, which has the potential to damage the product or cause the failure of critical elements within due to the repetitive application of stresses.

The response behaviour of cushioning or protective packaging materials under vibration excitation is central to the effective design of product packaging. The response characteristics of the cushioning material guide the design parameters of the product-transport cushion system. Conventionally, this is achieved by the measurement of the transmissibility or Frequency Response Function (FRF) of the product/cushion system by a Single Input-Single Output (SISO) approach assuming a linear relationship. However, the product/cushion system can exhibit strong nonlinear behaviour.

The Reverse Multiple Input-Single Output (R-MISO) approach has shown a greater ability to more accurately characterise the nonlinear package/cushion system. This greater accuracy will allow for the use of fewer materials with the benefit of cost and environmental savings.

The R-MISO approach revealed a significant difference in the natural frequency estimate between the SISO linear assumption and the linear frequency response function estimate of the R-MISO approach. A considerable difference in the magnitude of the transmissibility at the estimated natural frequency was also shown. These differences were accompanied by an improvement in coherence.

This work adds to the knowledge of the package designer through the study of the significance of the nonlinear behavior of a common cushioning material using the R-MISO method. This new approach to the vibration analysis of cushioning materials will allow the package designer to assess the nonlinear behavior of a packaging material.

Contents

1. Cushioning materials	1
1.1 Packaging distribution.....	3
1.2 Economic considerations	5
1.2.1 Distribution	6
1.2.2 Packaging as waste.....	9
1.3 Package testing standards.....	11
1.3.1 Distribution- vehicle vibrations	12
1.4 Research objective and significance	14
1.5 Organisation of thesis.....	21
2 Modelling the product and cushion.....	23
2.1 Linear and nonlinear systems.....	24
2.2 Frequency response functions	26
2.3 Coherence.....	28
2.4 Non-linear analysis review.....	29
2.5 Reverse Multiple Input-Single Output (R-MISO) analysis	34
2.6 Development of the Reverse Multiple Input-Single Output algorithm	37
2.7 Description of the Reverse Multiple Input-Single Output spectral decomposition algorithm.....	40
2.7.1 Component and total spectral density functions	43
2.7.2 Ordinary coherence functions	44
2.7.3 Cumulative coherence functions.....	45
2.8 The basis of the MISO technique.....	46
3 Hypothesis.....	48
4 Method	49
4.1 Equipment overview	52
4.1.1 Equipment requirements	52
4.1.2 Equipment used.....	52
4.1.3 Layout of equipment	54
4.2 Computer based implementation of the R-MISO algorithm.....	55

4.3	Validate and test the R-MISO computer implementation.....	56
4.4	Package cushion system.....	57
5	R-MISO Analysis	61
5.1	Example 1: Single Degree of Freedom (SDOF) linear system.....	63
5.2	Example 2: Duffing nonlinear equation.....	67
5.3	Example 3: Van-der Pol nonlinear equation	72
5.4	Example 4: Combined Duffing-Van-der Pol nonlinear equation	77
5.5	Introduction to results	82
5.5.1	Results for EPS grade S	82
5.5.2	Results for EPS grade SL.....	94
5.5.3	Effect of increasing averages for EPS grade S.....	105
5.5.4	Effect of increasing averages for EPS grade SL	107
6	Conclusion.....	109
6.1	Further work.....	111
	References.....	112
	APPENDIX A: Common packaging standards	117
	APPENDIX B: Equipment used during experimentation.....	121
	APPENDIX C: Compression curves of expanded polystyrene samples	122
	APPENDIX D: Summary of the natural frequency estimate.....	124
	APPENDIX E: Summary of the MATLAB files created	125
	Nomenclature.....	129

List of Figures

Figure 1-1 Growth in domestic freight transport in Australia (reproduced from Vic Roads 1995).....	5
Figure 1-2 Economic considerations for package/product optimisation.....	7
Figure 1-3 Relationship between AS, ASTM and ISO standards.....	12
Figure 1-4 Distribution of product fragility, level of cushioning and level of hazard.....	15
Figure 1-5 Critical element and product.....	17
Figure 1-6 Cushion curve for EPS.....	18
Figure 1-7 Typical cushion curve design plot.....	19
Figure 1-8 Typical vibration transmissibility design plot.....	19
Figure 2-1 Product cushion vibrating base model.....	23
Figure 2-2 Compression curve for EPS.....	24
Figure 2-3 Representation of a system H.....	25
Figure 2-4 Input - Output relationship for a linear system.....	27
Figure 2-5 Representation of general SDOF mechanical system.....	34
Figure 2-6 Single input-single output system with feedback.....	35
Figure 2-7 Reverse single input-single output SDOF system without feedback.....	35
Figure 2-8 Reverse single input-single output SDOF system with correlated inputs x_1 and x_2	35
Figure 2-9 Reverse single input-single output SDOF system with correlated inputs x_1 , x_2 and x_3	36
Figure 2-10 Multiple input-single output model.....	37
Figure 2-11 Multiple input-single output A response functions model.....	40
Figure 2-12 Multiple input-single output L response functions model.....	41
Figure 2-13 Multiple input-single output A response functions model.....	41
Figure 2-14 Three input-single output L response functions model.....	42
Figure 2-15 MISO model of Duffing equation.....	46
Figure 2-16 Duffing equation reverse single input/single output.....	46
Figure 2-17 Duffing equation two inputs/single output (time domain).....	47
Figure 2-18 Duffing equation two inputs/single output (frequency domain).....	47

Figure 4-1 Schematic of experimental setup.....	54
Figure 4-2 Flowchart of analysis program.....	55
Figure 4-3 Compression plot of eps grade sl at various displacement speeds.....	58
Figure 4-4 Raw compression plot of eps grade s.....	59
Figure 4-5 Cushion curve for eps grade s.....	60
Figure 5-1 SDOF linear system.....	63
Figure 5-2 SDOF linear system model.....	63
Figure 5-3 Force excitation time segment and histogram.....	64
Figure 5-4 Displacement response time segment and histogram.....	64
Figure 5-5 FRF estimate for SDOF system showing recovered system values...	65
Figure 5-6 Coherence result for SDOF system.....	66
Figure 5-7 Duffing equation nonlinear model.....	67
Figure 5-8 Duffing two input single output R-MISO model.....	68
Figure 5-9 Duffing system correlated inputs.....	68
Figure 5-10 Duffing system uncorrelated inputs.....	68
Figure 5-11 Force excitation and histogram for the Duffing nonlinear system...	69
Figure 5-12 Displacement response and histogram for the Duffing nonlinear system.....	69
Figure 5-13 FRF estimate for a Duffing system, showing recovered parameter values.....	70
Figure 5-14 Nonlinear FRF for a Duffing system showing recovered parameter value.....	70
Figure 5-15 Coherence plot analysis result for a Duffing system.....	71
Figure 5-16 Van der Pol nonlinear equation model.....	72
Figure 5-17 Van der Pol two input single output R-MISO model.....	73
Figure 5-18 Van der Pol system with correlated inputs.....	73
Figure 5-19 Van der Pol system with uncorrelated inputs.....	73
Figure 5-20 Force excitation and histogram for the Van der Pol nonlinear system	74
Figure 5-21 Displacement response and histogram for the Van der Pol nonlinear system.....	74
Figure 5-22 FRF estimate result for a Van der Pol system showing recovered parameter values.....	75

Figure 5-23 Nonlinear FRF estimate for a Van der Pol system showing recovered parameter values.....	75
Figure 5-24 Coherence for the Van der Pol nonlinear system.....	76
Figure 5-25 Combined Duffing-Van der Pol nonlinear equation model	77
Figure 5-26 Combined Duffing-Van der Pol two inputs/single output R-MISO model.....	78
Figure 5-27 Combined Duffing-Van der Pol system correlated inputs	78
Figure 5-28 Combined Duffing-Van der Pol system uncorrelated inputs	78
Figure 5-29 Force excitation and histogram for the combined Duffing Van der Pol nonlinear equation.....	79
Figure 5-30 Displacement response and histogram for the combined Duffing Van der Pol nonlinear equation	79
Figure 5-31 FRF estimate for a combined Duffing-Van der Pol system showing recovered parameter values.....	80
Figure 5-32 Nonlinear FRF for a combined Duffing-Van der Pol system showing recovered parameter values.....	80
Figure 5-33 Coherence for the combined Duffing-Van der Pol nonlinear system	81
Figure 5-34 FRF estimate for eps grade s @ 0.25g RMS	84
Figure 5-35 Nonlinear FRF estimate for eps grade s @ 0.25g RMS	85
Figure 5-36 Coherence plot for eps grade s @ 0.25g RMS	86
Figure 5-37 Excitation time history segment and histogram for eps grade s.....	87
Figure 5-38 Response time history segment and histogram for eps grade s.....	87
Figure 5-39 Excitation auto-spectrum @ 1125 averages for eps grade s	88
Figure 5-40 FRF estimate for eps grade s @ 0.40g RMS	89
Figure 5-41 Nonlinear FRF estimate for eps grade s @ 0.40g RMS	90
Figure 5-42 Coherence plot for eps grade s @ 0.40g RMS	91
Figure 5-43 Excitation time history segment and histogram for eps grade s.....	92
Figure 5-44 Response time history segment and histogram for eps grade s.....	92
Figure 5-45 Excitation auto-spectrum @ 1125 averages for eps grade s	93
Figure 5-46 FRF estimate for eps grade sl @ 0.25g RMS	95
Figure 5-47 Nonlinear FRF estimate for eps grade sl @ 0.25g RMS.....	96
Figure 5-48 Coherence plot for eps grade sl @ 0.25g RMS	97
Figure 5-49 Excitation time history segment and histogram for eps grade sl.....	98

Figure 5-50 Response time history segment and histogram for eps grade sl..... 98

Figure 5-51 Excitation auto-spectrum @ 1125 averages for eps grade sl 99

Figure 5-52 FRF estimate for eps grade sl @ 0.40g RMS..... 100

Figure 5-53 Nonlinear FRF estimate for eps grade sl @ 0.40g RMS..... 101

Figure 5-54 Coherence plot for eps grade sl @ 0.40g RMS 102

Figure 5-55 Excitation time history segment and histogram for eps grade sl.... 103

Figure 5-56 Response time history segment and histogram for eps grade sl..... 103

Figure 5-57 Excitation auto-spectrum @1125 averages for eps grade sl 104

Figure 5-58 FRF overlay of increasing averages for eps grade s @ 0.40g RMS
..... 105

Figure 5-59 Coherence overlay of increasing averages for eps grade s @ 0.40g
RMS 106

Figure 5-60 FRF overlay of increasing averages for eps grade sl @ 0.40g RMS
..... 107

Figure 5-61 Coherence overlay of increasing averages for eps grade sl @ 0.40g
RMS 108

Figure 6-1 Typical compression curve of various cushion materials 111

List of Tables

Table 4-1 Data capture and analysis details..... 53

Table 4-2 Material and load, experiment details..... 57

Table 5-1 Simulated system parameters 62

Table 5-2 Digital post processing parameters..... 62

Table 5-3 Material excitation and averaging table..... 82

Chapter 1

Introduction

1. Cushioning materials

During the distribution or delivery phase, products are often exposed to a variety of environmental hazards, which, if excessively severe, may cause damage to the product. Consequently, goods that are to be distributed must be protected against the hazards that occur during handling and transport. The design of this protective packaging requires a thorough understanding of the environment within which the package operates, and the response of the cushioning material to this environment.

Much of the mechanical damage to packages or products in shipment can be attributed to shocks and vibrations encountered during transportation. These vibrations, which are generally random in nature, can cause the shipment, or critical elements within, to resonate. This resonance has the potential to damage the product or cause the failure of critical elements due to the repetitive application of stresses.

The response behaviour of cushioning or protective packaging materials under vibration excitation is central to the effective design of product packaging. The response characteristics of the cushioning material guide the design parameters of the product-transport cushion system. Conventionally, this is achieved by the measurement of the transmissibility or linear Frequency Response Function (FRF) of the product/cushion system. However, commonly used cushioning materials can exhibit strong nonlinear behaviour.

This nonlinear behaviour is exacerbated when the cushioning system is placed under high static loads. Large static loads are often a result of attempts to minimise the environmental impact (as well as maximise the associated economic benefits) of packaging materials by reducing the amount of cushioning material used. Nonlinear behaviour can have significant implications for the design and optimisation of protective packaging systems, especially when trying to evaluate the transmissibility of the system.

Current transmissibility analysis techniques implicitly assume a linear relationship for the damping and stiffness in the behaviour of the cushioning material. As some common cushioning materials can exhibit nonlinear behaviour, the significance of the possible errors, using a linear analysis of these materials needs to be studied. The nonlinear behaviour of cushioning materials is largely ignored, consequently further research is needed. Also the application of a nonlinear analysis approach needs to be considered.

These factors lead to several observations:

- The distribution environment is continually expanding
- That there is a greater awareness of the human impact on the environment
- That globalisation is creating new distribution challenges.

They show that continual research into the design and behaviour of product package systems is essential.

1.1 Packaging distribution

A developed and progressive society, as successful as ours today in the economic, cultural and social arenas, is unachievable without mobility. Passenger and goods distribution are the foundation of national economies, and the distribution sector remains one of the principle linchpins of industry as a whole.

A global market and ever increasing need for resource management will lead to a further increase in distribution volume in Australia and elsewhere. Victorian Freight (2001) forecasts clearly indicate this. But more mobility not only brings evident benefits, it simultaneously inflicts burdens on people and the environment. Taking the broadest possible environmental perspective a modern economy must strive to limit its volume of transport. In order to keep the financial, social and ecological burdens of distribution within acceptable bounds, and if possible to reduce them overall, improvements must be accomplished in all areas of vehicle and distribution technology, more specifically packaging.

Packaging performs a number of fundamental services in today's modern society and is often overlooked or disregarded by critics focusing only on environmental issues. Packaging is not designed to be garbage (Packaging Council of Australia, 1994); it is a necessary link in the distribution chain. Packaging materials are used to perform a specific task. However there are hidden costs associated with over-packaging, the cost of extra materials, the cost of distributing excess volume, and an added cost to the environment due to the eventual disposal of this extra material.

The design of such packaging comes from our understanding of the distribution environment. Our ability to record and then simulate the distribution environment with greater accuracy will directly affect the package design outcomes. Optimum packaging can reduce the cost of goods, because its role as a protector can mean reduced product damage. Damage costs include package failure, damage to the packaged product, the outlay of shipping a product that is no longer saleable, and the disposal of un-saleable products. Obviously, such

optimum packaging is vitally important when shipping fragile and high technology goods.

Advanced measuring and testing techniques allow distribution systems to be analysed, and promote efficient use of capacities. Improved logistics coupled with technology helps to avoid unproductive routing, so as to be able to exploit the existing infrastructure to the full. Macroeconomic expansion and distribution are vital partners. Economic growth leads to higher consumption, which in turn increases the need for distribution services. In most markets today, only trucks can offer the flexibility and delivery assurance necessary to manage supply chains in the complex logistics systems that form the basis of our consumer societies. Rail infrastructure, which may have a lesser local impact, is slower to develop and to become economically viable. However, this increase in distribution traffic comes with an environmental cost.

During the past three decades, distribution services in Europe have grown by an average of 12 percent each year. In the past decade, truck distribution services have accounted for all of this increase (European Commission: White Paper, 2004). The European Union predicts that road distribution volume will rise by 50 percent between 1998 and 2010, but would like to limit this increase somewhat by encouraging rail and water-ways distribution (European Transport Policy for 2010, 2006).

In Australia a continual increase in road distribution places great pressure on the road infrastructure. As research contributes to our understanding of the dynamic interaction between the pavement and the vehicle, complementary research on the dynamic characteristics of cushioning materials responding to this excitation, will contribute significantly to tertiary package design. These factors will, through a reduction in volume and spoilage, help reduce distribution costs.

1.2 Economic considerations

The importance of vibrations generated by road vehicles is made more significant due to the fact that road transport still dominates the distribution industry and will probably do so for many years to come. Over the last 30 years the total movement of freight in Australia, and, it is expected, many developed countries, has tripled, as illustrated in Figure 1-1. According to a study by the National Transport Planning Taskforce (VicRoads, 1995), the growth in domestic freight is expected continue with that related to road mode predicted to increase three-fold over the next 20 years.

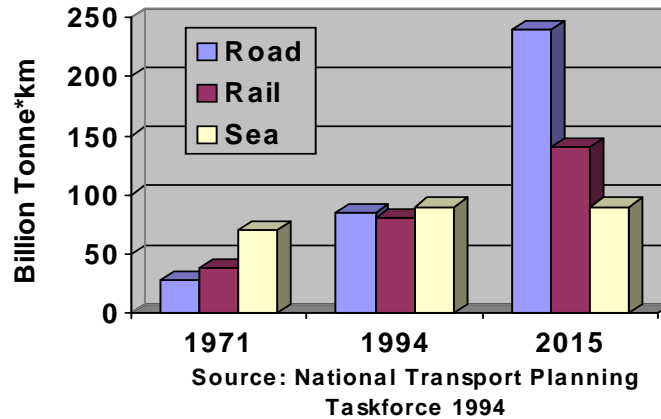


Figure 1-1 Growth in domestic freight transport in Australia (reproduced from Vic Roads 1995)

The cost associated with protective packaging for distribution and environmental costs of disposal are substantial. There is a strong case for continued research aimed at developing better techniques to optimise the design of protective packaging systems and reduce the amount of material required to protect products and shipments during distribution. In order to achieve a beneficial level of optimisation when designing protective packaging or cushioning systems, a thorough understanding of the nature of vehicle shocks and vibrations and their effect on the product and shipment, is essential.

For both economic and environmental reasons the packaging industry should seek to keep packaging material usage at the minimum required to satisfy technical, quality and performance standards. Resource usage and the environmental impacts of packaging should be taken into consideration when package design and manufacture is in the developmental stage.

Modern packaging technology is responsible for a significant contribution to our standard of living by enabling the preservation and distribution of goods on a large scale. It has been estimated that the annual expenditure on packaging material and machinery worldwide exceeds USD238 billion (Anon, 1996). Packaging is a significant contributor to the Australian economy. The Packaging Council of Australia conservatively estimates that the consumption of packaging has an annual value of \$4.5 billion and that in excess of 29,000 people are directly employed in the industry (The Packaging Council of Australia, 1994).

By providing an efficient means of distribution, packaging, together with improved distribution networks, enable manufacturing and production facilities to be centralized near the source of raw materials while the products are transported to consumer centres. Such large-scale operations offer significant economic benefits. Effective protective packaging makes it possible for the finished products to be transported across relatively large distances to consumer centres.

1.2.1 Distribution

The central role of protective packaging or cushioning systems is to shield from, or limit, the effects of excessive shocks and vibrations on the product, during distribution and transport. Figure 1-2 Economic considerations for package/product optimisation shows the region of adequate protection and the cost of insufficient protection and the rise in total cost in the case of excessive cushioning. In practice, the level of shocks and vibrations transmitted to the product, or critical element, is reduced by a cushioning or other vibration-absorbing element or devices.

The amount or level of protection required by a product is determined by the fragility (susceptibility to damage) of the shipment and the likely harshness of the hazards to be encountered. As well as requiring a comprehensive knowledge of the products' fragility, effective cushion design requires careful consideration of the cushioning materials' response to shocks and vibrations.

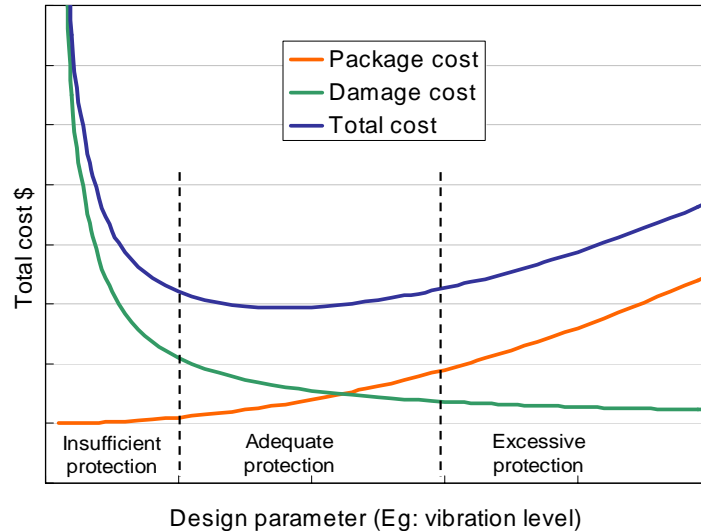


Figure 1-2 Economic considerations for package/product optimisation

Insufficient or ineffective packaging is easily identified as it is manifested through the occurrence of damage to the shipment during transport and handling. Over-packaging, however, is more difficult to establish. Over-packaging can be defined as the excess of protective cushioning material with respect to the expected risks of damage. In most cases, much of the material that makes up packages consists of cushioning elements included to protect the product against mechanical damage. In theory, cushioning systems are designed to provide protection for an expected or acceptable level of mechanical misuse during delivery. In practice, however, reliable knowledge of the likely intensity and occurrence of mechanical hazards are not always available.

The level and nature of mechanical misuse applied to freight during transportation and distribution (of which vehicle-related shocks and vibrations

are a major component) may be regarded as, on one hand, either normal or expected and, on the other, excessive or hazardous. Because severe levels of mechanical misuse, such as those generated by transport-vehicles are, to a certain extent, unpredictable and occur randomly, it is relevant to consider them as hazards. Such random and unpredictable extreme vibrations and shocks can cause the product or critical element within to undergo excessive irregular movement.

So far, in the packaging and distribution industries, much of the activity concerned with measuring and analysing vehicle-related shocks and vibrations has been concerned with simulation for the purpose of validating and testing protective packaging systems. The packaging testing or validation methods currently in use treat distribution-related hazards statistically and imply that the occurrence of incidents is unavoidable. Information on environmental hazards is not only used for package design but is also applied to define performance-testing schedules. Testing of packages in controlled laboratory conditions in which hazards are reproduced or simulated are widely considered superior to field testing (Sek, 2001). Hazards during handling and distribution are seen as the least predictable factor in package design. Insurers typically require the packaging to conform to performance standards, which, in turn, incorporate significant levels of over-packaging to compensate for the unpredictability of environmental hazards.

The problem is compounded by the reluctance of distribution companies to guarantee the limiting levels of hazards in their distribution chain such as the maximum level and number of shocks and frequency content and level of vibration (Rouillard, 2002).

These issues encourage packaging designers to take a conservative approach, which, in many cases, lead to over-packaging (Rouillard, 2002). In the E.U., it has been estimated that the hidden cost associated with over-packaging is 20 times higher than the cost of excessive packaging materials and has been valued at an estimated €130 billion per year (Oestergaard, 1991). These hidden costs include those associated with disposal, increased traffic, pollution, and

accelerated road deterioration due to excessive volume of over packaged goods. It is therefore evident that the reduction of over-packaging may lead to significant economical, environmental and social savings.

1.2.2 Packaging as waste

As a result of packaging's short life span, compared with the product it protects, packaging is often considered wasteful or excessive. Its durability and visibility in domestic waste, tends to strengthen the perception that there is just too much packaging. Its function is taken for granted and its contribution to our modern way of life is not appreciated or well understood.

Primary and secondary package development is continually refining and reducing the weight of packaging materials used. Packaging is 22% (by weight) of domestic waste and only 10% of the total waste stream (The Packaging Council of Australia, 1994).

Across Australia, there is a goal to reduce waste (including packaging waste) by 50% by 2008 (National Packaging Covenant, 2005). Some examples of the reduction in weight of the primary packaging are:

- The weight of the 375ml glass beer stubby has been reduced by 35% since 1980
- The weight of a standard 440gm sliced fruit can has been reduced by 18% since 1980
- A weight saving of 29% has been made to 375ml aluminium beer and soft drink cans since their introduction in 1969
- The weight of 200ml polystyrene yoghurt tubs has been reduced by 20% since 1986
- Since its Australian debut in 1980, the HDPE milk bottle has been reduced in weight by 30%
- The PET soft drink bottle weight has been reduced by 38% since its introduction in the late seventies.

Continuing research into new materials has greatly reduced the weight of package containers and has a follow on effect, on the design of the tertiary or transportation package.

Directive 94/62/EC of the European Parliament on Packaging and Packaging Waste was introduced in December 1994 as part of the Europe-wide rules on packaging. Directive 94/62/EC says in part, packaging must now be manufactured so that *“its volume and weight is limited to the minimum adequate amount to maintain the necessary level of safety, hygiene and acceptance of the packed product for the consumer.”*

This directive stems directly from the pressures of waste disposal within Europe. Australia as a large, lightly populated continent is not yet under such immediate visible pressures. However, a growing awareness of our impact, most particularly of our waste products, as a society on the environment, local and global should lead us to a more responsible attitude.

Much of the drive to reduce packaging has been based on the immediate economic benefit during production with the final disposal responsibility passed to the purchaser. Within Europe, in particular Germany, this disposal responsibility has been legislated back to the manufacturer (Eichstadt, Carius, Kraemer, 1999). This then, creates even more pressure upon the designer to produce tertiary package designs that protect whilst reducing waste.

It is not in our or industry's best interest to use excessive packaging or to over package on either economic or environmental grounds as it adds to cost and product price, reduces competitiveness and is less acceptable in the marketplace. Resource usage and the environmental impacts of packaging should be taken into consideration when both, the product and package design and manufacture, are in the development stage.

1.3 Package testing standards

In 1992 an Environmental Code of Practice for Packaging was released in Australia (The Package Council of Australia, 1992). New package design now incorporates an environmental impact study; with technological development allowing lighter weight packaging without loss of performance. Along with a growing environmental awareness, reuse and recycling are gaining acceptance within society and are increasing.

Product and package manufacturers coexist in a highly competitive market. Unnecessary packaging adds to manufacturing and delivery costs. The package manufacturer has to ensure that there is neither too much (over packaging) nor too little (under packaging). Over packaging leads to extra delivery costs and waste, under packaging may result in waste due to damaged and unsaleable products. Legislation exists regarding the suitability of certain containers for particular purposes and products.

For both economic and environmental reasons the packaging industry seeks to keep packaging material usage to the minimum required to satisfy technical, quality and performance standards. The harsh and complex nature of the packaging environment highlighted the need for a set of performance standards and an appropriate testing schedule. This need is met by package design and performance standards developed by various regulatory bodies in Europe, America and Australia.

Figure 1-3 shows the relationship between the Australian Standard (AS), American Society for Testing and Materials (ASTM) and the International Organisation for Standardization (ISO) standards. However, the International Safe Transit Association (ISTA) is generally considered the more common of the testing schedules and as such is the most widely used.

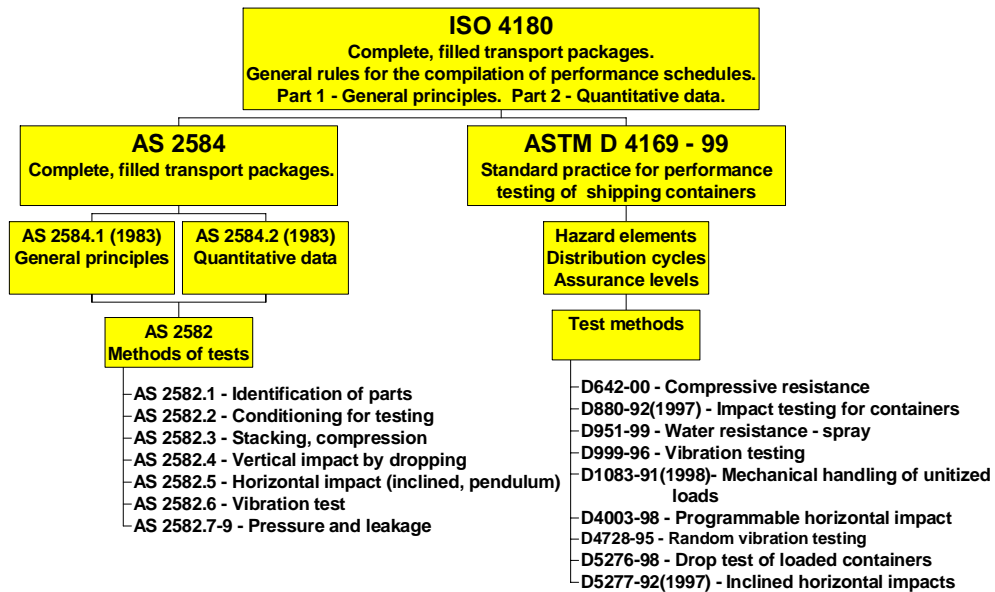


Figure 1-3 Relationship between AS, ASTM and ISO standards

1.3.1 Distribution- vehicle vibrations

In the distribution environment, transport, and in particular, road transport is a major source of hazardous shocks and vibrations. These shocks and vibrations may have a detrimental effect on the freight. Products and the critical elements within suffer damage primarily due to excessive levels of vibration and shocks generated by the vehicle.

All mechanical systems will exhibit resonance when subjected to vibration inputs. In package systems, vibrations during transport can generate considerable responses. Godshall (1971) identified the resonance of a stack of filled paperboard boxes at between 8 and 18 Hz with a resonant transmissibility of well above six (6). Cushioned packs were found to exhibit vibration transmissibilities of up to 10 at resonance (Zell, 1969). These resonances can result in sustained and large dynamic stresses and eventually in damage or failure of the package, product or one of its components (critical elements). Electronic goods and fresh fruit and vegetable produce are prime examples of products which are vulnerable

to vibration induced damage. The types of damage may range from surface abrasion (scuffing), loosening of fasteners and connectors, loss of calibration, metal fatigue and cracking of plastic components (Caldicott, 1991).

Depending on the environmental conditions, the premature collapse of paperboard boxes due to excessive vibrations has also been observed (Gordon, 1980). Materials such as glass, hard plastics and some types of metals fail primarily due to excessive stress levels. Repetitive stress applications below the strength limit have negligible effects on the material's ability to withstand stresses. However many materials, which are used in products and protective packaging systems, are ductile and are affected by the repetitive application of stress even at relatively low amplitudes. In such cases, the material's ability to withstand further stress application is gradually eroded until failure occurs (Kipp, 2000).

It is obvious that the primary source of vertical vibrations generated by road vehicles can be attributed to the unevenness of the road pavement surface. When vehicles travel irregular surfaces, the interaction between the vehicle and terrain gives rise to a dynamic process that produces complex forces and motions within the vehicle. Pavement surface irregularities are generally random in nature; this causes the resulting vehicle vibrations to be random. Furthermore, the levels of vibrations are not solely dependent on the pavement roughness but are also a function of vehicle type, payload and speed. The effects of these parameters tend to make the complex mechanical interactions between the vehicle and pavement surface difficult to characterise and predict. It is therefore widely acknowledged that the analysis and simulation of road-related vehicle vibrations demands some level of sophistication.

Regulatory standards are by their nature a baseline, rather than a driving force for optimisation. Therefore assumptions are made that simplify the environmental signal, and whilst adequate there is much room for improvement. Current road simulation techniques, based on a frequency domain Power Spectral Density (PSD), remove transient effects, which are the likely cause of package damage.

Other distribution hazards such as vibrations, compressive loads and climatic variations are often considered as secondary effects. However, mechanical vibration and resonance are potentially the most damaging. As a result, the main design parameter for protective packaging systems is the level and nature of shocks and vibrations that will be encountered.

1.4 Research objective and significance

During the distribution phase, products are often exposed to a variety of environmental hazards, which, if excessively severe, may cause damage to and even destroy the product. Consequently, goods that are to be distributed must be protected against these hazards that occur during handling and transport. Among these hazards, vibrations and thus resonance are potentially the most damaging. Mechanical vibrations and shocks arise as a result of the vehicle travelling over uneven pavements. As a result, the main design parameter for protective packaging systems is the level and nature of this unevenness.

The design of protective packaging or cushioning systems have so far relied heavily on simplified models and fundamental assumptions with respect to the nature of shocks and vibrations generated during distribution and transport (Sek, 2001). These will be elaborated upon further in this thesis and, at this stage, suffice to mention that these simplified models and assumptions have encouraged the adoption of a conservative approach to packaging design which, in many cases, leads to over-packaging (Sek, 2001).

The terms 'excessive packaging' and 'over packaging' are not synonymous and should not be confused with one another. Excessive packaging implies that there is too much used in total. This is often the case where advertising or “presence on display” is the priority; however, display is not the primary task of packaging. Over-packaging, meaning more than is necessary, can suggest a lack of knowledge of the product-package mix or of the environment that a package must withstand, to perform efficiently and satisfactorily in its life cycle.

Cushion design, like any other design process, requires the goal, the materials and the design criteria to be fully understood before a successful solution can be achieved.

The most widely accepted method for the development of optimised package-product systems is the so-called Six-Step Method (Root, 1997) comprising the following steps:

1. Evaluate and quantify distribution hazards
2. Determine product robustness (cf. fragility)
3. Increase product robustness
4. Characterise protective packaging material
5. Design protective packaging
6. Test and validate product/package against simulated distribution hazards

As illustrated in Figure 1-4 the Six-Step Method importantly promotes the concept of the optimum product / package system. This concept, being characterised by improved product robustness, as well as a sufficient (optimum) amount of protective packaging to withstand the environmental hazards.

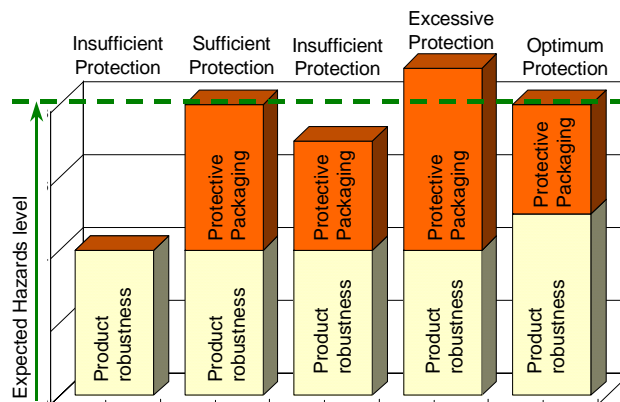


Figure 1-4 Distribution of product fragility, level of cushioning and level of hazard

This Six-Step Method is guided by economical considerations, which control the design of products and packages for distribution and handling as illustrated previously in Figure 1-2.

This further illustrates the need for compromise between the costs associated with increasing the product's robustness, on one hand, and improved levels of protective packaging, on the other, in order to attain an optimised system.

Step 1: Evaluate and quantify the distribution environment.

Before the design of the cushion can be considered, the environment within which the package will travel must be investigated. There are two approaches available here;

1. Record and quantify the actual real world experience of a test package over the expected route of delivery,
- or
2. Estimate the delivery environment and use an appropriate standard as the maximum expected hazard level. If the package delivery route varies greatly then the use of a standard may be more appropriate.

Step 2: Determine the product robustness.

Depending on its robustness the product will have a natural ability to withstand and absorb shocks and vibration from the distribution environment. Shocks are evaluated by the method of dropping the product from a determined drop height. Resonance behaviour, when the excitation vibration occurs at the natural frequency of the cushioning material, should be avoided as the product will undergo an amplification of the excitation leading to possible failure of the critical element. The critical element within the product, that is the most susceptible to damage, will be the design cost factor.

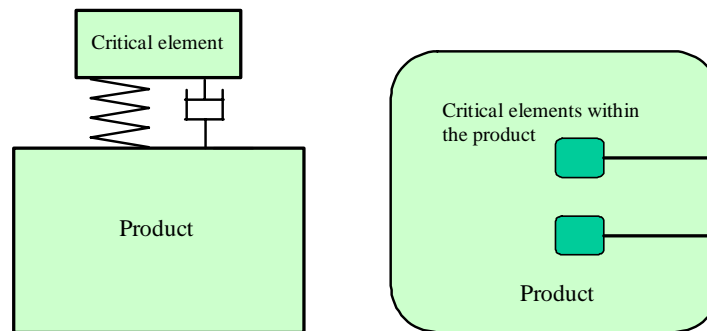


Figure 1-5 Critical element and product

The critical element defined as the part or component of the product most susceptible or prone to damage. It can be modelled as a small mass attached to the product by an elastic element (spring) and a damper as illustrated in Figure 1-5. This represents the critical elements natural capacity to dissipate shock and vibration energy. Damage will obviously occur when the spring fails due to excessive deflection.

The point at which the critical element fails must be quantified for the design process to continue. This may be done by the generation of damage boundary curves (Sek et al, 2000) or through design calculations.

Step 3: Increase the products robustness.

It is at this point that the product robustness may be reviewed. After the generation of the damage boundary curves it may be possible, through a product redesign, to increase the products robustness and therefore save on cushioning and packaging. This step has of course economic consequences.

Step 4: Characterise the protective packaging material.

The accurate characterisation of the package cushioning material is important for the efficient design of protective cushioning. The vibration transmissibility and shock attenuation are essential engineering information.

It is in this area that this thesis seeks to add to and extend the current body of knowledge. To begin to characterise the material experiments are performed on the material to determine its actual response to certain excitations. To then use the experimental response of the material in further study a mathematical model is formulated. This mathematical model will allow the simulation and design of the product-package unit

The cushion curve of a package material is a representation of the shock transmission characteristics of the material. It depicts the peak acceleration transmitted by the cushioning material, of a given thickness, of a mass dropped from a known drop height as a function of static load. Figure 1-6 shows a typical cushion curve for an expanded polystyrene material for two drop heights, 50 cm and 100 cm. The ordinate is the maximum acceleration transmitted to the tested mass. The abscissa is the static load, or ratio of weight to cushion bearing area.

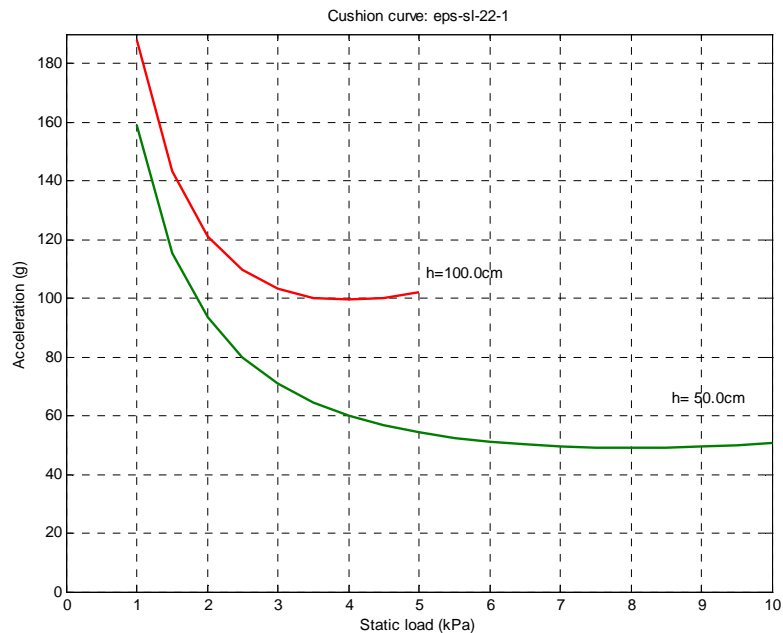


Figure 1-6 Cushion curve for EPS

Figure 1-7 shows a typical cushion curve with the horizontal line representing the fragility/robustness limit or maximum acceleration limit (g) of the critical element within the product. The region beneath the curve and fragility limit line, describes the extent of the range of static loads over which the cushion will provide adequate protection.

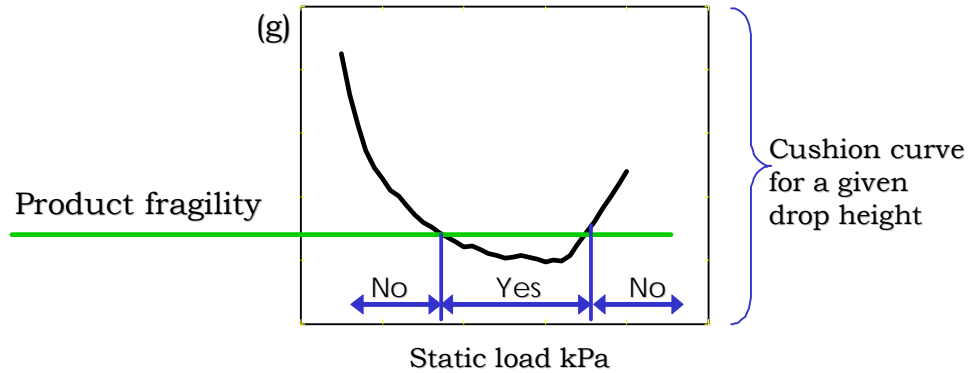


Figure 1-7 Typical cushion curve design plot

Figure 1-8 is a typical transmissibility amplification/attenuation plot of a common cushion material. It is shown with the frequency of excitation/response as a function of static load.

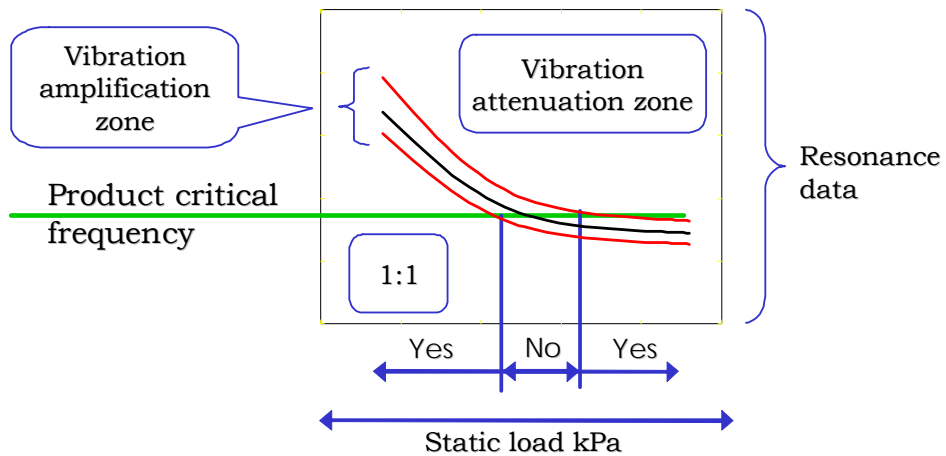


Figure 1-8 Typical vibration transmissibility design plot

From the area beneath the product fragility line in Figure 1-7 the range of static load is determined and used on Figure 1-8 with the product critical frequency, to determine the frequency range over which the cushion will provide adequate protection. The amplification/attenuation range is taken from the magnitude of the Bode plot, for a linear system.

Typically the transmissibility plot is obtained by sine sweep. The sine sweep range and rate being determined by a standard such as ASTM D3580-95 (see appendix A). The accurate characterization of the transmissibility behavior of the cushion material is vital information for the designer of a package under a static load due to the vulnerability of the critical element. These two figures demonstrate (by yes/no/yes) the possible conflict between the requirements for protection from shocks and the need to avoid a vibration resonance situation.

Step 5: Design protective packaging.

The design of the packaging follows from the knowledge of the distribution environment, the product or critical element's fragility, and the accurate characterisation of the cushioning material.

The initial cushion curve design requires that the maximum expected shock level or drop height be defined. This is usually determined by estimating the statistical likelihood of a certain design drop height from data describing the probability of occurrence. In most cases, such statistical distributions are constructed using limited sets of data and, as such, cannot represent all possible drop heights. A test recording device may be sent over the expected distribution route recording the acceleration it is subjected to. This data can be analysed and a drop height calculated.

Step 6: Test and validate product/package against simulated distribution hazards

Upon completion of the protective cushion design the complete product/package is tested to ensure the design criteria has been met. The testing may consist of real world experience, i.e. on the expected vehicles and on the expected or

similar delivery route. Random vibration tests may also be conducted in which the vibration is of a frequency range and magnitude to mimic the real world motions of transportation vehicles.

These six steps are interdependent and can be separated into three main categories, environment, product and material. The cushioning material, its vibration transmission characteristics and analysis, are the focus of this research. The behaviour of the material under vibration is an important design consideration for the protection of the critical element.

1.5 Organisation of thesis

This chapter has highlighted the importance and further development of mobility and distribution whilst also considering the burdens on people and the environment. It stresses the significance of continued research aimed at promoting and improving the design of protective packaging systems. It also underlines the damaging effect of vibrations and resonance on the package.

In Chapter 2 a mathematical model is developed to study the characteristics of a cushioning material. It is found that a cushioning material system can exhibit strong nonlinear behaviour. This nonlinear behaviour further adds to the difficulty of relating and predicting the response of protective packaging systems. Chapter 2 presents a brief review with a focus on existing nonlinear analysis techniques. The Reverse Multiple Input-Single Output (R-MISO) analysis technique is studied and its engineering significance is discussed. This technique is shown to have an aptitude in promoting and contributing to a more reliable analysis of nonlinear systems. The technique will be used to further study the nonlinear response of packaging systems.

Chapter 3 formulates the hypothesis that, the design decisions based on an analysis of a nonlinear system by an analysis technique that considers such nonlinearities would be an improvement and refinement over current practice.

Chapter 4 explains the method adopted to examine the response of a typical cushioning material, expanded polystyrene, to random broadband vibration excitation. It outlines the material details and experiments the cushioning material was subjected to. The development of a computer based implementation of the R-MISO algorithm is described. A detailed outline of the equipment required and how this was organised is depicted.

Chapter 5 expounds upon the R-MISO analysis software and presents the analysis results for simulations of known nonlinear equations. A single degree of freedom dynamic system is simulated and the R-MISO analysis results compared to the known simulation values. Various nonlinear systems are simulated and analysed, this leads to a greater understanding of the process. The chapter further presents the R-MISO analysis results for the nonlinear analysis of a common cushioning material, expanded polystyrene and presents some interesting comparisons.

Chapter 6 in conclusion, summarises the significance of the results and discusses possible future research areas.

Chapter 2

Vibration transmissibility
of cushioning materials

2 Modelling the product and cushion

To study the characteristics of cushioning material, a mathematical model is developed. Recalling the initial model of the product and cushion in Figure 2-1, this representation may be extended by defining the direction of vibration:

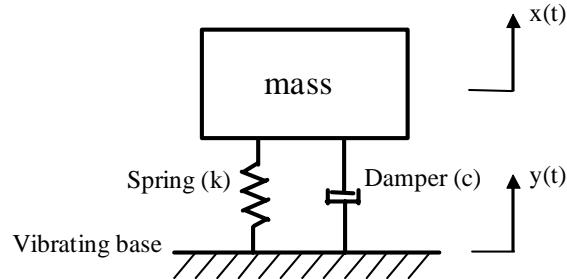


Figure 2-1 Product cushion vibrating base model

Figure 2-1 shows a representation of a single degree of freedom system with mass, spring and damper. The equation for this model with vibrating base excitation (displacement) becomes:

$$-f_1(x-y) - f_2(\dot{x}-\dot{y}) = m\ddot{x}, \quad (2-1)$$

where: $f_1(x-y)$ describes stiffness as a function of displacement

and $f_2(\dot{x}-\dot{y})$ describes the damper coefficient as a function of velocity.

This equation is a general situation with no assumptions of nonlinearity.

An accurate characterisation requires a closer look at the terms of Equation (2-1). The damping or dissipative term (c) and the spring term (k) may or may not be nonlinear. To investigate the spring/restorative force and the damping a compression curve plot is generated for the cushion material as illustrated in Figure 2-2.

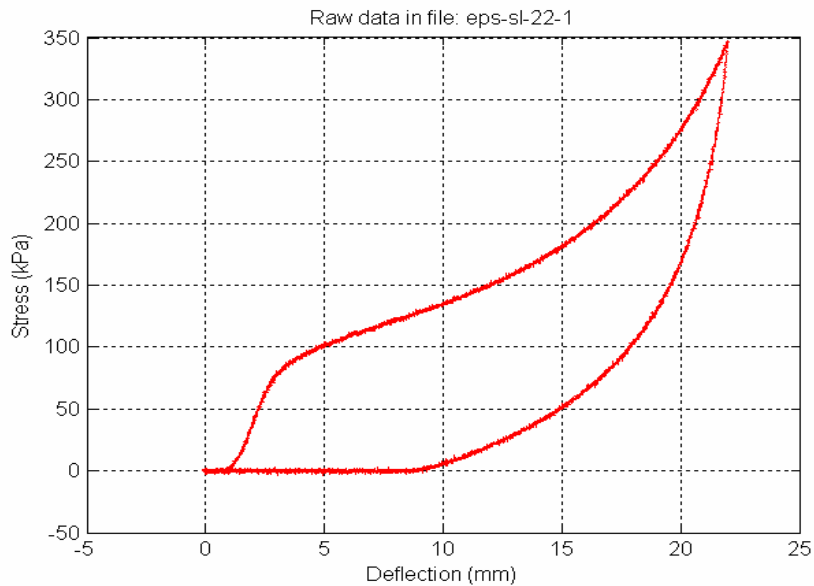


Figure 2-2 Compression curve for EPS

Figure 2-2 shows a typical compression curve for expanded polystyrene compressed to 65% of its original thickness, at a rate of 1mm per second. It is obvious from Figure 2-2 that the spring /restorative force behaviour is nonlinear, and it can also be seen that there are hysteretic damping effects present. So it follows that the mathematical model, incorporating these terms as nonlinear functions, will be nonlinear.

2.1 Linear and nonlinear systems

At this point a brief review of the strict definition of linear and nonlinear systems and the practical meaning of these to the testing and analysis of such systems is warranted.

The simplest representation of a structure with an input (a) being changed in some way by the system (H) resulting in an output (b) is shown in Figure 2-3.

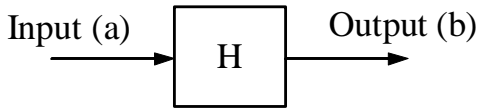


Figure 2-3 Representation of a system H

A system H is defined as linear if, for any inputs $x_1 = x_1(t)$ and $x_2 = x_2(t)$, and for any constants c_1, c_2 :

$$H[c_1x_1 + c_2x_2] = c_1H[x_1] + c_2H[x_2] \quad (2-2)$$

This equation contains two properties required of linear systems:

- Additive Property
- Homogeneous Property.

Should a system not satisfy either of the above two properties, the system is considered nonlinear. This is defined as follows:

A system H is nonlinear if, for any inputs $x_1 = x_1(t)$ and $x_2 = x_2(t)$, and for any constants c the system input/output relations are not additive and/or are not homogeneous. Such that:

$$H[x_1 + x_2] \neq H[x_1] + H[x_2] \quad (2-3)$$

$$H[cx] \neq cH[x_1] \quad (2-4)$$

These nonlinear operations will produce non-Gaussian output data when the input data are Gaussian, whereas linear operations preserve the Gaussian structure. Non-Gaussian output data will also occur when the input data is non-Gaussian, for example sine waves.

Any physical system that must operate over a very wide dynamic input range will ultimately exhibit nonlinear behavior. In the case of a cushioning system this is because of the possibility of stiffening of the cushion at extreme deflections. Therefore, a product-package system should be judged to be linear or nonlinear

depending on its specific properties for a desired type and level of input. The test, type and level of input should match as closely as possible, the expected distribution environment. No general theory is available for the analysis of nonlinear systems such as that which exists for linear systems. Instead, different approaches and techniques are required for the study of specific nonlinear systems.

Conventional spectral analysis techniques assume that the system adheres to the additive and homogeneous properties of the input, nonlinear systems however, do not adhere to these properties. This leads to the possibility of errors in the analysis and possibly wrong conclusions drawn from this analysis. Research shows that errors, resulting from the analysis of a nonlinear system by linear system analysis techniques, can be significant. (Bendat, 1990, Potter et al, 1996).

Product-package systems include cushioning materials, which can exhibit strong nonlinear behavior. This nonlinear behavior adds to the challenge of describing and predicting the response of such systems. The accurate modeling and design of these packaging systems necessitates the use of a nonlinear analysis approach. However for any such nonlinear analysis approach to gain wide spread acceptance it is desirable that it follows on or extends upon current practice.

2.2 Frequency response functions

Linear Single Input-Single Output (SISO) analysis is widely used within the packaging industry and this section will review the concepts of frequency response function and coherence.

SISO analysis involves the simultaneous measuring and recording of two channels of data. The most significant application of this approach is in the measurement of Frequency Response Functions. The frequency response function represents the ratio of output/response to input/excitation in the frequency domain and can fully characterise a stable time invariant physical system.

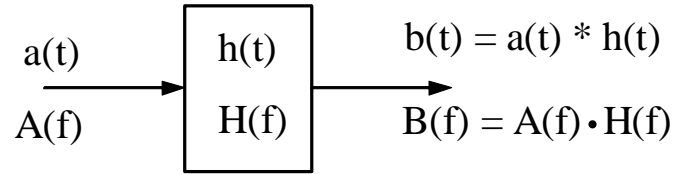


Figure 2-4 Input - Output relationship for a linear system

Figure 2-4 shows the relationship between the input and output signal for a stable linear time-invariant system in the absence of noise. The system is characterised by its impulse response $h(t)$ such that the output signal $b(t)$ is the convolution of $a(t)$ with $h(t)$, thus:

$$b(t) = a(t) * h(t) \quad (2-5)$$

By the convolution theorem, it follows that

$$B(f) = A(f) \cdot H(f), \quad (2-6)$$

where $H(f)$ is the Fourier transform of $h(t)$. Thus the Frequency Response Function can be obtained from:

$$H(f) = \frac{B(f)}{A(f)} \quad (2-7)$$

Equation (2-5) may be tailored in various ways so as too give a range of conclusions. For example, if the numerator and denominator are both multiplied by the complex conjugate of A , an FRF version known as $H1$ is obtained:

$$H1(f) = \frac{B(f)}{A(f)} \cdot \frac{A^*(f)}{A^*(f)} = \frac{S_{AB}(f)}{S_{AA}(f)} = \frac{G_{AB}(f)}{G_{AA}(f)} \quad (2-8)$$

This is the cross-spectrum, between input and output from A to B , normalised by the autospectrum of the input spectrum. Bendat & Piersol (1993) show that, with noise in the output signal, this definition minimises the error in the result.

Similarly if the complex conjugate of B is the multiplier, another version known as H2 is obtained:

$$H2(f) = \frac{B(f) \cdot B^*(f)}{A(f) \cdot B^*(f)} = \frac{S_{BB}(f)}{S_{BA}(f)} = \frac{G_{BB}(f)}{G_{BA}(f)} \quad (2-9)$$

This is the output autospectrum normalised by the cross-spectrum, between output and input from B to A. This version has advantages in various situations such as when there is noise in the input signal, (Mitchell, 1982).

2.3 Coherence

Coherence gives a measure of linear dependence between two signals as a function of frequency, and is an important factor in the assessment of the goodness of fit of a mathematical model to the measured data. It is calculated from the two autospectra and the cross-spectrum:

$$\gamma^2(f) = \frac{|G_{AB}(f)|^2}{G_{AA}(f) \cdot G_{BB}(f)} \quad (2-10)$$

The coherence can be interpreted as a least squares correlation coefficient (expressing the degree of linear dependence between the two variables), with the autospectral estimates corresponding to the variances of the two variables, and the cross-spectral estimate to the covariance.

The coherence function may also be used to calculate the signal-to-noise ratio defined as:

$$S/N = \frac{\gamma^2}{1 - \gamma^2} \quad (2-11)$$

When noise in the measured output is assumed to be the only factor influencing coherence, then the coherent power (proportional to γ^2) gives a measure of the

signal appearing in the output, while the non-coherent power (proportional to $1-\gamma^2$) gives a measure of the noise in the output.

Coherence is a widely recognised and accepted measure of the ‘goodness of fit’ of a proposed linear model to recorded data. As such, an ability to quantify a similar parameter to coherence, in any nonlinear analysis approach, would be desirable.

2.4 Nonlinear analysis review

With the determination that the cushioning material can exhibit strong nonlinear behaviour, a nonlinear analysis approach becomes necessary. A requirement of any such approach is that it would be relatively easily incorporated into current vibration testing programs. This would encourage the use and quicker uptake of such a proposal.

Most of the previous research into nonlinear system theory has been directed toward defining a widely applicable mathematical model able to convert a single input data record into the many terms that comprise various possible nonlinear output records. The nonlinear formulation with the most universal application was found to be the Volterra series (Rugh, 1981).

The Volterra series and its derivative Wiener series are based on Taylor series expansion of time-invariant nonlinear systems (Rugh, 1981). The Volterra series model assumes that the nonlinear response data can be expanded into a "power series with memory" with an N-integral kernel associated with each nth order component. This approach leads to higher order spectra such as bi spectra and tri spectra that are based on higher order moments of the input data. Some of the disadvantages of the Volterra series are the sensitivity to a Gaussian assumption of the input data, and the possibility of large random errors in estimates that require excessive amounts of data for acceptable confidence limits.

Parametric identification methods are techniques to estimate the parameters of a given model. Parametric identification methods include Output Error, State Space and Auto Regressive Moving Average models. These models are a numerical search algorithm to identify the parameters values that give the best agreement between the simulated or predicted models output and the measured one. In general prediction error methods, for example Least Squares, Maximum Likelihood, Output Error Identification, the parameters of the model are simply chosen so that the sum of the squares of certain residuals is minimised.

Preliminary work was undertaken to assess various nonlinear analysis techniques and concluded that, for the purpose of this study, the reverse multiple input/single output (R-MISO) system identification technique has the most promise. The algorithm introduced by Bendat and Piersol (1982) will be the starting point for the development of an analysis tool for the investigation of the nonlinear characteristics of cushioning systems. Their research paper discussed single input-single output (SISO) square law systems. The authors proposed a procedure in which the input data and the input data squared are treated as two partially correlated inputs to the system, thus giving a two input-single output model. Later Bendat and Piersol (1986) used this approach for modelling the wave forces arising from Morison's equation, which contains a linear and a quadratic term representing the inertial and drag forces.

Rice and Fitzpatrick (1988) then extended this approach to show how to deal with any arbitrary nonlinear systems using spectral analysis. They developed a spectral approach based on linear multi-variant analysis for the identification of Single-Degree-Of-Freedom (SDOF) systems including nonlinearity. Also, procedures for estimating the nonlinear contributions to responses were detailed. This method was applied to numerically simulated SDOF models with nonlinear stiffness and damping.

Bendat (1990) made a detailed description of the use of random vibration excitations for the analysis and identification of many classes of practical engineering systems featuring the general nonlinearity, in parallel and series with arbitrary linear operators. He established the procedure for the mathematical

reversing of the roles of input and output of a SDOF model in order to form a R-MISO model. He also formulated the spectral conditioning technique for removing the correlation effects from one input to other inputs. The advantages of this method are that it is non-iterative, does not require any starting value and is robust as well as computationally efficient. This new simpler frequency domain technique approach is easier to compute and interpret than the Volterra functional series (Schetzen, 1980).

Rice and Fitzpatrick (1991) continued their inversion approach, which in many respects is comparable to the reverse path method, to the analysis of a two-degree-of-freedom system such that a multiple input-single output (MISO) model is configured. Using spectral conditioning techniques, the frequency response functions of the various linear and nonlinear paths may be isolated. The SDOF system input/output analysis procedure set forth earlier may then be used to complete the identification of the model and system parameters.

Bendat and Piersol (1993) further emphasised the procedure for identifying optimum nonlinear system properties from simultaneous measurement of the input/output data and spectral analysis. Formulae are stated for two engineering problems that represent nonlinear wave force models and nonlinear drift force models. Error functions and multiple and partial coherence functions, are given to quantify how well each term of the model fits the data at specific frequencies of interest.

Spanos and Lu (1995) addressed the problem of nonlinearity in structural systems when the nonlinearity is caused by the interaction of a fluid and structural dynamics. They used an inversion method similar to the reverse path method to study, single and two degree of freedom, systems excited by various nonlinear types of wave forcing functions. The forcing functions were decomposed into a set of base functions or were expanded in terms of the wave and structural kinematics. The simulations showed that the wave force parameters could be estimated accurately under different levels of observational noise.

Bendat (1998) published an extensive revision and replacement of his previous book on Nonlinear System Analysis and Identification from Random Data, taking into account advances in technology and further work in the field. New techniques called Direct and Reverse MISO techniques are introduced. General nonlinear models consisting of linear systems in parallel with arbitrary or special nonlinear models (Duffing, Van der Pol, Mathieu and dead-band) were introduced.

Also applications for more complex multi-degree-of-freedom oceanographic, automotive and biomedical systems were presented. The identification of the nonlinear system response properties of naval vessels is discussed in detail. Coherence functions were again emphasised as indicators of the accuracy of the choice of the inputs to the MISO analysis.

Narayanan *et al.* (1998) demonstrated a practical application of the R-MISO identification technique on a moored sphere, treated as a SDOF system, exhibiting nonlinear behaviour due to the nonlinearity of mooring line restoring forces and hydrodynamic excitations. Given the input wave characteristics, the wave force and the system response, they identified the hydrodynamic drag and inertia coefficients from the wave model formulated by the relative-motion Morison equation. In addition to the method presented by Spanos and Lu (1995), this study was also able to identify the structural properties.

Richards and Singh (1998) made an attempt to adapt the reverse path method for SDOF systems to multi-degree-of-freedom systems. The most challenging objective of this research was to address the problem of identification of nonlinearity, which may exist at or away from the excitation locations. However, similarly to the reverse path method, the nonlinearity is described by analytical functions, whose coefficients can be determined by computing the conditioned frequency response functions. This implies that, from a system identification point of view, the types of nonlinearity and their location must be known. The method presented by Richards and Singh enables the estimation of the linear and nonlinear parameters at or away from the excitation locations; an example with a maximum of five degrees of freedom is presented.

Panneer, Selvam and Bhattacharyya (2001) studied a compliant marine SDOF system. They considered four different data combination scenarios, and developed an iterative scheme for the identification of the hydrodynamic coefficients. They also identified the nonlinear Duffing stiffness parameter in the relative velocity model of Morison's equation. Their analysis procedure used the R-MISO technique and their findings showed the approach was efficient and robust for both weak and strong nonlinear systems.

Liagre (2002) adapted the R-MISO approach to address distributed parameter Multi-Degree-Of-Freedom (MDOF) systems with general damping-restoring types of nonlinearities. An application with respect to a compliant deepwater offshore platform was modelled with the system parameters identified. These included the frequency dependant added mass and damping coefficients. The results presented demonstrate that the methodology can yield accurate values of the identified system parameters.

Panneer, Selvam and Bhattacharyya (2003) studied a large floating body, as a compliant marine SDOF system, with linear and cubic nonlinear stiffness terms. The R-MISO technique was used to identify the system parameters, particularly the frequency dependent added mass and radiation damping, and linear and nonlinear stiffness coefficients.

This review demonstrates the 'reverse path' system identification technique is topical and has the potential to facilitate a more accurate analysis of a nonlinear system. The method has a foundation in current dual channel analysis, and gives results in a relatively understandable format. Specifically, there is a need to extend this system identification technique to distributed parameter systems and to explore its ability to accurately model common cushioning material systems.

2.5 Reverse Multiple Input-Single Output (R-MISO) analysis

The following is an explanation of the R-MISO analysis method based on the work of Bendat (1990). An extensive class of Single Degree of Freedom (SDOF) nonlinear systems shown in Figure 2-5 are described by the following nonlinear differential equation of motion:

$$m\ddot{u}(t) + c\dot{u}(t) + ku(t) + p(u, \dot{u}, t) = F(t) \quad (2-12)$$

where;

$F(t)$ = force input

$u(t)$ = displacement output

m = system mass

c = linear viscous damping coefficient

k = linear elastic stiffness coefficient

and $p(u, \dot{u}, t)$ = general nonlinear damping-restoring term.

The linear SDOF case occurs when $p(u, \dot{u}, t) = 0$.

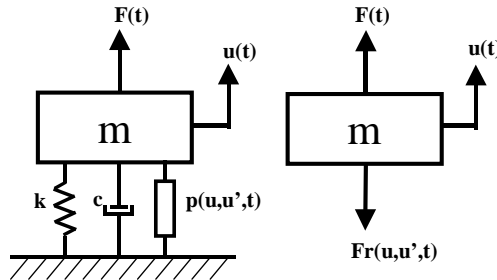


Figure 2-5 Representation of general SDOF mechanical system

The reverse MISO technique of spectral analysis makes use of a reverse dynamic nonlinear system that interchanges the input and output roles of the actual measured physical excitation and response data. The displacement output $u(t)$ is considered as a mathematical input $x(t)$ and the applied force input $F(t)$ is established as a mathematical output $y(t)$.

Through this purely mathematical manipulation the problem modelled as shown in Figure 2-6 of a Single Input-Single Output (SISO) system with feedback becomes a Reverse Multiple Input-Single Output (R-MISO) system without feedback, as illustrated in Figure 2-7.

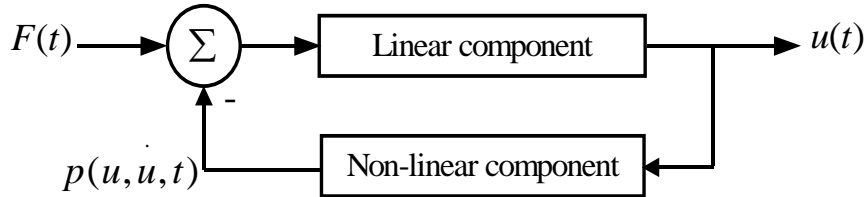


Figure 2-6 Single input-single output system with feedback

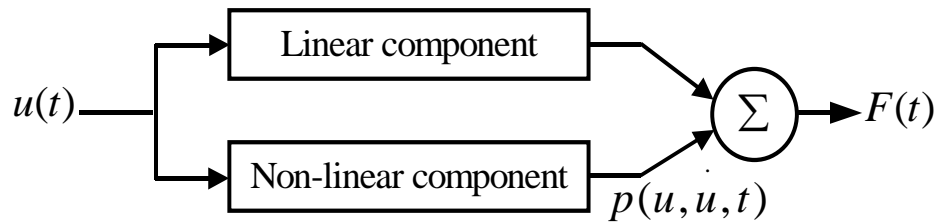


Figure 2-7 Reverse single input-single output SDOF system without feedback

The model can now be further shown as a multiple input single output SDOF linear model with correlated inputs x_1 and x_2 noise (n), see Figure 2-8.

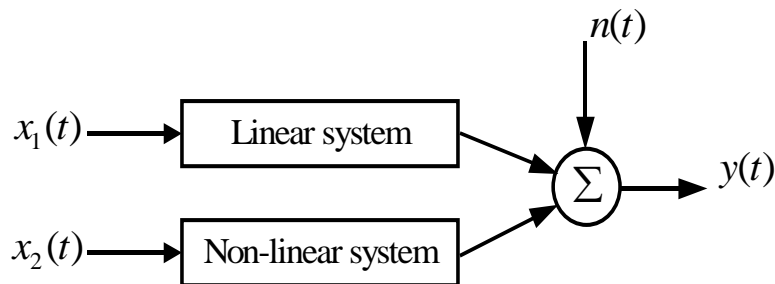


Figure 2-8 Reverse single input-single output SDOF system with correlated inputs x_1 and x_2

This mathematical manipulation changes the nonlinear differential equation of motion of the modelled problem to:

$$m\ddot{x}(t) + c\dot{x}(t) + kx(t) + p(x, \dot{x}, t) = y(t), \quad (2-13)$$

where;

$y(t)$ = force input

$x(t)$ = displacement output

m = system mass

c = linear viscous damping coefficient

k = linear elastic stiffness coefficient

and $p(x, \dot{x}, t) = p(u, \dot{u}, t)$ = general nonlinear damping-restoring term.

The linear SDOF case occurs when $p(x, \dot{x}, t) = 0$.

This general idea may be further developed to multiple inputs $x_1(t)$, $x_2(t)$, and $x_3(t)$ passing through constant parameter systems having frequency response functions A_1 and A_2 and A_3 producing the single measured response $y(t)$ with some noise $n(t)$.

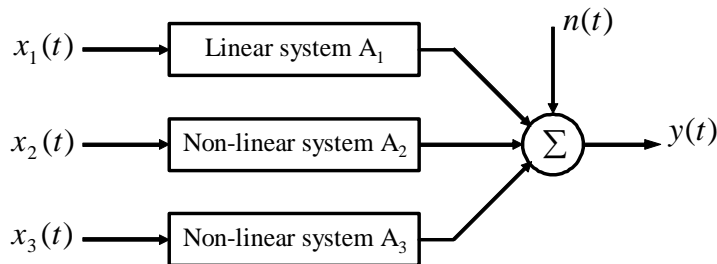


Figure 2-9 Reverse single input-single output SDOF system with correlated inputs x_1 , x_2 and x_3

Reverse analysis changes a Single Input-Single Output (SISO) system with feedback to a Multiple Input-Single Output (MISO) system without feedback. The presence of feedback requires the solution algorithm to involve iterative procedures which may lead to serious errors when it is assumed the input data $x(t)$ is Gaussian.

Without the presence of feedback, the nonlinear system may be analysed using conventional SISO approaches. It can be clearly seen from Figures 2-6 to 2-9 such mathematical reversal is a significant step towards the analysis of these nonlinear systems.

The R-MISO method shows a significant improvement in modelling accuracy and consequently much better prediction of vibrations. The method also recognizes, through the coherence functions, the contribution of each nonlinear function. The errors possible through a reliance on the linear approximation of a nonlinear system are shown in Chapter 5 through an example R-MISO analysis of several classical nonlinear equations.

2.6 Development of the Reverse Multiple Input-Single Output algorithm

Consider the Multiple Input-Single Output model in Figure 2-10, shown below. The multiple inputs to the system $x_i(t)$, with $i=1,2,\dots,q$ are held to be stationary with zero mean. The inputs are uncorrelated with the output noise output $n(t)$ also with zero mean. So that:

$$G_{x_i n}(f) = 0, \dots, i = 1, 2, \dots, q.$$

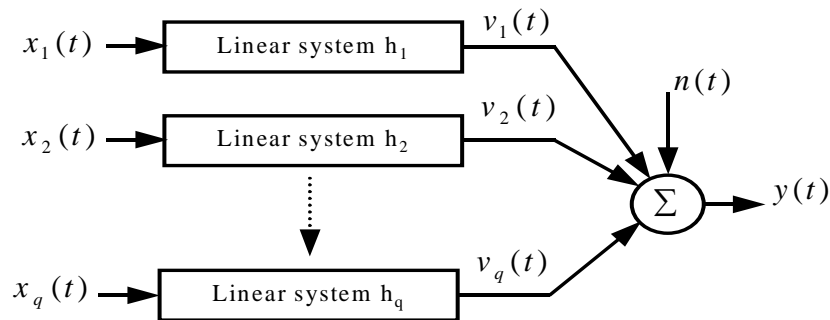


Figure 2-10 Multiple input-single output model

From the relationship $y(t) = \sum_{i=1}^q v_i(t) + n(t)$ the autospectral densities are:

$$G_{yy} = \sum_{i=1}^q \sum_{j=1}^q G_{v_i v_j} + G_{nn} \quad (2-14)$$

and

$$G_{yy} = \sum_{i=1}^q \sum_{j=1}^q H_i^* H_j G_{x_i x_j} + G_{nn} . \quad (2-15)$$

Also the cross-spectral densities are:

$$G_{x_j y} = \sum_{i=1}^q G_{x_j v_i} \quad (2-16)$$

and

$$G_{x_j y} = \sum_{j=1}^q H_j G_{x_i x_j}, j = 1, 2, \dots, q. \quad (2-17)$$

As with SISO analysis the best possible frequency response function is found by minimizing the output noise power spectral density. So by rearranging the above, the output noise power spectral density is:

$$G_{nn} = G_{yy} - \sum_{i=1}^q G_{y v_i} - \sum_{i=1}^q G_{v_i y} + \sum_{i=1}^q \sum_{j=1}^q G_{v_i v_j} \quad (2-18)$$

and

$$G_{nn} = G_{yy} - \sum_{i=1}^q H_i G_{y x_i} - \sum_{i=1}^q H_i^* G_{v_i y} + \sum_{i=1}^q \sum_{j=1}^q H_i^* H_j G_{x_i x_j} . \quad (2-19)$$

To minimize noise the derivative of G_{nn} with respect to H_k is set to zero, such

that: $\frac{\partial G_{nn}}{\partial H_k^*} = 0$

$$G_{ky} = \sum_{j=1}^q H_j G_{kj}, k = 1, 2, \dots, q \quad (2-20)$$

Expressing this in matrix form:

$$\begin{bmatrix} H_1 \\ H_2 \\ \vdots \\ H_q \end{bmatrix} = \begin{bmatrix} G_{11} & G_{12} & \dots & G_{1q} \\ G_{21} & G_{22} & \dots & G_{2q} \\ \vdots & \vdots & & \vdots \\ G_{q1} & G_{q2} & \dots & G_{qq} \end{bmatrix}^{-1} \begin{bmatrix} G_{1y} \\ G_{2y} \\ \vdots \\ G_{qy} \end{bmatrix} \quad (2-21)$$

Note, that for the best possible frequency response function, the output noise will automatically be uncorrelated with the inputs, in view of the fact that:

$$G_{kn} = 0, k = 1, 2, \dots, q.$$

For the singular case when the inputs are uncorrelated with each other,

$$G_{kj} = 0, k \neq j,$$

we have the simple relationship given by

$$H_{kk} = \frac{G_{ky}}{G_{kk}}, k = 1, 2, \dots, q.$$

This is identical to the Single Input-Single Output case, referred to as H1 in Equation (2.8).

2.7 Description of the Reverse Multiple Input-Single Output spectral decomposition algorithm

The basis of the R-MISO method begins first with the record chosen for x_1 , x_2 , and x_3 as the recorded reversed output, (now the input (x)). This is left as is, squared and cubed respectively giving x_1 as x , x_2 as x^2 , and x_3 as x^3 as shown in Figure 2-11.

These generally correlated input records are then changed using the conditioned spectral density techniques (in the frequency domain) to uncorrelated inputs.

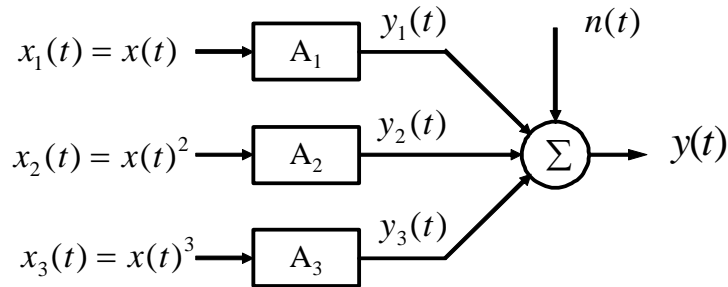


Figure 2-11 Multiple input-single output A response functions model

The generally correlated inputs are changed so that the first input x_1 is left as is, the second input x_2 becomes $x_{2:1}$ where the linear effects of x_1 are removed from x_2 and the third input x_3 becomes $x_{3:2}$ where the linear effects of x_2 and x_1 are removed from x_3 . These mutually uncorrelated input records become the inputs to the MISO model as illustrated in Figure 2-12.

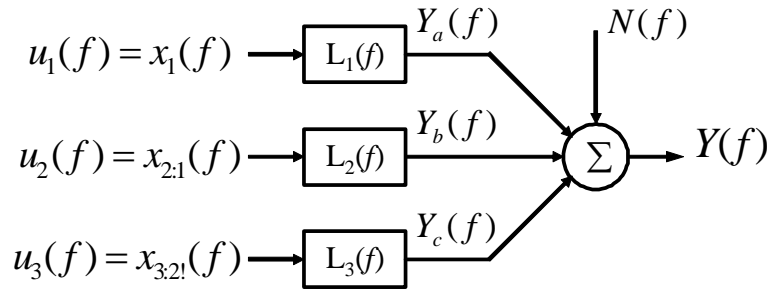


Figure 2-12 Multiple input-single output L response functions model

The noise output record $N(f)$ and the total output record $Y(f)$, are unchanged. However y_1, y_2 , and y_3 are replaced by the uncorrelated records y_a, y_b , and y_c and the three linear systems A_1, A_2 , and A_3 are replaced by three new linear systems L_1, L_2 , and L_3 . The L systems can be identified by SISO linear techniques which then give the A systems by algebraic equations.

Ordinary coherence functions can be computed giving the percentage of the total output spectral density function due to each uncorrelated input record. The coherence functions quantify the appropriateness of the chosen inputs.

For the case of the system identification problem, from the measurements of both the input and output, the object is the identification of the optimum frequency response functions A_1, A_2, A_3 etc, as shown in Figure 2-13.

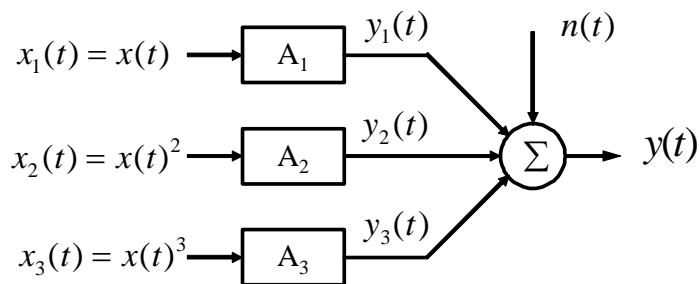


Figure 2-13 Multiple input-single output A response functions model

This example describes the case of a three input- single output nonlinear model where the inputs may be correlated as shown in Figure 2-13. The three inputs being $x_1(t) = x(t)$, with $x_2(t)$ and $x_3(t)$ the square and cubic of $x(t)$ respectively.

$$x_1(t) = x(t) \qquad x_2(t) = x^2(t) \qquad x_3(t) = x^3(t)$$

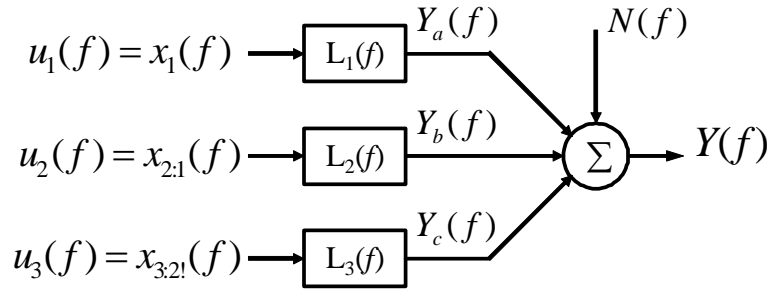


Figure 2-14 Three input-single output L response functions model

The noise output record $N(f)$ and the total output record $Y(f)$, are unchanged. However this representation is changed with x_1 , x_2 , and x_3 replaced by the uncorrelated records u_1 , u_2 , and u_3 and the three systems A_1 , A_2 , and A_3 are replaced by three new linear systems L_1 , L_2 , and L_3 , see Figure 2-14. The L systems can be identified by SISO linear techniques which then give the A systems by the following algebraic equations:

$$H_0(f) = \frac{G_{xy}(f)}{G_{xx}(f)} = L_1(f) \tag{2-22}$$

$$L_1(f) = \frac{G_{1y}(f)}{G_{11}(f)} = \frac{G_{u_1y}(f)}{G_{u_1u_1}(f)} \tag{2-23}$$

$$L_2(f) = \frac{G_{2y,1}(f)}{G_{22,1}(f)} = \frac{G_{u_2y}(f)}{G_{u_2u_2}(f)} \tag{2-24}$$

$$L_1(f) \neq A_1(f)$$

$$L_3(f) = \frac{G_{3y,2l}(f)}{G_{33,2l}(f)} = \frac{G_{u3y}(f)}{G_{u3u3}(f)} \quad (2-25)$$

$$A_3(f) = L_3(f) \quad (2-26)$$

$$A_2(f) = L_2(f) - \frac{G_{23,1}(f)}{G_{22,1}(f)} A_3(f) \quad (2-27)$$

$$A_1(f) = L_1(f) - \frac{G_{12}(f)}{G_{11}(f)} A_2(f) - \frac{G_{13}(f)}{G_{11}(f)} A_3(f) \quad (2-28)$$

These A systems are the frequency response functions for the model inputs. A_1 is the linear frequency response function estimate for the input x , A_2 is the nonlinear frequency response function estimate for the input x^2 , and A_3 is the nonlinear frequency response function estimate for the input x^3 . This continues for the number of model inputs.

2.7.1 Component and total spectral density functions

The component and total spectral density functions of the model are described in Equations (2-29 to 2-32).

$$G_{y_a y_a}(f) = |L_1(f)|^2 G_{u1u1}(f) = \gamma_{u1y}^2(f) G_{yy}(f) \quad (2-29)$$

$$G_{y_b y_b}(f) = |L_2(f)|^2 G_{u2u2}(f) = \gamma_{u2y}^2(f) G_{yy}(f) \quad (2-30)$$

$$G_{y_c y_c}(f) = |L_3(f)|^2 G_{u3u3}(f) = \gamma_{u3y}^2(f) G_{yy}(f) \quad (2-31)$$

$$G_{yy}(f) = G_{y_a y_a}(f) + G_{y_b y_b}(f) + G_{y_c y_c}(f) + G_{nn}(f) \quad (2-32)$$

The total output spectral density function being the addition of the individual output spectrums of the respective inputs and the noise autospectrum.

2.7.2 Ordinary coherence functions

The coherence function is a measure of the ‘goodness of fit’ of the model to the recorded data. It is used here, as the first ordinary coherence being the percentage of the total output spectral density function due to the first input correlated record, then the second ordinary coherence being the percentage of the total output spectral density function due to the second input correlated record. The third ordinary coherence becomes the percentage of the total output spectral density function due to the third input correlated record. The total or multiple coherence function is the sum of the ordinary coherence functions.

$$\text{First ordinary coherence function } \gamma_{u_1y}^2(f) = \frac{|G_{u_1y}(f)|^2}{G_{u_1u_1}(f)G_{yy}(f)} \quad (2-33)$$

$$\text{Second ordinary coherence function } \gamma_{u_2y}^2(f) = \frac{|G_{u_2y}(f)|^2}{G_{u_2u_2}(f)G_{yy}(f)} \quad (2-34)$$

$$\text{Third ordinary coherence function } \gamma_{u_3y}^2(f) = \frac{|G_{u_3y}(f)|^2}{G_{u_3u_3}(f)G_{yy}(f)} \quad (2-35)$$

$$\text{Multiple coherence function } \gamma_{xy}^2(f) = \gamma_{u_1y}^2(f) + \gamma_{u_2y}^2(f) + \gamma_{u_3y}^2(f) \quad (2-36)$$

The uncorrelated noise spectrum is that which is not related to the correlated inputs to the model.

$$\text{Uncorrelated noise spectrum } G_{nn}(f) = [1 - \gamma_{y:x}^2(f)]G_{yy}(f) \quad (2-37)$$

2.7.3 Cumulative coherence functions

The cumulative coherence functions are also a measure of the ‘goodness of fit’ of the model inputs to the recorded data. The first cumulative coherence being the percentage of the total output spectral density function due to the first input uncorrelated record, then the second cumulative coherence being the percentage of the total output spectral density function due to the first and second uncorrelated input records. The third cumulative coherence becomes the percentage of the total output spectral density function due to the second cumulative coherence function and the percentage of the total output spectral density function due to the third uncorrelated input record.

$$\text{First cumulative function} = \gamma_{u_1y}^2(f) \quad (2-38)$$

$$\text{Second cumulative function} = \gamma_{u_1y}^2(f) + \gamma_{u_2y}^2(f) \quad (2-39)$$

$$\text{Third cumulative function} = \gamma_{u_1y}^2(f) + \gamma_{u_2y}^2(f) + \gamma_{u_3y}^2(f) \quad (2-40)$$

2.8 The basis of the MISO technique

The Multiple Input-Single Output (MISO) technique has applications in multiple exciter frequency response analysis, excitation source identification in operating systems, estimation of path characteristics from operating data and estimation of system response. This last point is the area of interest for this work.

Consider the case of the classical *Duffing* nonlinear equation:

$$m \ddot{x} + c \dot{x} + kx + k_3 x^3 = F(t). \quad (2-41)$$

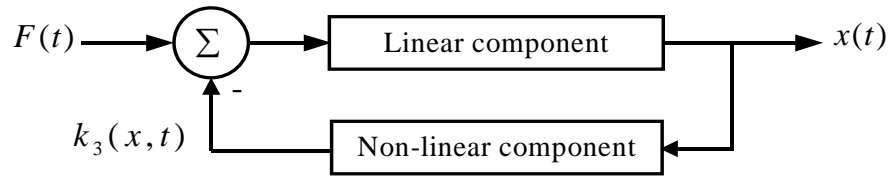


Figure 2-15 MISO model of Duffing equation

This may be analysed, in the reverse manner, as a measurable input $x(t)$ and with this input cubed passing through a constant parameter linear system having frequency response functions (H) producing the single measured response $F(t)$.

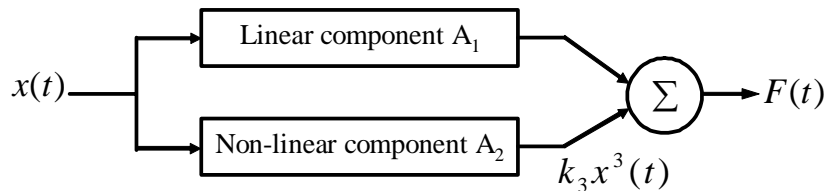


Figure 2-16 Duffing equation reverse single input-single output

This may be further developed to multiple inputs $x(t)$ and $x^3(t)$ with some noise $n(t)$ passing through constant parameter systems having frequency response functions A_1 and A_2 and A_n producing the single measured response $F(t)$.

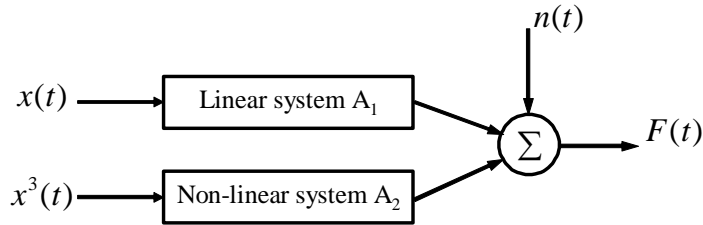


Figure 2-17 Duffing equation two inputs/single output (time domain)

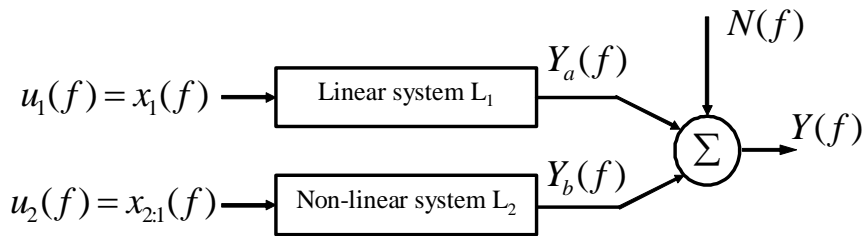


Figure 2-18 Duffing equation two inputs/single output (frequency domain)

The R-MISO method shows a significant improvement in modelling accuracy and consequently much better prediction of vibrations. The method also recognizes, through the coherence functions, the contribution of the nonlinear functions, and if there is no nonlinearity, the system will be shown as linear. Chapter 5 demonstrates by example, using classic nonlinear equations, the errors possible through reliance on the linear approximation of a nonlinear system.

Chapter 3

Hypothesis

3 Hypothesis

In the previous chapters was presented a discussion on the current approach to package cushion design and testing. The design of protective cushioning can be separated into three main categories, (a) environment, (b) product and (c) material. The cushioning material, its vibration transmission characteristics and analysis, are the focus of this research. The behaviour of the cushion material under vibration excitation is an important design consideration for the protection of the critical element.

Errors resulting from the current assumptions of linearity, and the analysis of a nonlinear system by linear analysis techniques, may be significant Bendat (1990), Parker et al (2005). It follows naturally, that a fully optimised design of protective packaging requires the thorough characterisation of the properties of the cushioning material and therefore, a designer can make the maximum use of a cushioning material.

So, the question becomes, would the description of a cushioning system with a Frequency Response Function accommodating some nonlinear effects make a difference to the resulting characterisation? Mindlin (1945), Bendat et al (1990), Parker et al (2005), have shown significant errors due to the analysis of a nonlinear system by linear analysis techniques. Additionally, would the conclusions derived from the characterisation results make a difference to the design of cushioning for a critical element? If there are errors in the analysis of the cushioning material, then the subsequent design based on these flawed results will not result in an optimum product.

Chapter 4

Methodology

4 Method

A package, during distribution is subjected to vibrations and transient events, sometimes called shocks. To optimise the design of a cushioning system to protect the product or critical element within, an accurate description of the vibration response of the cushioning material is required. This chapter describes the approach taken to analyse the response of a common cushioning material, expanded polystyrene, allowing for system nonlinearity, to random broadband excitation.

A product and cushion system may be described as a Single Degree Of Freedom (SDOF) second order dynamic system with the product as the mass and the cushioning material having stiffness and damping characteristics. The stiffness and/or damping characteristics of such a system may be nonlinear. The systems response will then exhibit nonlinear behaviour.

The definition of a nonlinear system as previously discussed states that its response to an excitation is dependant upon the frequency of excitation and the amplitude of that excitation. The excitation to such a system can be sinusoidal, or random. This leads to the idea that to closely study the response of a nonlinear system, we need to excite the system with a random broadband signal, that has a range of frequencies, to reveal through the analysis of the systems response either linear or nonlinear behaviour.

To test common cushioning materials and be able to draw meaningful conclusions, the test frequency range, and amplitude, of excitation should follow closely the expected range and amplitude of the transport environment.

The system is to be excited by random broadband white noise over the range of frequencies recommended by the standards. Band limited white noise will be used as the excitation. A flat spectrum will be used however, as ISTA 4 (appendix A) notes the spectrum may be different for the different modes of travel.

This approach will closely follow current practice with the new analysis approach giving the same results in the case of a linear system yet revealing, if any, the nonlinear characteristics of the system.

The amplitude of the excitation signal will depend on the response of the mass to the excitation. Bouncing of the mass will cause the system to behave in a nonlinear manner as when the mass is at the top of a bounce and disconnected from the base it is the characteristics of flight in a gravitational field that are being recorded not the characteristics of the cushioning material.

The cushioning material is subjected to a compressive test and the compression curve recorded. This compression curve was developed via software into a cushion curve for the particular material (Sek, 2001). A mass is chosen to suit the cushion curve with the natural frequency of the package model related to the stiffness of the cushioning material. This then leads to the determination of the frequency range of interest being from 3-100 Hz. ASTM 4728 suggests for truck transport 1-100 Hz, a rail car a frequency range of 1-100 Hz, and for aircraft 1-200 Hz.

The ASTM standard approach, sine dwell excitation test, results in a excitation/response transmissibility plot. This two dimensional plot implicitly assumes a linear system, such that doubling the magnitude of the excitation would simply result in the doubling of the response and that if the excitation were to involve multiple excitations the response would be equal to the sum of the responses caused by each individual excitation. A linear system's transmissibility, by definition, is dependant on the frequency of the excitation only so this approach would suffice. However, in cases where nonlinearity is present in a system, the response of the system to an excitation will be dependent on both the frequency and amplitude of the excitation, with the response of a system excited at a certain frequency involving contributions from other frequencies.

Constant amplitude excitation is the standard testing approach, however in testing a nonlinear system the response may have contributions from other frequencies and be the result of the system operating within a different region of the nonlinearity. Constant response magnitude, in other words varying the level of the input excitation such that the response remains approximately constant, is one method of ensuring a pseudo linear response of a nonlinear system.

The drawbacks of the sine dwell test are the length of time such a test can take and that the vibration response may not accurately reflect the real world transportation environment. For this we need to consider broadband excitation. Broadband excitation encompasses noise, impulse etc. White noise or more correctly band-limited white noise, limited to suit the transportation environment, does by its nature contain multiple frequencies and is a faster method of vibration testing.

The following approach has been formulated in response to the questions raised in the hypothesis:

- Develop a computer based implementation of the R-MISO algorithm
- Validate and test the computer implementation
- Select a common cushioning material and investigate its vibration transmissibility using R-MISO.

The aim is to develop an analysis approach superior to current standard practices yet understandable by current definitions, that will attempt to reveal the, if any, nonlinear characteristics of a cushioning system.

4.1 Equipment overview

The following chapter explains the processes and the equipment used in the generation of the experimental data.

4.1.1 Equipment requirements

The equipment necessary is first described in terms of overall requirement and then in the specifics of the machines used.

This work is on the vibration response of various cushioning materials and so a vibration source or shaker is required. The shaker should be programmable to allow for different excitation frequencies and amplitudes. The cushion material's vibration transmissibility is to be studied, so an experimental rig is needed to facilitate the recording of response of a mass resting on the cushion material. The rig should restrain, with minimum friction, the resulting motion to vertical only. This will allow the use of accelerometers on both the shaker platen and the mass. The excitation to the system and the response of the mass are to be recorded simultaneously so a suitable data capture and storage arrangement is required with the flexibility to select various data capture rates. These data are then processed and analysed before producing a graphical representation of the outcome.

4.1.2 Equipment used

An electro-magnetic shaker was used as the excitation source, Vibration Test Systems model 500, the particulars of which are in appendix B. A computer equipped with a vibration controller and Signal Calc® software was used to drive the electro-magnetic shaker with a feedback loop to ensure the appropriate response to the drive signal. A specially designed test frame with a central guide rod and Teflon slide guide was used to hold the variable mass and restrain the vibration to vertical motion only.

Accelerometers were used to record the acceleration of the shaker platen and that of the mass. A computer running HP VEE® software was used as the data capture and record device. The data capture specifics are listed in Table 4-1.

Table 4-1 Data capture and analysis details

Excitation type	BLWN
frequency range	3 – 100 Hz
RMS	0.25g / 0.40g
sampling frequency f	1024 Hz
fft size	4096
Δt	4 s
Δf	0.25 Hz
Individual record length T	500 s
number of distinct averages N_{d1}	125
number of distinct averages N_{d2}	250
number of distinct averages N_{d3}	500
number of distinct averages N_{d4}	1125

The data records were processed using four (4) sets of distinct averages (N_d), this was to observe the change in the estimate of natural frequency and coherence, if any, over longer averaging.

4.1.3 Layout of equipment

The equipment arrangement is shown in Figure 4-1. The excitation signal generator controls the shaker. The sample is on the shaker platen and a guided mass rests on the sample. The Teflon slide guide allows the mass to vibrate vertically. An accelerometer attached to the shaker platen monitors the excitation signal and an accelerometer attached to the guide monitors the response signal. These signals are amplified and then recorded simultaneously before the data acquisition computer saves both to a data file.

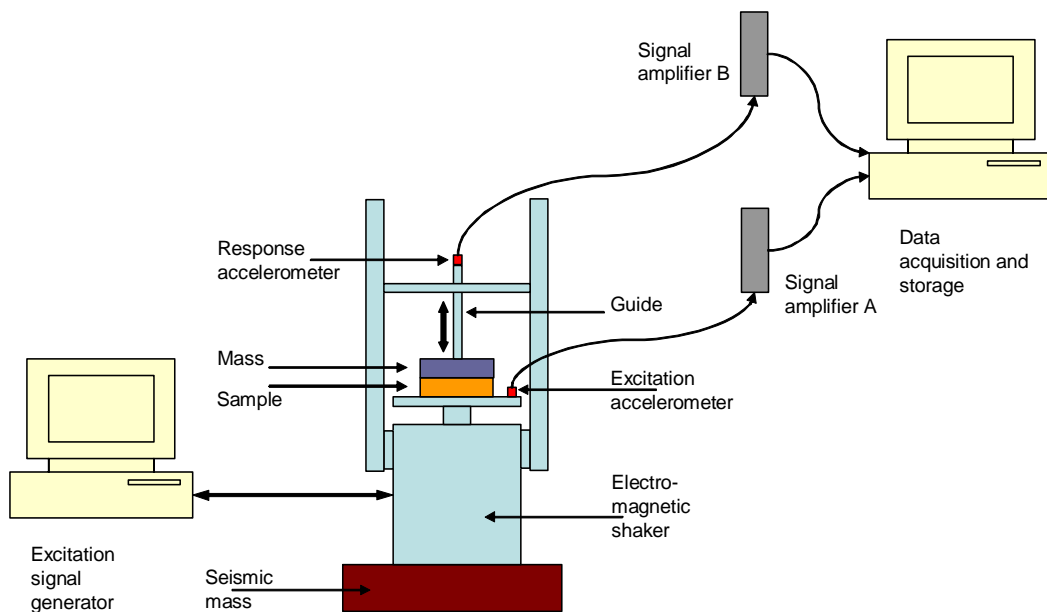
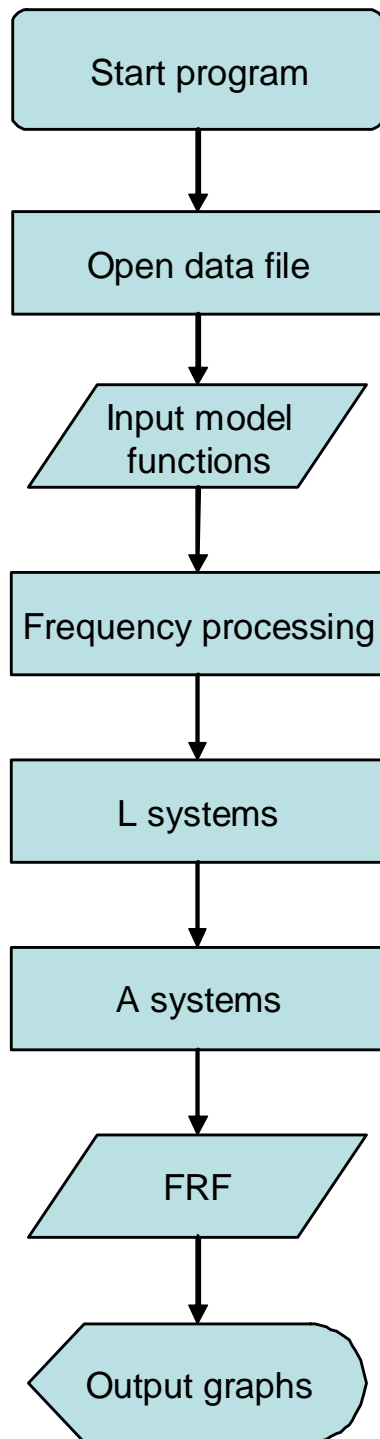


Figure 4-1 Schematic of experimental setup

4.2 Computer based implementation of the R-MISO algorithm



The data file containing the simultaneously recorded excitation and response accelerations is opened and separated into input and output files.

The functions chosen as inputs are entered and the process performed on the reversed response output, now the input to the model.

The frequency domain process, Fast Fourier Transform is applied with windowing and averaging, to all the records.

The result are the correlated L systems as described earlier and then through further manipulations the A system frequency response function estimates.

The recovered Frequency Response Function estimates are then devolved and prepared for plotting.

The output is twofold; one, the graphical representation of the Frequency Response Function estimates and, two, the Frequency Response Functions as a description of the material model.

Figure 4-2 Flowchart of analysis program

4.3 Validation and testing of the RMISO computer implementation

The use of R-MISO analysis in the study of the characteristics of packaging materials is relatively new. Some previous work has been done (Parker et al, 2005) showing the possible significance of the materials nonlinear behaviour on its vibration transmissibility. However, before the computer implementation of the R-MISO algorithm can be relied upon to analyse experimental data, a reasonable level of confidence in the software results is required.

The computer implementation of the R-MISO algorithm was tested on simulated excitation and response data. The simulations modeled known linear and nonlinear equations and were analysed using the R-MISO computer implementation to confirm the program results. Although the parameter recovery feature will not be used in the case of experimental acceleration transmissibility, the recovery of the simulated, and thus known, system parameters, in the case of force excitation and displacement response, was a clearer validation of the accuracy of the technique. The Duffing, Van der Pol and combined Duffing-Van der Pol nonlinear equations were analysed using the R-MISO computer implementation.

The results and discussion of the computer implementation of the R-MISO algorithm are shown in Chapter 5.

4.4 Package cushion system

Section (2.8) discussed modelling the typical package cushion arrangement as a single degree of freedom dynamic system. This model is used in the following experiments. A cushion curve was generated for each material and a static load determined (Sek, 2001). Table 4-2 lists the mass and material used in the experiments and analysis.

Table 4-2 Material and load, experiment details

Material	Grade	Density (kg/m ³)	Mass (kg)	Sample dimensions (mm)
EPS	S	13.5	5.2	80x80x30
EPS	SL	14.0	5.2	80x80x30
EPS	H	24.5	4.4	80x80x30
EPS	L	13.0	4.4	80x80x30
EPS	VH	27.0	4.4	80x80x30
EPS	X	35.0	6.4	80x80x30

Expanded polystyrene, a common cushioning material, of varying densities will be studied. The experimental variables are:

- The excitation type, band limited white noise has been chosen
- The frequency range, 3Hz to 100 Hz has been chosen
- The levels of excitation are, 0.25g RMS and 0.40g RMS
- The size of the sample, 80x80x30mm, to suit the experimental rig
- The mass, chosen to suit a stress level relevant to the material from the materials cushion curve.

The cushioning material was compressed to 65% strain, until it exhibited hardening, i.e. the compression graph started to asymptote.

The material was compressed at 1, 50, 100, 200 mm/s and it was seen the effect of strain rate quickly saturates at 50 mm/s, 100 mm/s, this is an interesting feature; however for the analysis of vibration transmissibility we are only interested in the confirmation of nonlinear behaviour.

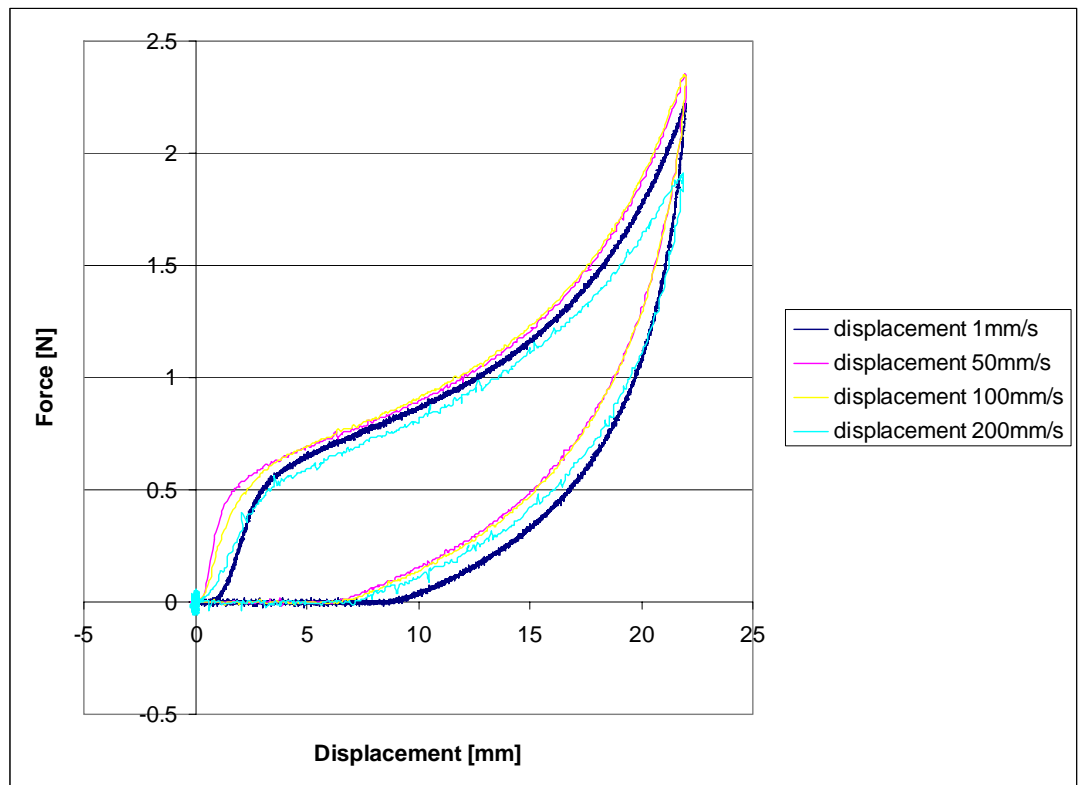


Figure 4-3 Compression plot of eps grade sl at various displacement speeds

The compression curve in figure 4-4 reveals the nonlinear behaviour of the material. It can be seen that the stiffness of the material is linear over a very small range of deflection (1.5-3 mm). A assumption that the system is linear would be misleading. The cushion mass system will be nonlinear as the mass and cushion are not physically connected. A prime example is bouncing of the mass.

Further compression plots and the cushion curves are shown in appendix C.

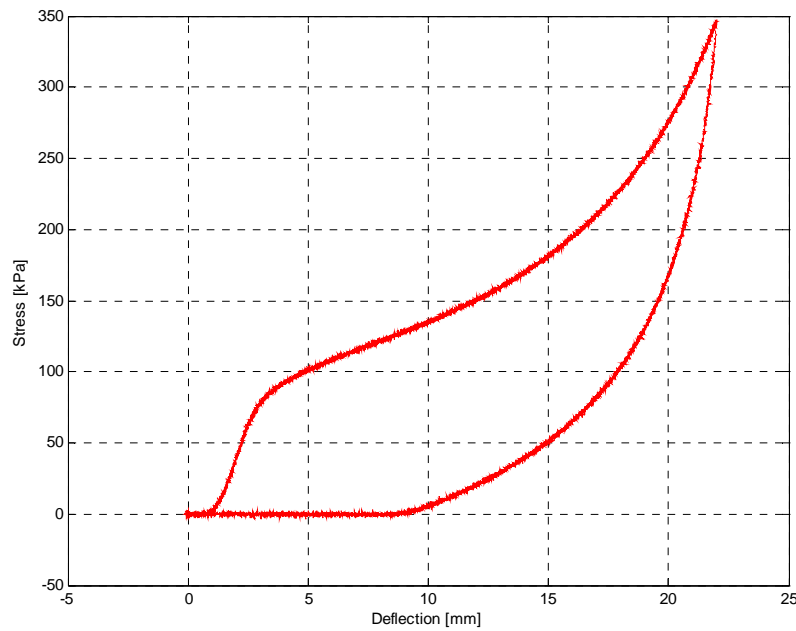


Figure 4-4 Raw compression plot of eps grade s

Figure 4-5 shows the developed cushion curve (Sek, 2001) for expanded polystyrene grade s. The upper line signifies a drop height of 100cm and the lower line a drop height of 50cm. Shown on the graph are the initial estimates of natural frequency, stiffness and the estimated mass for the vibration experiments.

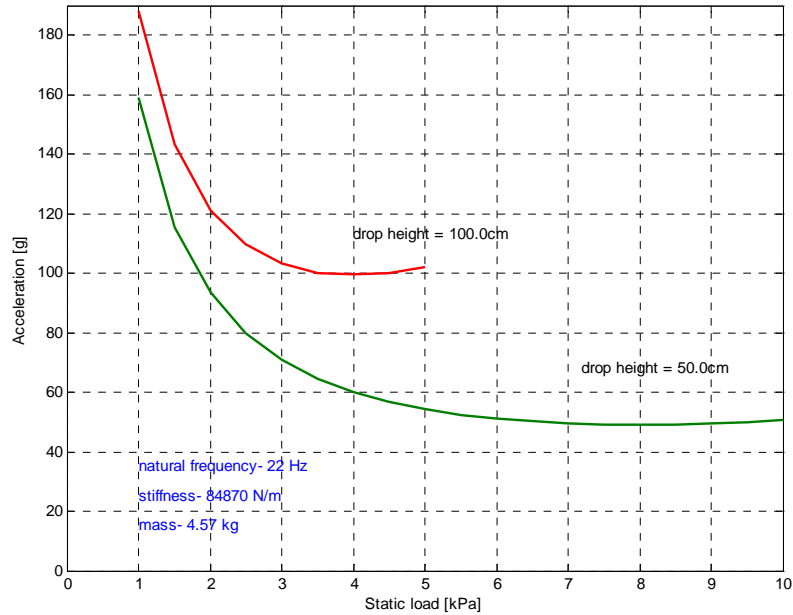


Figure 4-5 Cushion curve for eps grade s

Chapter 5

Results

5 R-MISO Analysis

This chapter discusses the R-MISO algorithm validation, and the verification of the analysis program results for nonlinear equations with a known nonlinearity. The program was written in Matlab®, based on the Reverse Multiple Input-Single Output algorithm, to analyse the excitation and response signals of the expanded polystyrene packaging material. The Matlab® program was verified by the analysis of a simulated nonlinear Single Degree Of Freedom (SDOF) dynamic system based on the Duffing and Van-der Pol classical nonlinear equations.

A linear SDOF system was first analysed as a control using both the linear Single Input-Single Output (SISO) analysis method and the R-MISO technique. The results, of the analysis of the control nonlinear equations, show very strong agreement with previous work by Bendat, 1993.

A SDOF linear system was analysed first, then the Duffing nonlinear equation which has the addition of a nonlinear stiffness component (k_3u^3), then, the classic Van-der Pol nonlinear equation which has the addition of a nonlinear damping component ($c_3 u.u^2$). Finally, the combined Duffing-Van-der Pol nonlinear equation, which has the addition of the nonlinear stiffness and nonlinear damping components (k_3 and c_3) was analysed. These were analysed and assessed by both the SISO and R-MISO methods.

The values used in the digital data post processing and the simulation of the SDOF linear system, Duffing system, and the Van-der Pol and combined Duffing-Van der Pol nonlinear equations are listed in Table 5-1 Simulated system parameters, and Table 5-2 Digital post processing parameters.

Table 5-1 Simulated system parameters

Mass (kg)	$m = 1.0$
Linear damping coefficient	$c = 3.77$
Linear stiffness coefficient	$k = 355.3$
Duffing nonlinear constant	$k_3 = 2 \times 10^7$
Van-der Pol nonlinear constant	$c_3 = 2 \times 10^6$
Natural frequency (Hz)	$f_n = (1/2\pi)\sqrt{k/m} = 3.0\text{Hz}$
Damping ratio	$\zeta = c/(2\sqrt{km}) = 0.10$
Excitation	BLWN 0.1 Hz – 50Hz

Table 5-2 Digital post processing parameters

$\Delta t =$	0.02 sec
$N =$	512 samples
$T = N\Delta t =$	10.24 sec
$n_d =$	16
$N_{total} = n_d N =$	8,192
$T_{total} = n_d T =$	163.84 sec
$f_c = \text{Nyquist cutoff frequency} = 1/2\Delta t =$	25 Hz
$\Delta f = \text{bandwidth resolution} = 1/T =$	0.097 Hz

5.1 Example 1: Single Degree Of Freedom (SDOF) linear system

Consider the case of the following linear equation:

$$m \ddot{x} + c \dot{x} + kx = F(t) \tag{5-1}$$

This is a linear system with a forcing function $F(t)$ as the excitation. This may be analysed as a Single Input-Single Output (SISO) system. This example system has no nonlinear components. In R-MISO analysis the measurable output $x(t)$, now the reversed input, is the input to the model. This input passes through, a constant parameter linear system frequency response function called (A_1) resulting in the system producing the single measured reversed force response $y(t)$.

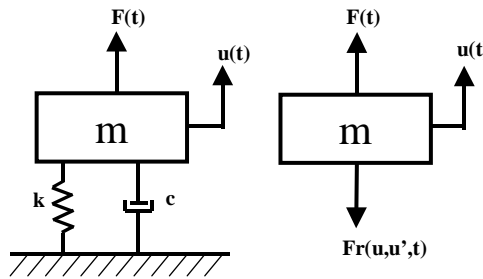


Figure 5-1 SDOF linear system

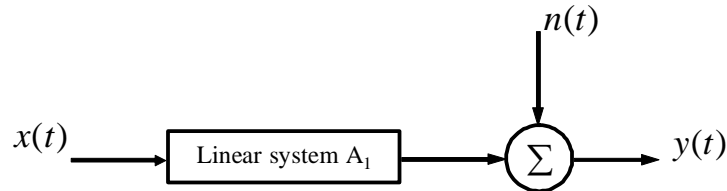


Figure 5-2 SDOF linear system model

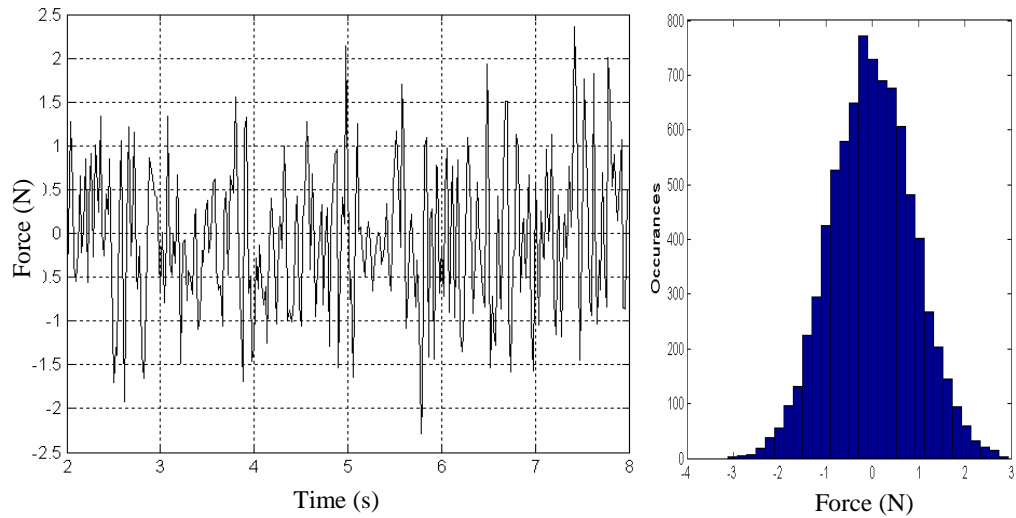


Figure 5-3 Force excitation time segment and histogram

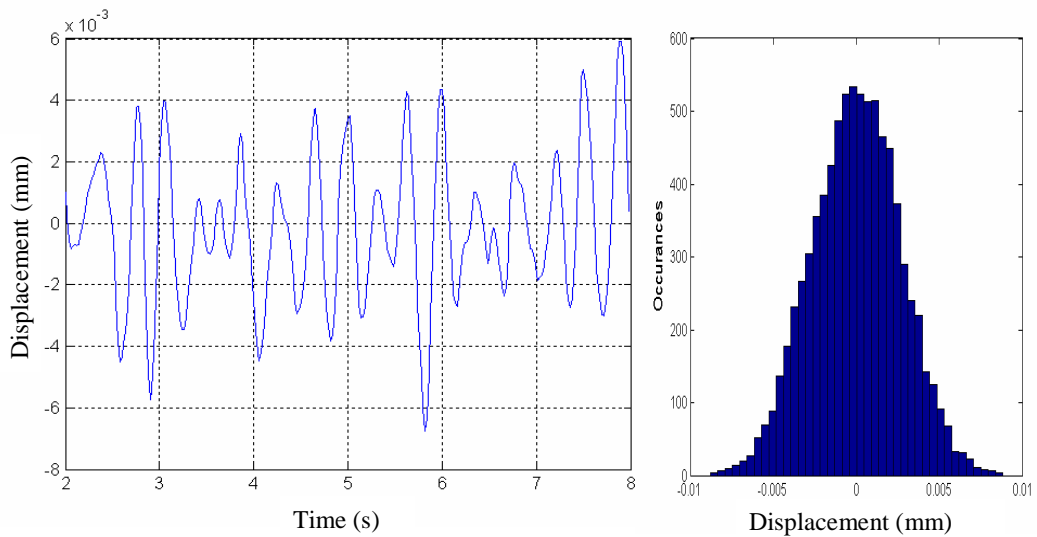


Figure 5-4 Displacement response time segment and histogram

Figures 5-3 to 5-6 relate to the analysis of the linear single degree of freedom dynamic system. Figure 5-3 is a time history segment of the simulated force excitation and histogram of the excitation showing the close to Gaussian distribution of the input. Figure 5-4 shows the corresponding time history segment of the simulated displacement response and histogram of the response showing the close to Gaussian distribution of the output of the simulation model.

Figure 5-5 is the SISO and R-MISO linear frequency response function estimates with the recovered parameters of natural frequency and stiffness. The recovered values compare very well with the simulated system parameters in Table 5-1.

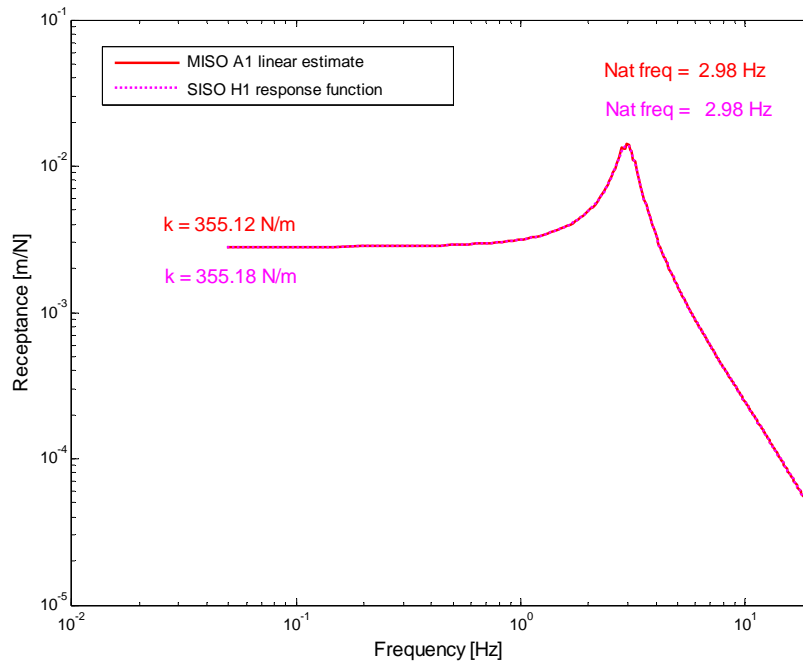


Figure 5-5 FRF estimate for SDOF system showing recovered system values

Figure 5-6 is the coherence plot of the simulation model showing very good coherence. These graphs confirm the R-MISO analysis approaches ability to analyse a linear system.

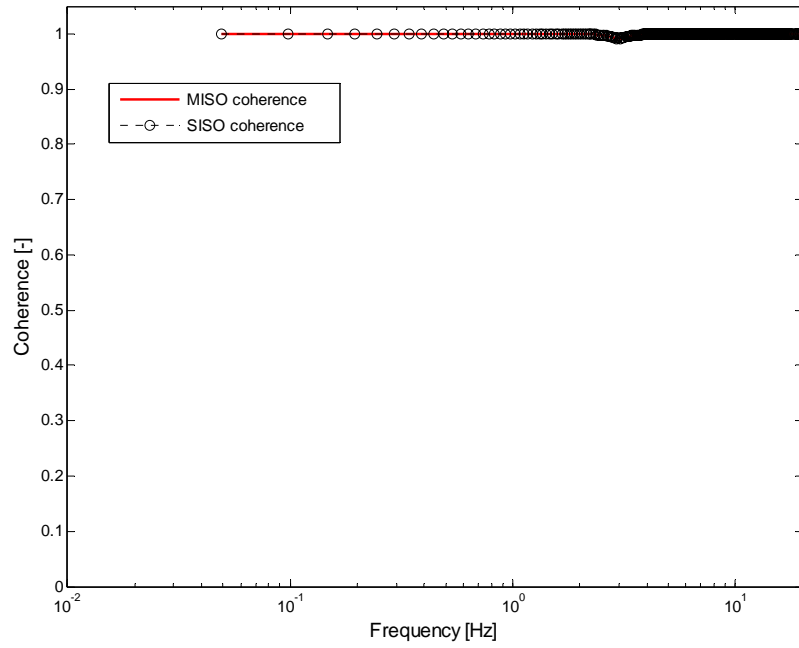


Figure 5-6 Coherence result for SDOF system

5.2 Example 2: Duffing nonlinear equation

Consider now the case of the classical Duffing nonlinear equation with nonlinear stiffness k_3x^3 :

$$m \ddot{x} + c \dot{x} + kx + k_3x^3 = F(t) \quad (5-2)$$

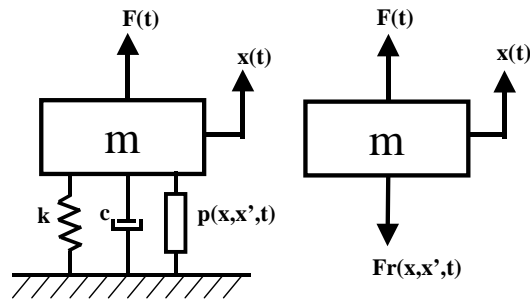


Figure 5-7 Duffing equation nonlinear model

This system may be analysed as a reverse two input/single output nonlinear system. The measurable output $x(t)$, reversed now as the input, is the first input and is also used, cubed, as the second input to the model. These two inputs pass through, a constant parameter linear system and a constant parameter nonlinear system respectively, having frequency response functions (A_1 and A_2). The system with the two inputs, producing the single measured, reversed force, response $F(t)$, Figure 5-9.

The results shown here are for the Duffing nonlinear equation SISO and R-MISO analysis. From the simulations of force input and displacement output, the estimates of the linear and nonlinear frequency response functions (A_1 and A_2) are computed. An estimate of the system parameters, natural frequency, stiffness and the nonlinear coefficient, may also be recovered by the R-MISO method these show very close agreement with the simulation values used.

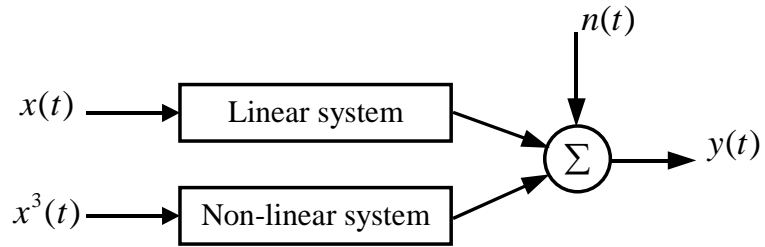


Figure 5-8 Duffing two inputs/single output R-MISO model

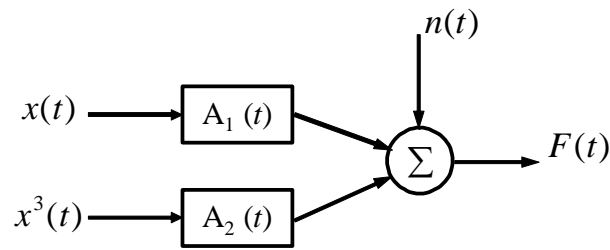


Figure 5-9 Duffing system correlated inputs

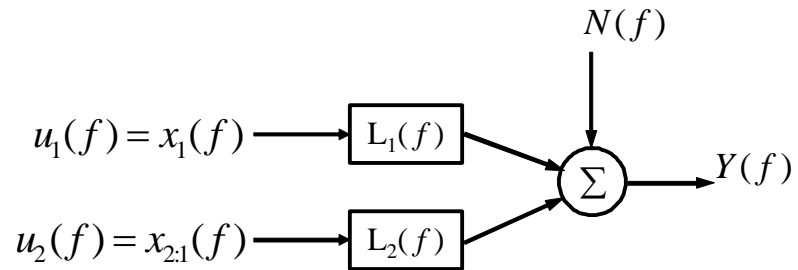


Figure 5-10 Duffing system uncorrelated inputs

Figures 5-11 and 5-12 show the time history segment and histogram for the force excitation and displacement response. Note the slight deviation of the displacement response histogram from a Gaussian distribution. This shows that the system is nonlinear however; this histogram plot would not be a reliable signifier of nonlinearity.

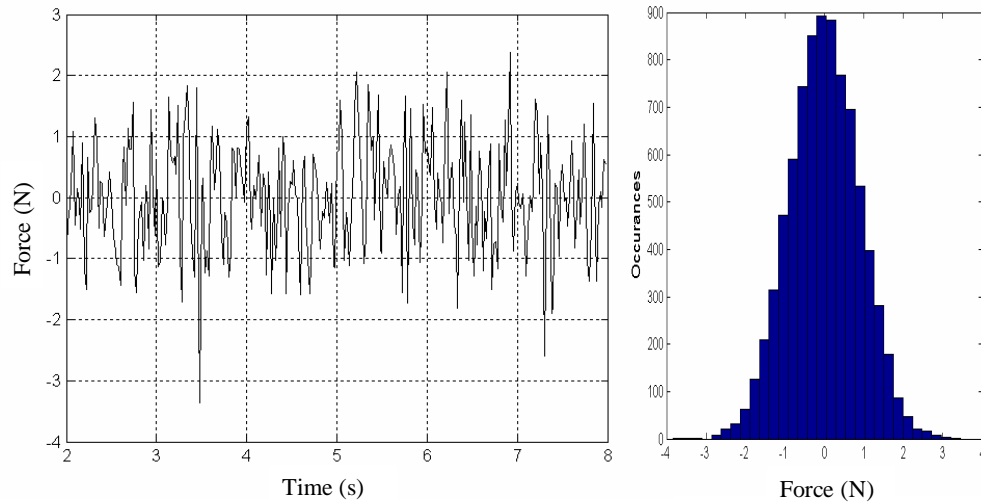


Figure 5-11 Force excitation and histogram for the Duffing nonlinear system

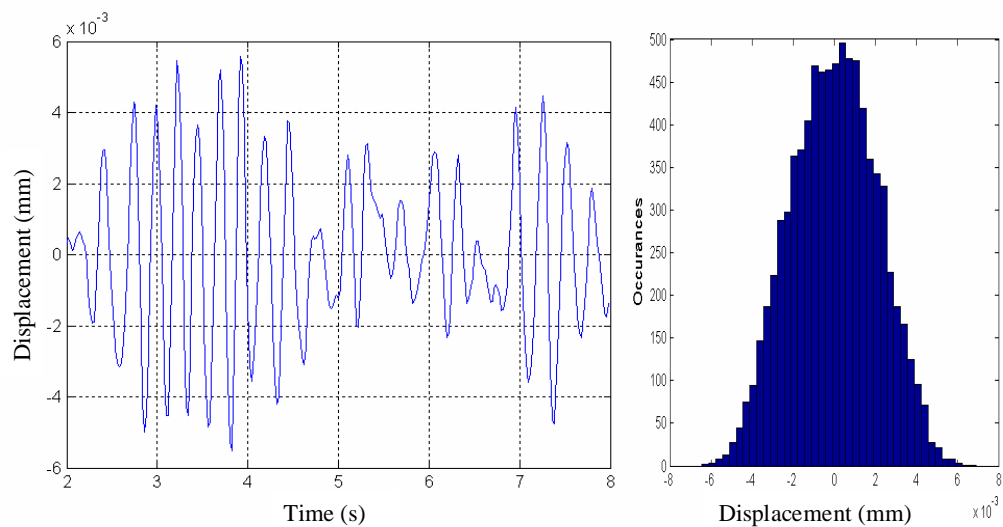


Figure 5-12 Displacement response and histogram for the Duffing nonlinear system

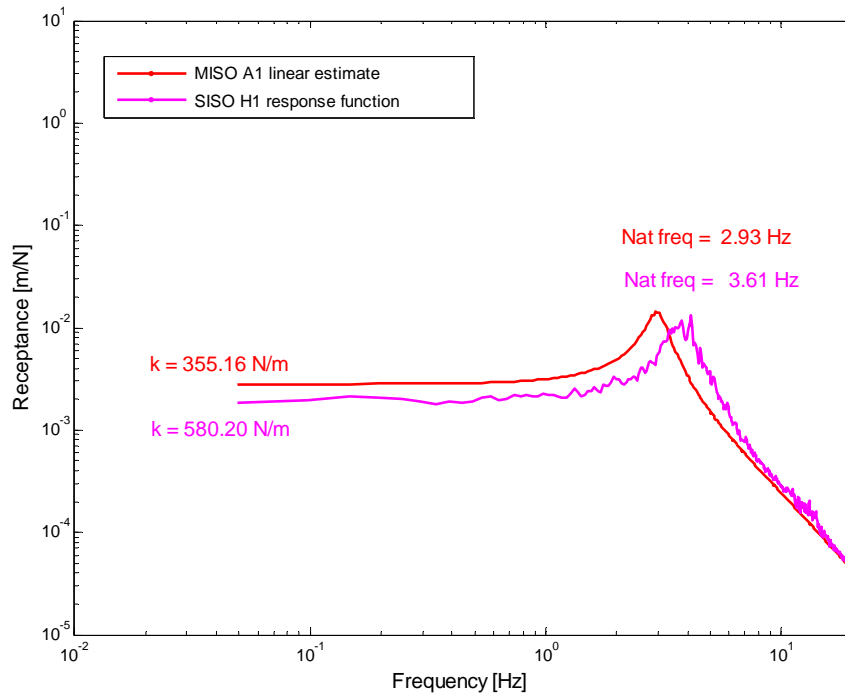


Figure 5-13 FRF estimate for a Duffing system, showing recovered parameter values

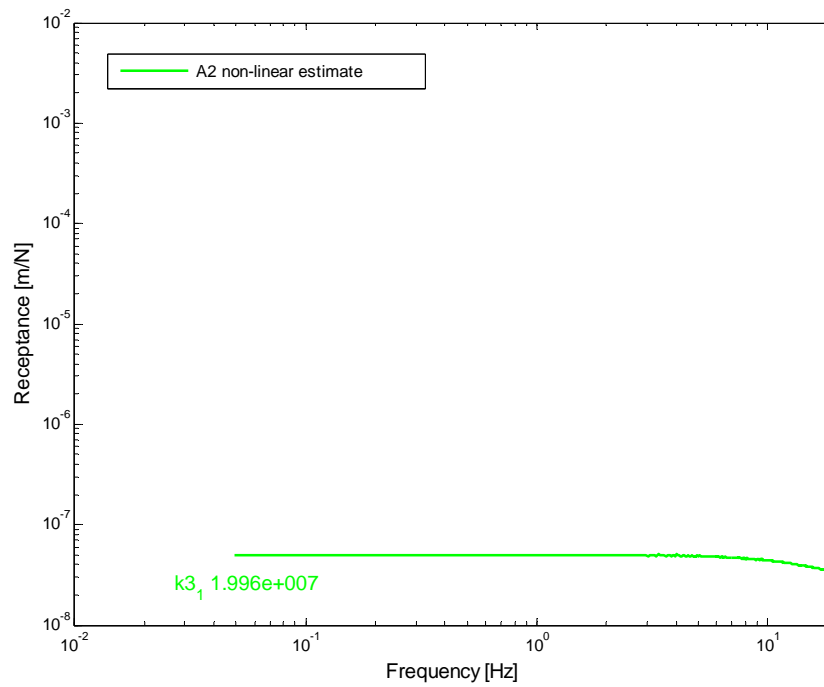


Figure 5-14 Nonlinear FRF for a Duffing system showing recovered parameter value

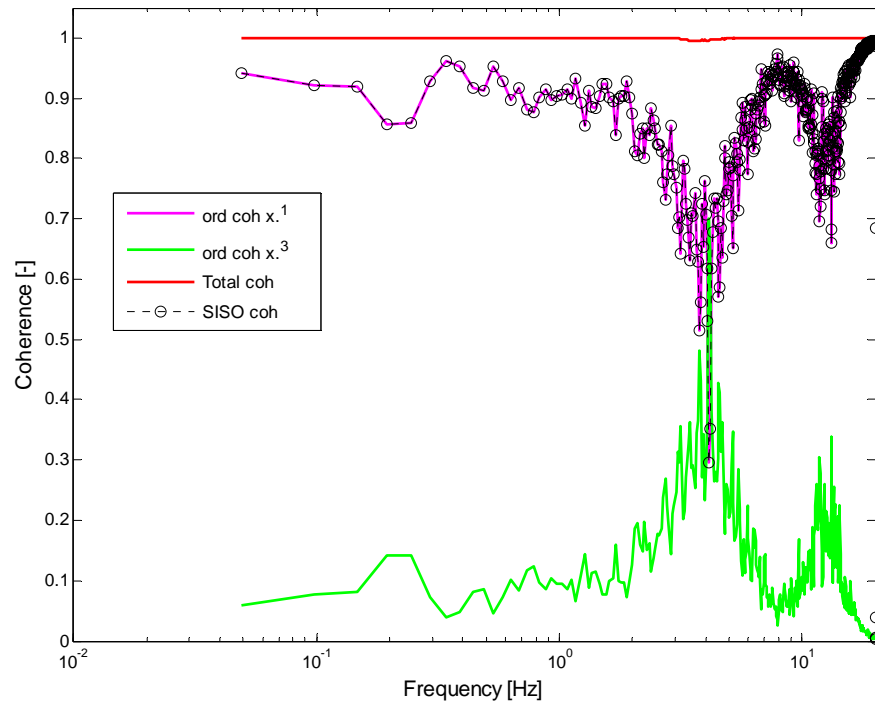


Figure 5-15 Coherence plot analysis result for a Duffing system

Figure 5-13 shows the Linear Frequency Response Function estimates as recovered by the R-MISO and conventional SISO analysis methods. Figure 5-14 shows the nonlinear Frequency Response Function estimate and Figure 5-15 shows the coherence plot for the model analysis. Figures 5-13 and 5-14 should be read together as they show the same frequency base. Using the standard spectral analysis parameter recovery approach, the natural frequency and stiffness values for both the R-MISO and conventional SISO analysis methods are shown. This clearly demonstrates the errors possible when using a linear analysis of a nonlinear system.

5.3 Example 3: Van-der Pol nonlinear equation

Consider now the case of the classical Van der Pol nonlinear equation with nonlinear damping c_3x^2 :

$$m \ddot{x} + c \dot{x} + kx + c_3 x^2 \dot{x} = F(t) \quad (5-3)$$

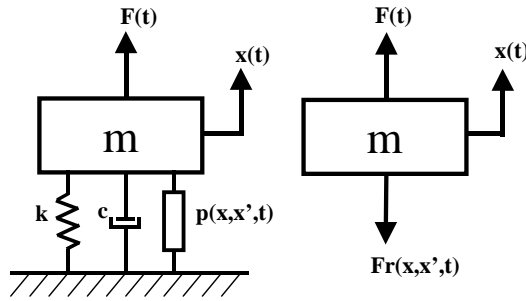


Figure 5-16 Van der Pol nonlinear equation model

This system may be analysed as a reverse two input single output nonlinear system. The measurable output $x(t)$, reversed now as the input, is the first input and is also used, cubed, as the second input to the model. These two inputs pass through, a constant parameter linear system and a constant parameter nonlinear system respectively, having frequency response functions (A_1 and A_2). The system with the two inputs, producing the single measured, reversed force, response $F(t)$ see Figure 5-17.

The results are shown here are for the R-MISO analysis of the Van der Pol nonlinear equation. From the simulations of force input and displacement output, the estimates of the linear and nonlinear frequency response functions (A_1 and A_2) are computed. An estimate of the system parameters, natural frequency, stiffness and the nonlinear coefficient, may also be recovered by the R-MISO method these show very close agreement with the simulation values used.

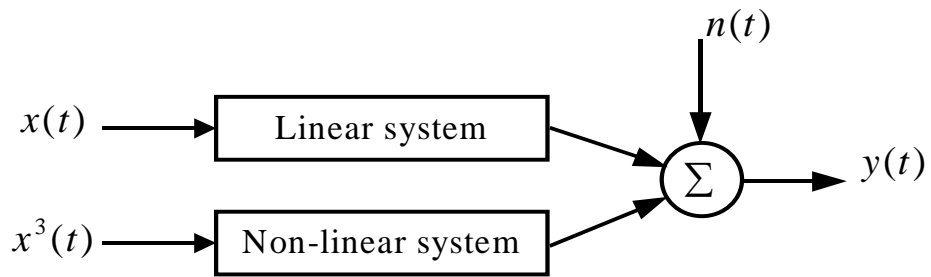


Figure 5-17 Van der Pol two inputs/single output R-MISO model

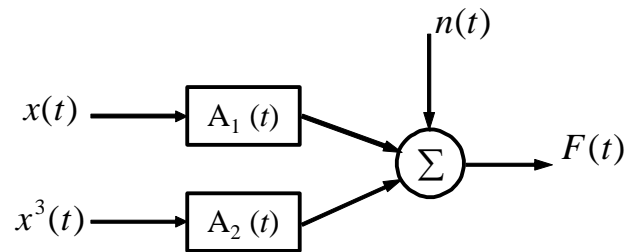


Figure 5-18 Van der Pol system with correlated inputs

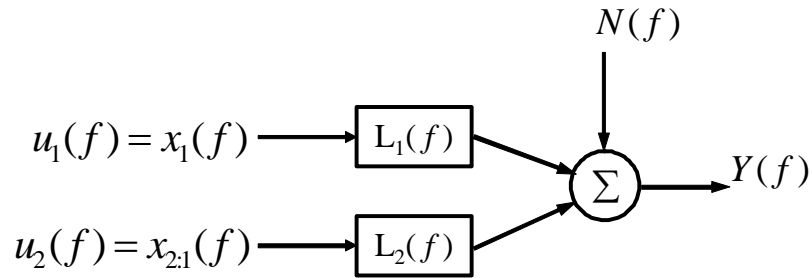


Figure 5-19 Van der Pol system with uncorrelated inputs

Figures 5-20 to 5-21 show a time history segment of the force excitation and histogram and corresponding time history segment and histogram of the displacement response. Note the significant distortion from a Gaussian distribution of the response histogram. This again, clearly demonstrates the errors possible when using a linear analysis of a nonlinear system.

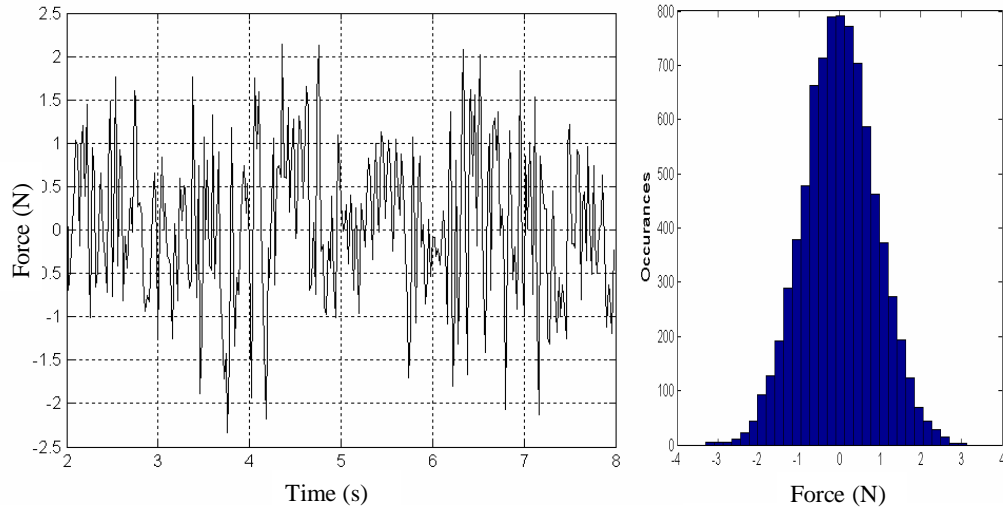


Figure 5-20 Force excitation and histogram for the Van der Pol nonlinear system

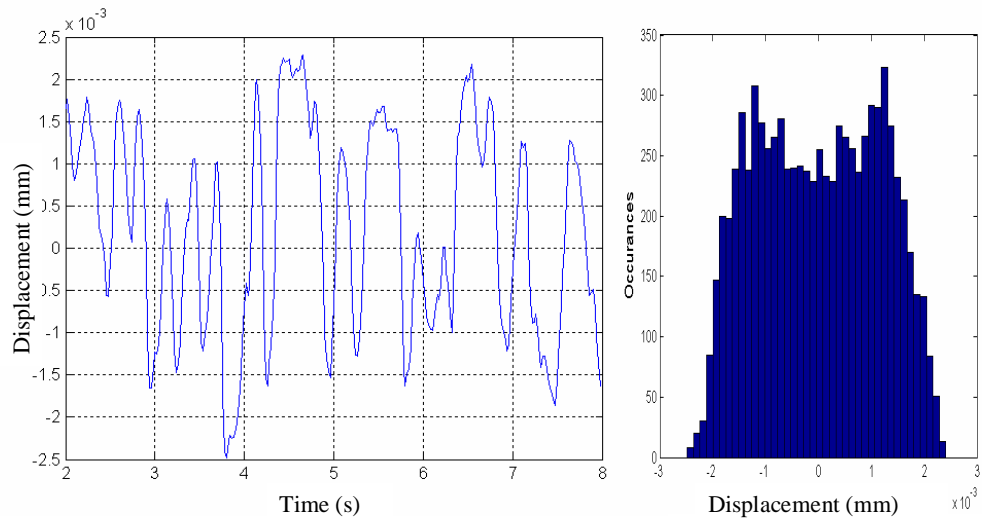


Figure 5-21 Displacement response and histogram for the Van der Pol nonlinear system

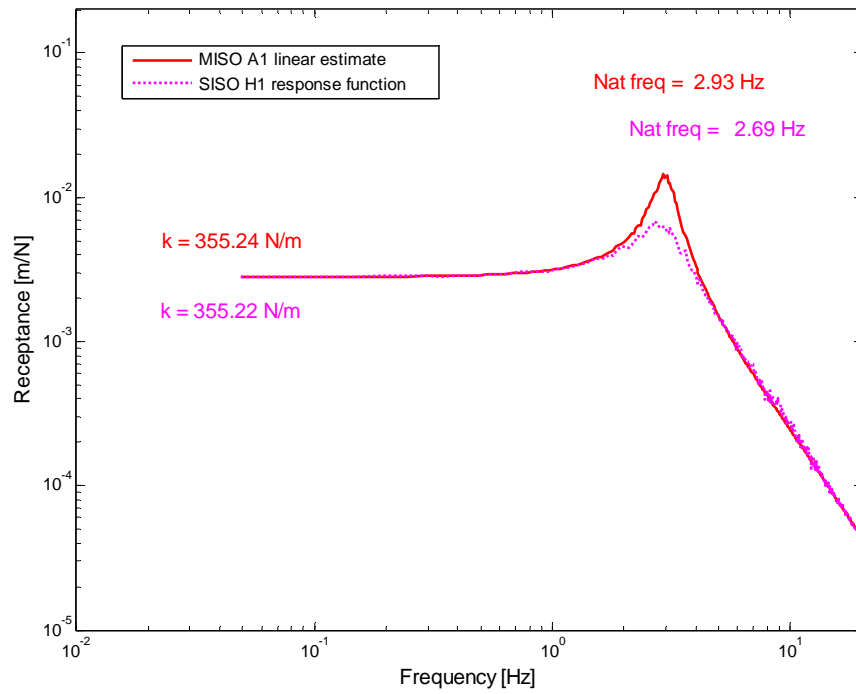


Figure 5-22 FRF estimate result for a Van der Pol system showing recovered parameter values

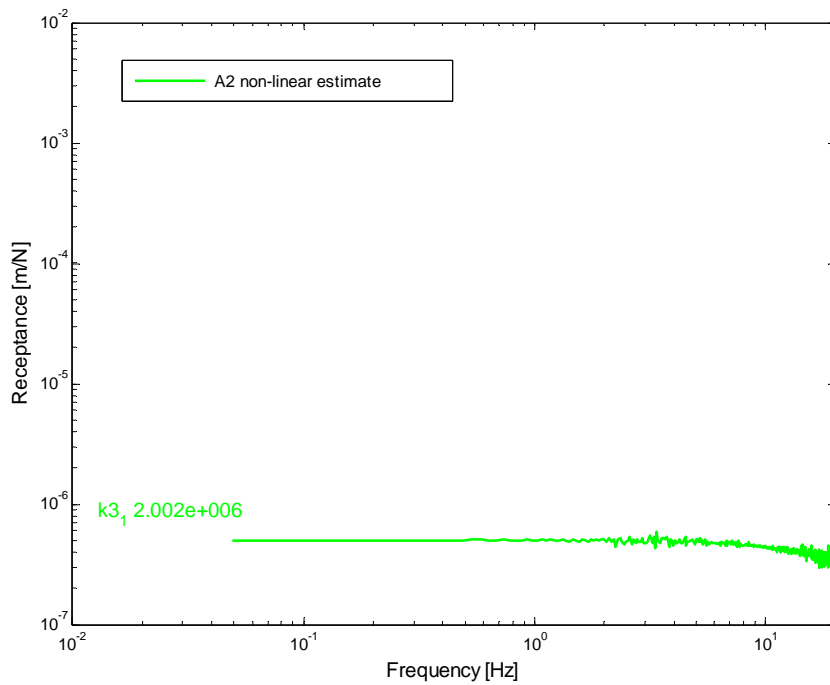


Figure 5-23 Nonlinear FRF estimate for a Van der Pol system showing recovered parameter values

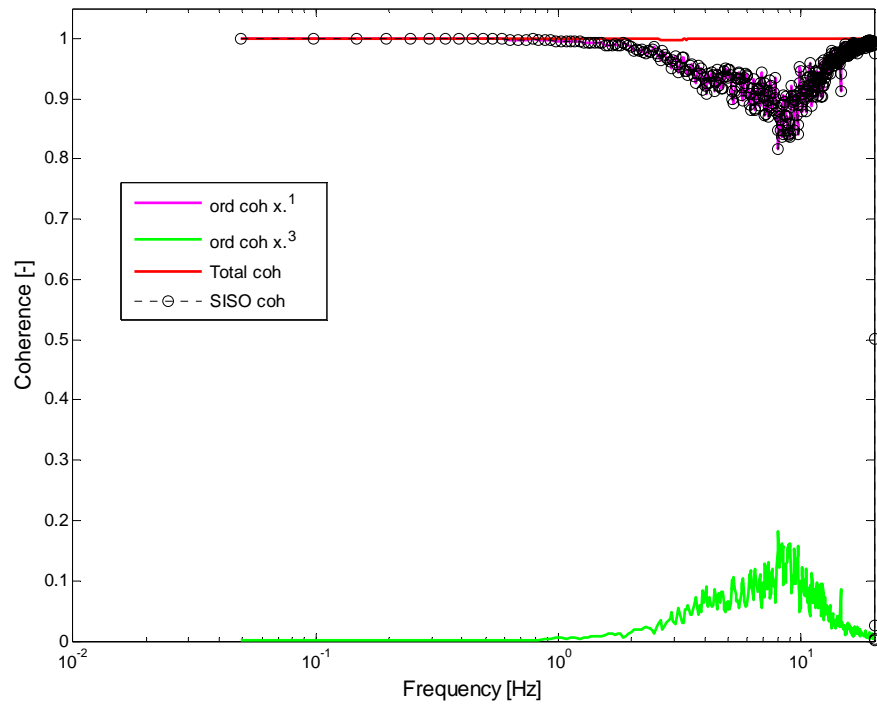


Figure 5-24 Coherence for the Van der Pol nonlinear system

Figure 5-22 shows the Linear Frequency Response Function estimates as recovered by the R-MISO and conventional SISO analysis methods. Figure 5-23 shows the nonlinear Frequency Response Function estimate and Figure 5-24 shows the coherence plot for the model analysis. Using standard spectral analysis parameter recovery, the natural frequency and stiffness values for both the R-MISO and conventional SISO analysis methods are shown. Note the difference in the recovered estimates of natural frequency. However, the recovery of the stiffness coefficient is very good for both methods. Table 5-1 lists the system parameters used in the simulation.

5.4 Example 4: Combined Duffing-Van-der Pol nonlinear equation

Consider now the case of the combined Duffing-Van der Pol nonlinear equation with both, nonlinear stiffness and nonlinear damping:

$$m \ddot{x} + c \dot{x} + kx + c_3 x^2 \dot{x} + kx^3 = F(t) \quad (5-4)$$

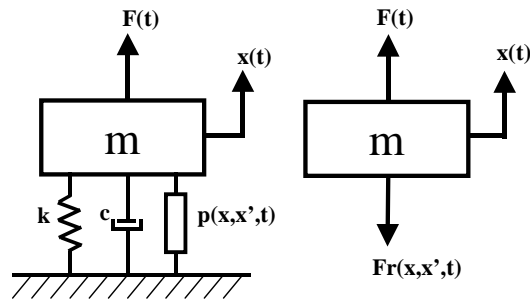


Figure 5-25 Combined Duffing-Van der Pol nonlinear equation model

This system may also be analysed as a reverse two input/single output nonlinear system. The measurable output $x(t)$, reversed and now the input, is the first input and is also used, cubed, as the second input to the model. These two inputs pass through, a constant parameter linear system and a constant parameter nonlinear system respectively, having frequency response functions (A_1 and A_2). The system with the two inputs, producing the single measured, reversed force, response $F(t)$ see Figure 5-26.

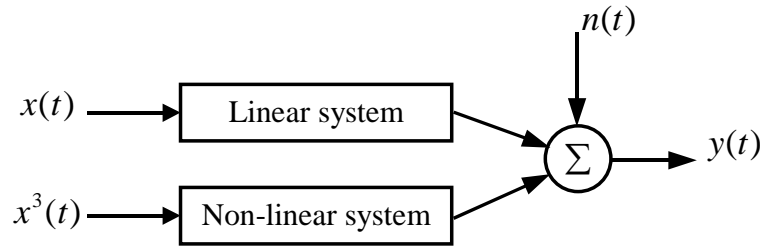


Figure 5-26 Combined Duffing-Van der Pol two inputs/single output R-MISO model

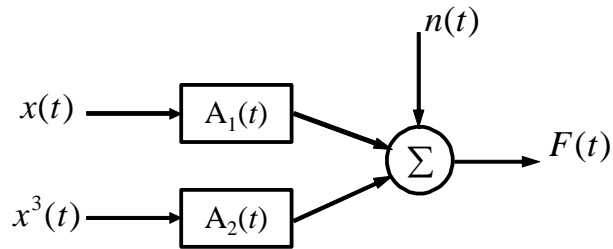


Figure 5-27 Combined Duffing-Van der Pol system correlated inputs

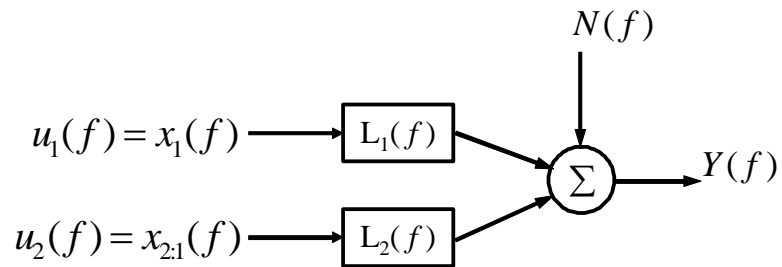


Figure 5-28 Combined Duffing-Van der Pol system uncorrelated inputs

Figures 5-29 to 5-30 show a time history segment of the force excitation and histogram and corresponding time history segment and histogram of the displacement response. Note the significant distortion from a Gaussian distribution of the response histogram. This again, clearly demonstrates the errors possible in this case of linear analysis of a nonlinear system.

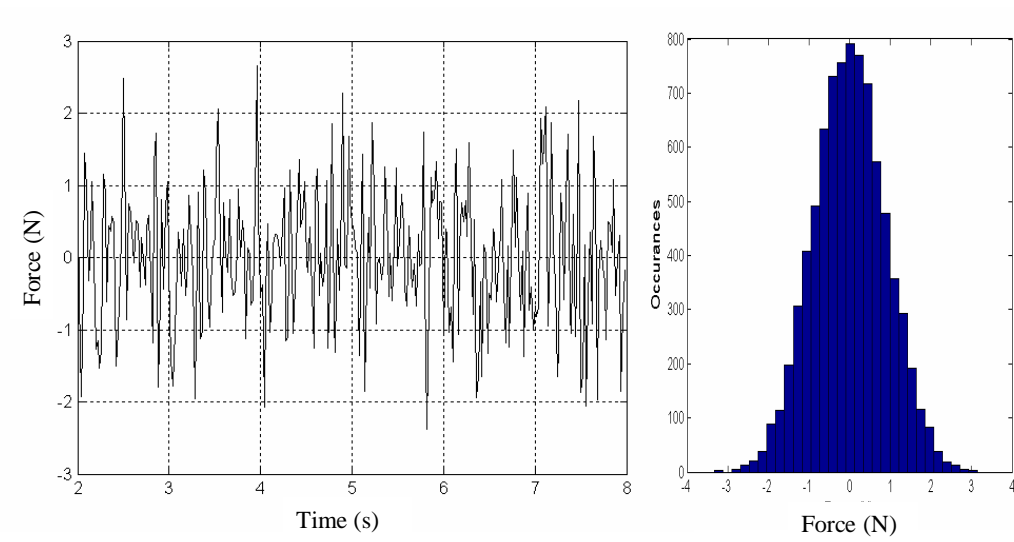


Figure 5-29 Force excitation and histogram for the combined Duffing Van der Pol nonlinear equation

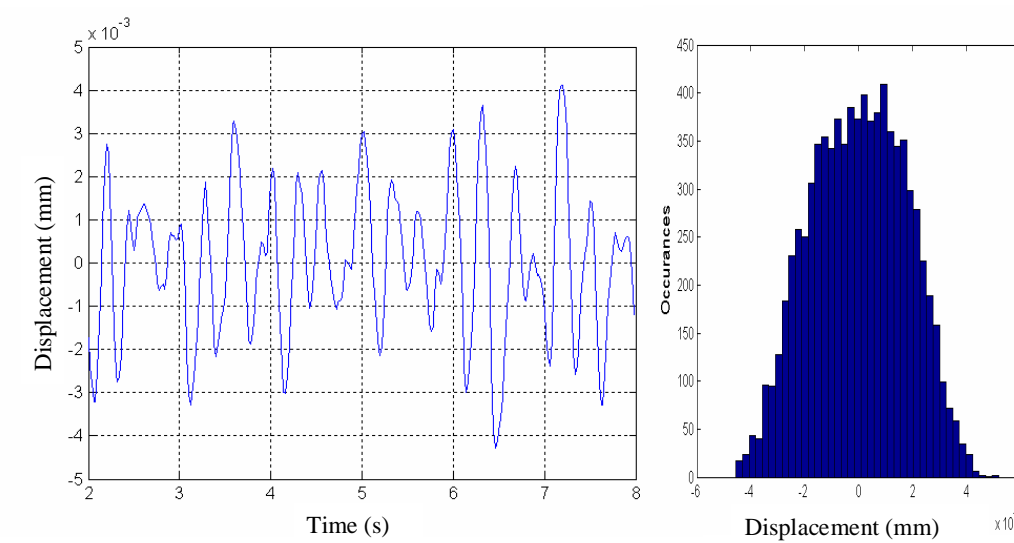


Figure 5-30 Displacement response and histogram for the combined Duffing Van der Pol nonlinear equation

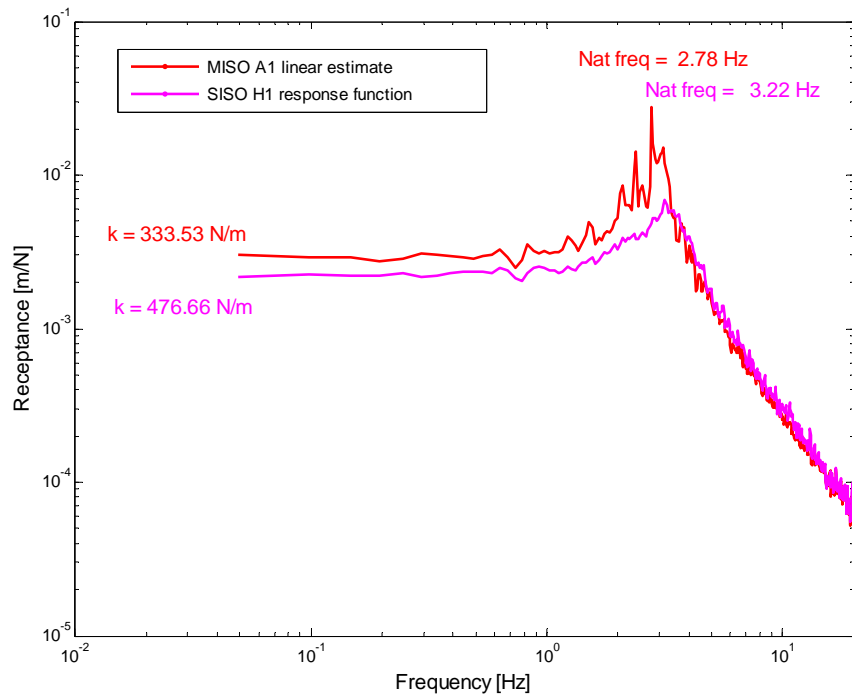


Figure 5-31 FRF estimate for a combined Duffing-Van der Pol system showing recovered parameter values

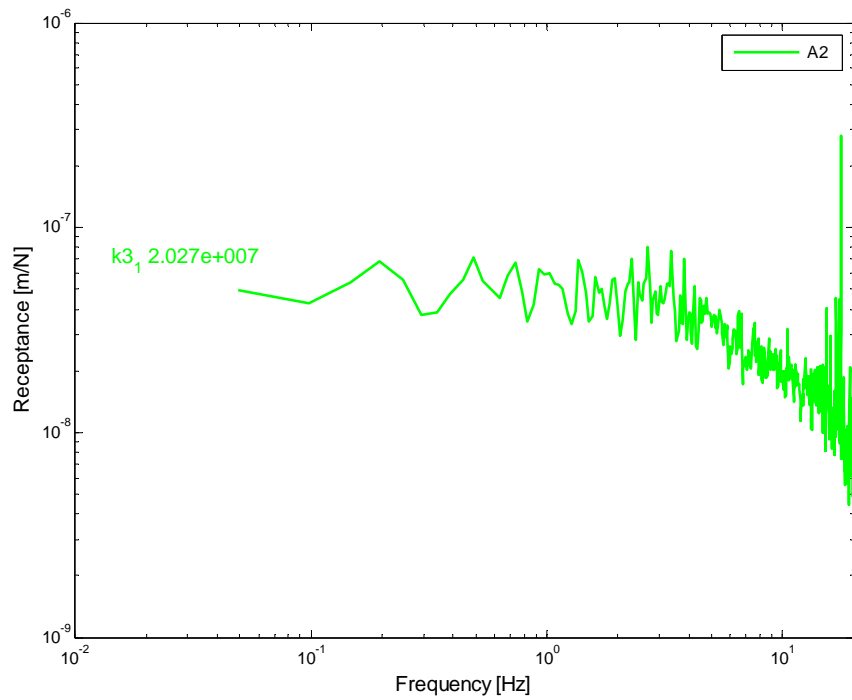


Figure 5-32 Nonlinear FRF for a combined Duffing-Van der Pol system showing recovered parameter values

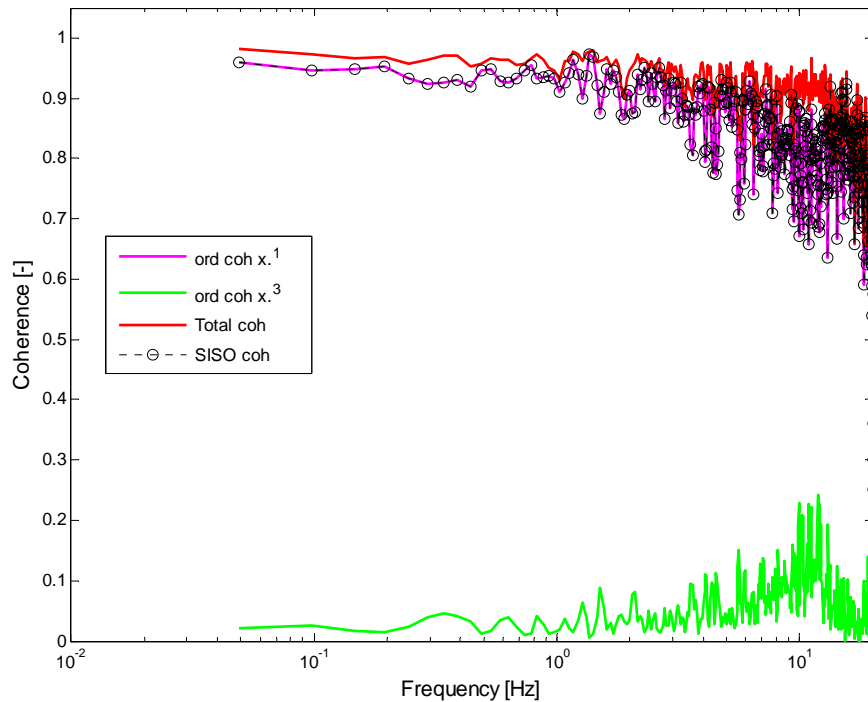


Figure 5-33 Coherence for the combined Duffing-Van der Pol nonlinear system

Figure 5-31 shows the Linear Frequency Response Function as recovered by the R-MISO and conventional SISO analysis methods. Figure 5-32 shows the nonlinear Frequency Response Function estimate and Figure 5-33 shows the coherence plot for the model analysis. Using standard spectral analysis parameter recovery techniques, the natural frequency and stiffness values for both the R-MISO and conventional SISO analysis methods are shown. Note the difference in the recovered estimates of natural frequency and the stiffness coefficient. Table 5-1 lists the system parameters used in the simulation.

The R-MISO analysis of the simulated SDOF linear, Duffing and Van der Pol dynamic systems has clearly demonstrated the ability of the software implementation to separate the linear and nonlinear FRF estimates. And in this case of force excitation and displacement response recoup, through standard spectral analysis parameter recovery techniques, the system parameters. The R-MISO approach has also shown the significant difference in the linear FRF estimates when analysing a nonlinear system by linear means.

5.5 Introduction to results

The previous sub sections have demonstrated the ability of the software implementation to reveal the linear and nonlinear estimates of a simulated nonlinear system. The following sections will discuss the results of the R-MISO vibration transmissibility analysis experiments on expanded polystyrene.

Table 5-3 lists the materials, excitation they were subjected to, and the number of distinct averages used for comparison in the analysis.

Table 5-3 Material excitation and averaging table

cushion material	excitation	number of averages
EPS grade S	BLWN	125, 250, 500, 1125
EPS grade SL	BLWN	125, 250, 500, 1125
EPS grade X	BLWN	125, 250, 500, 1125
EPS grade L	BLWN	125, 250, 500, 1125
EPS grade VH	BLWN	125, 250, 500, 1125
EPS grade H	BLWN	125, 250, 500, 1125

The material expanded polystyrene (EPS) grade S and grade SL will be described fully as being typical of the experimental results.

5.5.1 Results for EPS grade S

The following are the results of the R-MISO analysis of the expanded polystyrene material grade S. The sample was, as previously discussed, excited by band limited white noise at an RMS of 0.25g and 0.40g. The excitation and response data was analysed using the R-MISO software tool and the following results plotted:

- Figure 5-34 and 5-40 R-MISO linear estimate and SISO transmissibility FRF plot
- Figure 5-35 and 5-41 R-MISO nonlinear estimate FRF plot
- Figure 5-36 and 5-42 Total coherence plots

- Figure 5-37(left) and 5-43(left) A time domain segment of the excitation signal
- Figure 5-37(right) and 5-43(right) Normalised histogram of the excitation signal
- Figure 5-38(left) and 5-44(left) A time domain segment of the response signal
- Figure 5-38(right) and 5-44(right) Normalised histogram of the response signal
- Figure 5-39 and 5-45 Auto-spectrum of the excitation signal

The following graphs show the analysis results for a two input dynamic system model. The two inputs (a) response x , and (b) response $x * \text{abs}(x)$ pass through a constant parameter linear system and a constant parameter nonlinear system respectively, having frequency response functions (A_1 and A_2). The system with the two inputs, producing the single measured, reversed input, response $y(t)$, The first set of results are at 0.25g RMS excitation and the second set at 0.40g RMS excitation and are after 1125 distinct averages. They show the improvement of the R-MISO model incorporating a nonlinear term over the SISO linear assumption model.

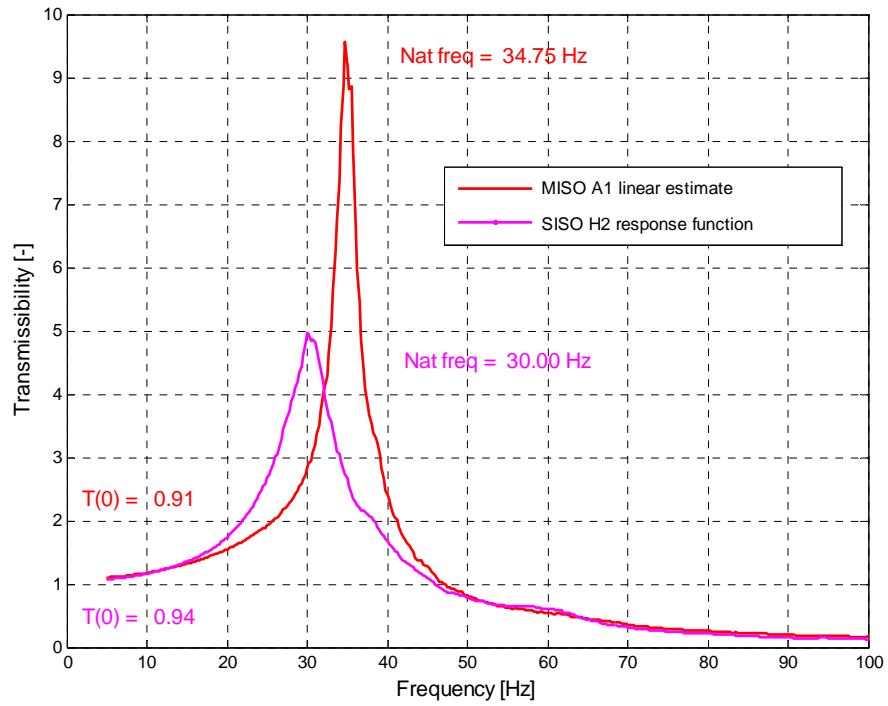


Figure 5-34 FRF estimate for eps grade s @ 0.25g RMS

Figure 5-34 shows the R-MISO linear frequency response function estimate and the SISO frequency response function estimate. Also shown are the peak frequency estimates. The difference between the R-MISO and SISO, transmissibility magnitude and peak frequency, can be clearly seen.

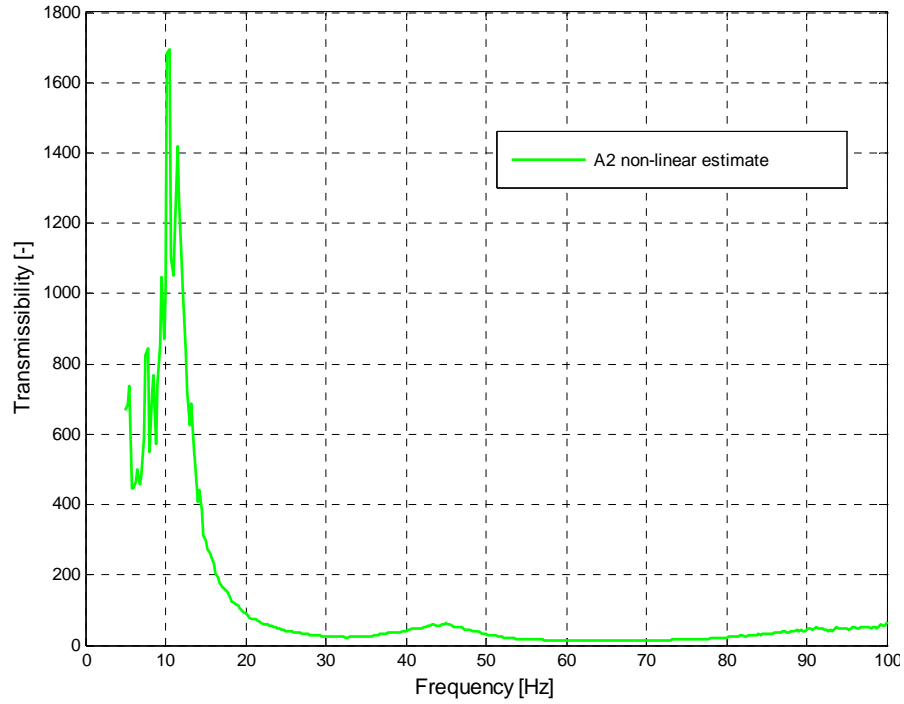


Figure 5-35 Nonlinear FRF estimate for eps grade s @ 0.25g RMS

Figure 5-35 shows the R-MISO nonlinear frequency response estimate for the second input $(b)-(x*\text{abs}(x))$. This is the magnitude plot of the nonlinear component of the system model and shows the contribution of the second term over the frequency range.

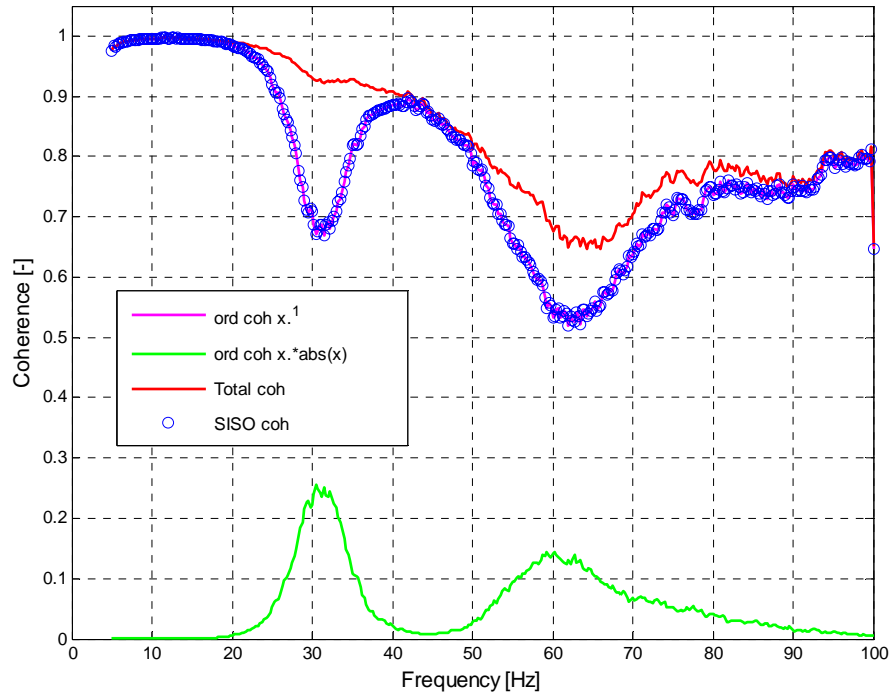


Figure 5-36 Coherence plot for eps grade s @ 0.25g RMS

Figure 5-36 shows the R-MISO, ordinary and total coherence, and the SISO coherence for the system model. The contribution of the nonlinear term can be clearly seen. Note the particular improvement of the coherence in the region near the peak frequency and the continuous improvement in coherence at higher frequencies.

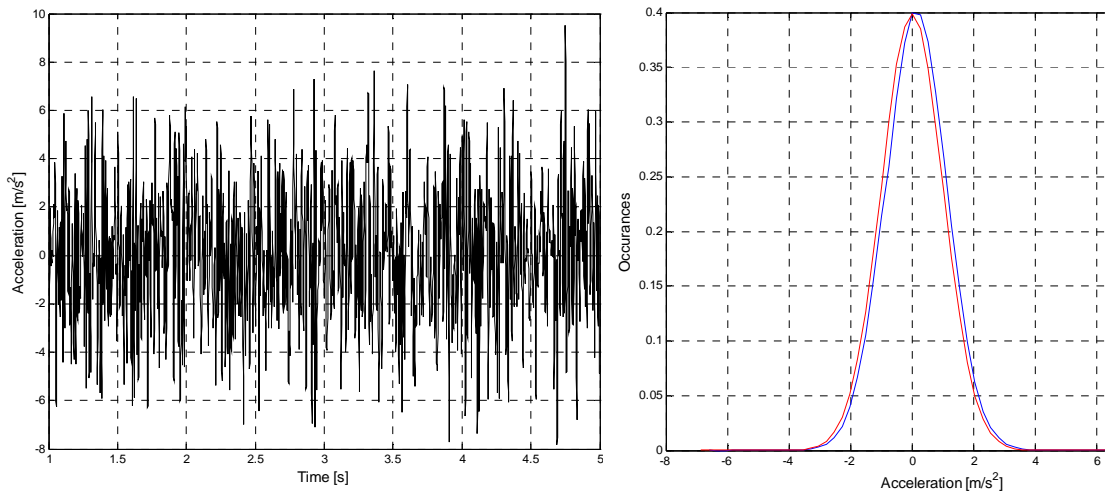


Figure 5-37 Excitation time history segment and histogram for eps grade s

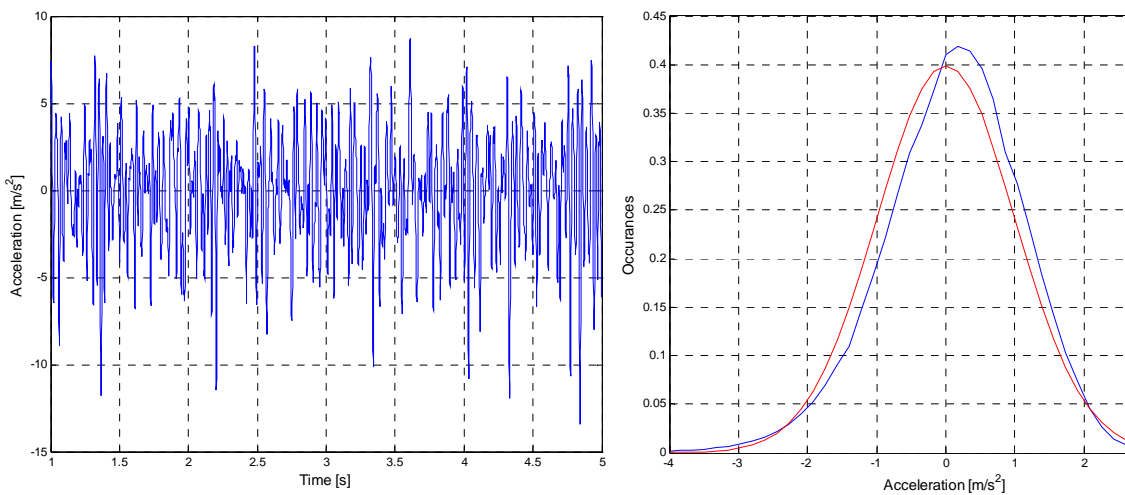


Figure 5-38 Response time history segment and histogram for eps grade s

Figures 5-37 and 5-38 relate to the excitation and response of the system. Figure 5-37 shows a time history segment of the excitation and the corresponding normalised histogram. The normalised probability density function plot shows the close to Gaussian distribution of the excitation signal (normalised Gaussian distribution in red). Figure 5-38 is a time history segment of the system response and the corresponding normalised histogram (normalised Gaussian distribution in red). Note the shift to the right of the response histogram compared to a Gaussian

distribution. This non-Gaussian distribution clearly shows the nonlinearity of the response.

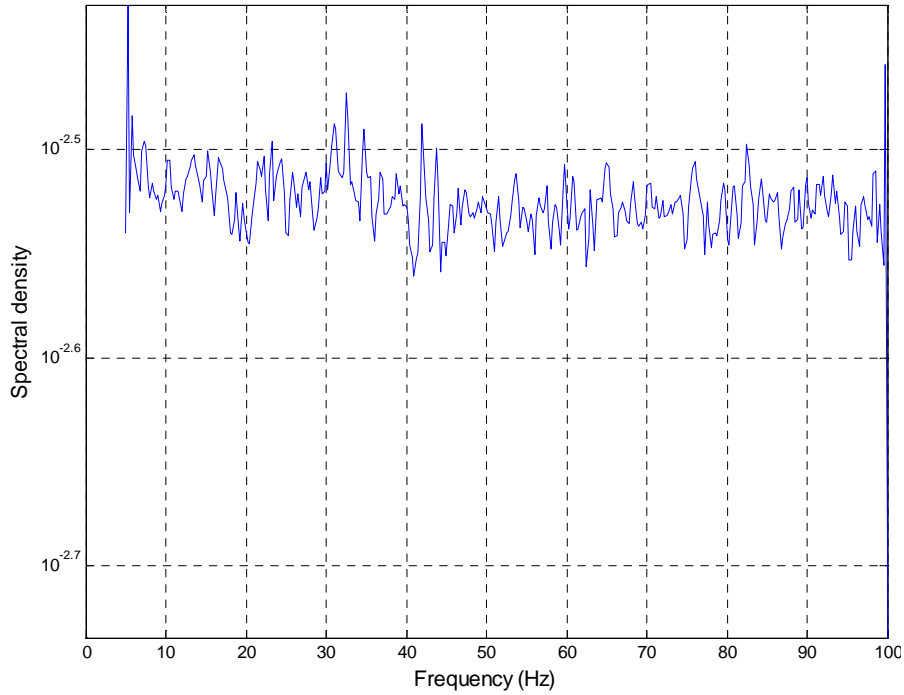


Figure 5-39 Excitation auto-spectrum @ 1125 averages for eps grade s

Figure 5-39 shows the excitation auto-spectrum after 1125 averages and confirms the expected error of less than 3%. The expected error calculation is:

$$error = \frac{1}{\sqrt{N_d}} \quad \text{where } N_d \text{ is the number of distinct averages.}$$

In this case, of 1125 averages, the calculated error equates to approximately 3%.

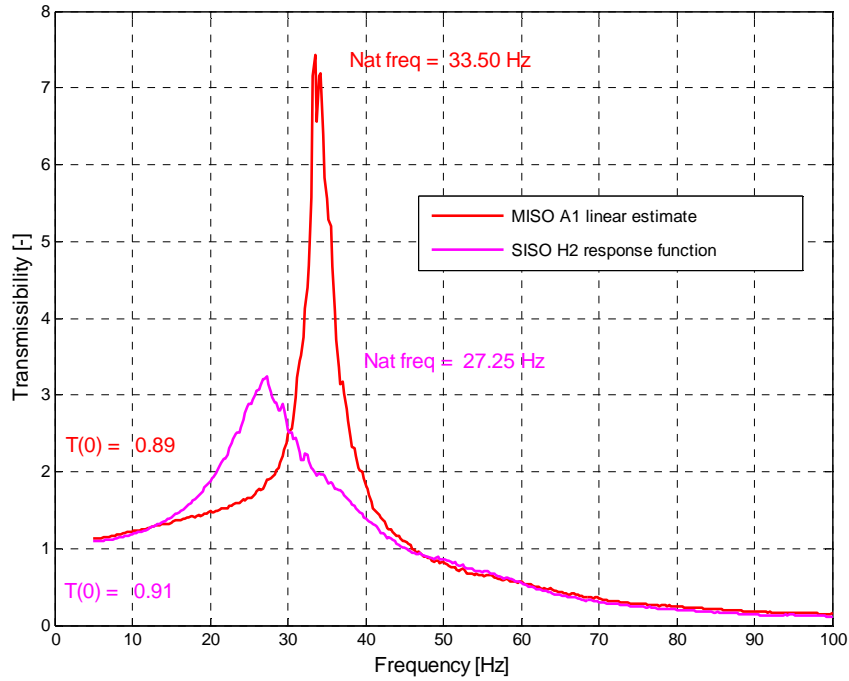


Figure 5-40 FRF estimate for eps grade s @ 0.40g RMS

Figure 5-40 shows the R-MISO linear frequency response function estimate and the SISO frequency response function estimate. Also shown are the peak frequency estimates. The difference between the R-MISO and SISO, transmissibility magnitude and peak frequency, can be clearly seen.

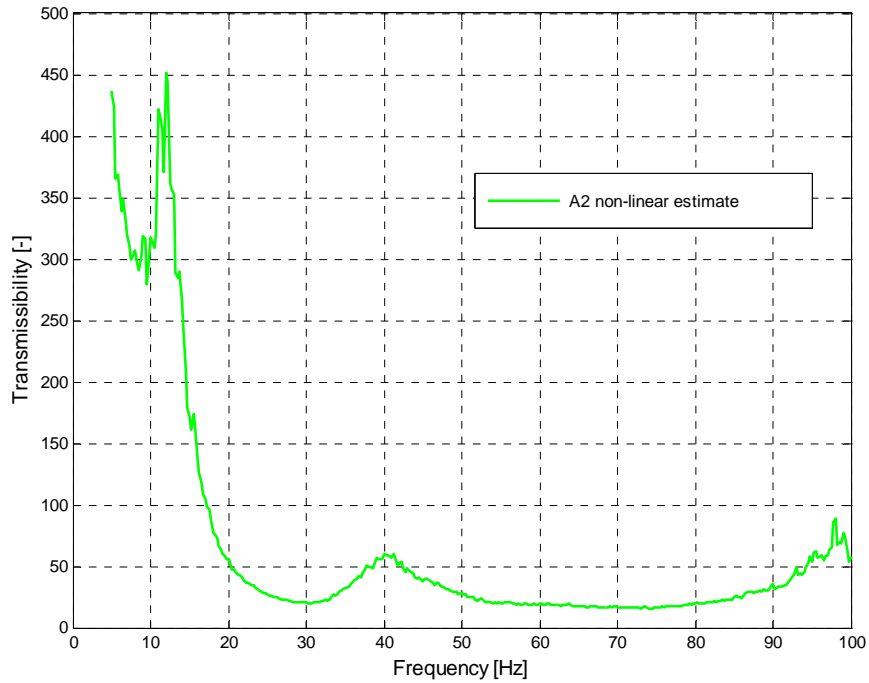


Figure 5-41 Nonlinear FRF estimate for eps grade s @ 0.40g RMS

Figure 5-41 shows the R-MISO nonlinear frequency response estimate for the second input ($x \cdot \text{abs}(x)$). This is the magnitude plot of the nonlinear component of the system model and shows the contribution of the second term over the frequency range.

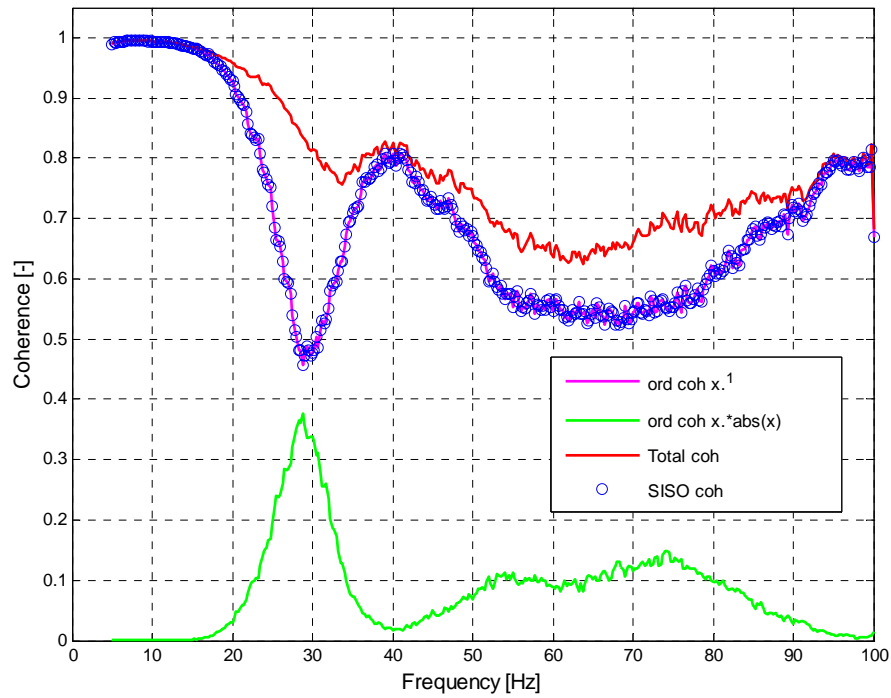


Figure 5-42 Coherence plot for eps grade s @ 0.40g RMS

Figure 5-42 shows the R-MISO, ordinary and total coherence, and the SISO coherence for the system model. The contribution of the nonlinear term can be clearly seen. Note the particular improvement of the coherence in the region near the peak frequency and the continuous improvement in coherence at higher frequencies.

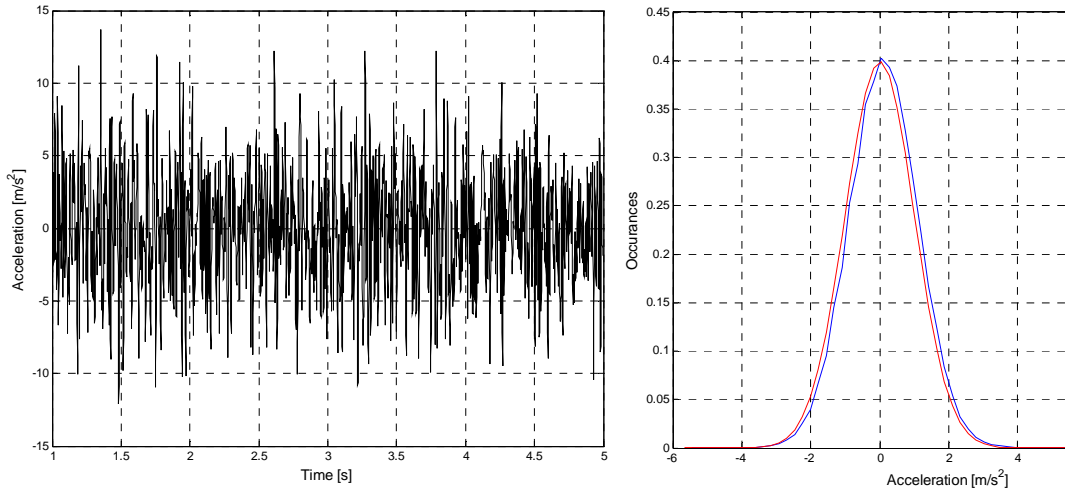


Figure 5-43 Excitation time history segment and histogram for eps grade s

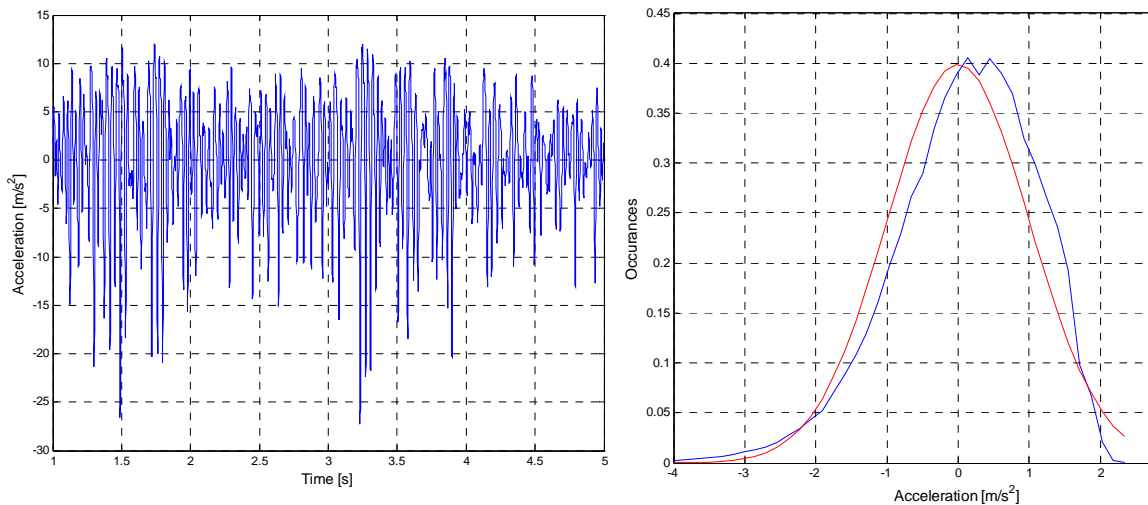


Figure 5-44 Response time history segment and histogram for eps grade s

Figures 5-43 and 5-44 relate to the excitation and response of the system. Figure 5-43 shows a time history segment of the excitation and the corresponding normalised histogram. The normalised probability density function plot shows the close to Gaussian distribution of the excitation signal (normalised Gaussian distribution in red). Figure 5-44 is a time history segment of the system response and the corresponding normalised histogram (normalised Gaussian distribution in red). Note the shift to the right of the response histogram compared to a Gaussian

distribution. This non-Gaussian distribution clearly shows the nonlinearity of the response.

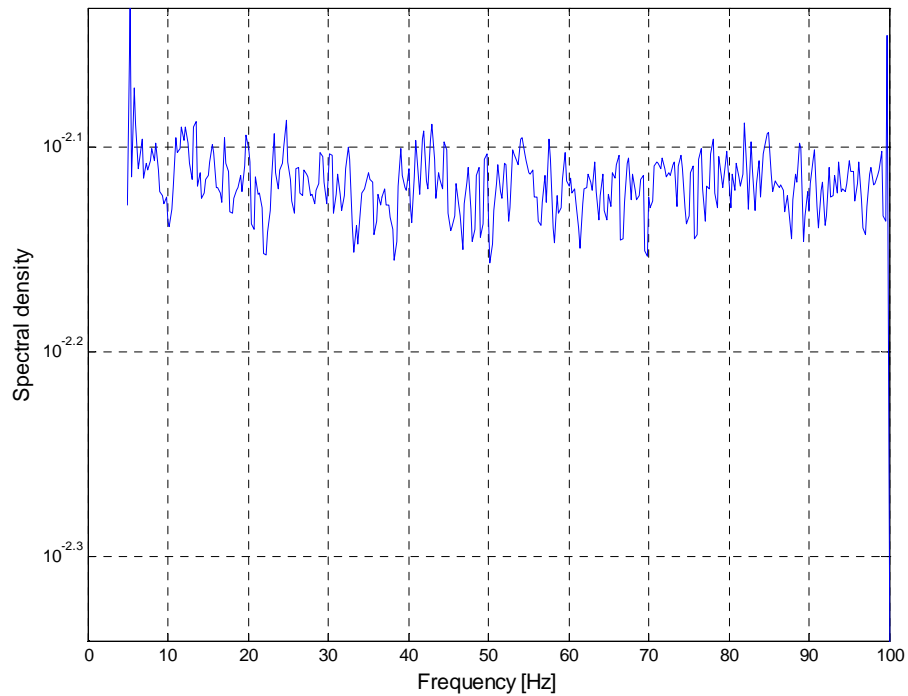


Figure 5-45 Excitation auto-spectrum @ 1125 averages for eps grade s

Figure 5-45 shows the excitation auto-spectrum after 1125 averages and confirms the expected error of less than 3%. The expected error calculation is:

$$error = \frac{1}{\sqrt{N_d}} \text{ where } N_d \text{ is the number of distinct averages.}$$

In this case, of 1125 averages, the calculated error equates to approximately 3%.

5.5.2 Results for EPS grade SL

The following will describe the results of the R-MISO analysis of the expanded polystyrene material grade SL. The sample was, as previously discussed, excited by band limited white noise at an RMS of 0.25g and 0.40g. The excitation and response data was analysed using the R-MISO software tool and the following results graphed for 125, 250 500 and 1125 distinct averages.

- Figure 5-46 and 5-52 R-MISO linear estimate and SISO transmissibility FRF plot
- Figure 5-47 and 5-53 R-MISO nonlinear estimate FRF plot
- Figure 5-48 and 5-54 Total coherence plots
- Figure 5-49(left) and 5-55(left) A time domain segment of the excitation signal
- Figure 5-49(right) and 5-55(right) Normalised histogram of the excitation signal
- Figure 5-50(left) and 5-56(left) A time domain segment of the response signal
- Figure 5-50(right) and 5-56(right) Normalised histogram of the response signal
- Figure 5-51 and 5-57 Auto-spectrum of the excitation signal

The following graphs show the analysis results for a two input dynamic system model. The two inputs (a) response x , and (b) response $x * \text{abs}(x)$ pass through a constant parameter linear system and a constant parameter nonlinear system respectively, having frequency response functions (A_1 and A_2). The system with the two inputs, producing the single measured, reversed input, response $y(t)$, The first set of results are at 0.25g RMS excitation and the second set at 0.40g RMS excitation and are after 1125 distinct averages. They show the improvement of the R-MISO model incorporating a nonlinear term over the SISO linear assumption model.

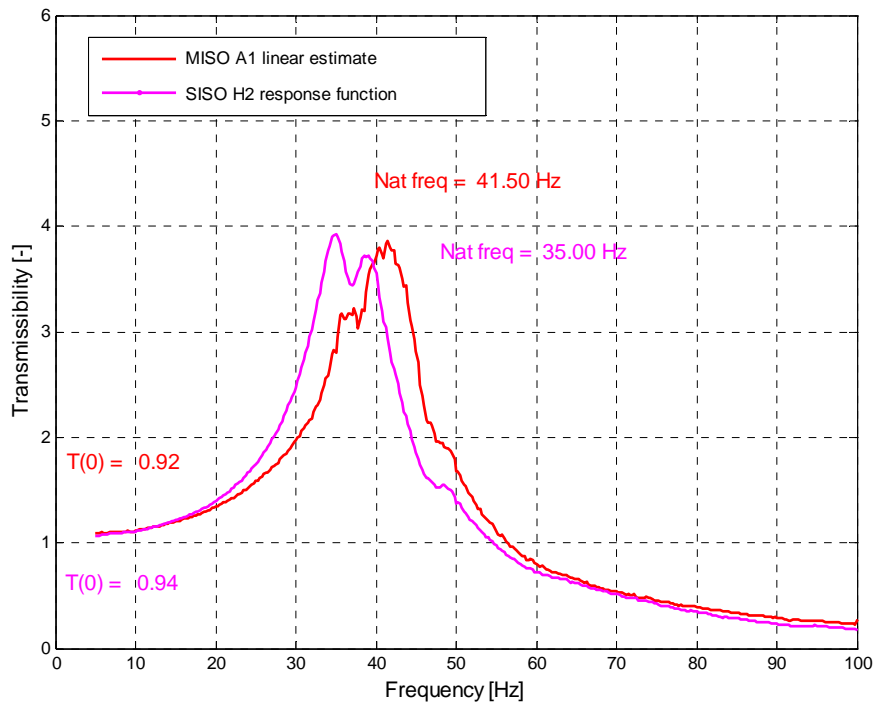


Figure 5-46 FRF estimate for eps grade sl @ 0.25g RMS

Figure 5-46 shows the R-MISO linear frequency response function estimate and the SISO frequency response function estimate. Also shown are the peak frequency estimates. The difference between the R-MISO and SISO, transmissibility magnitude and peak frequency, can be clearly seen.

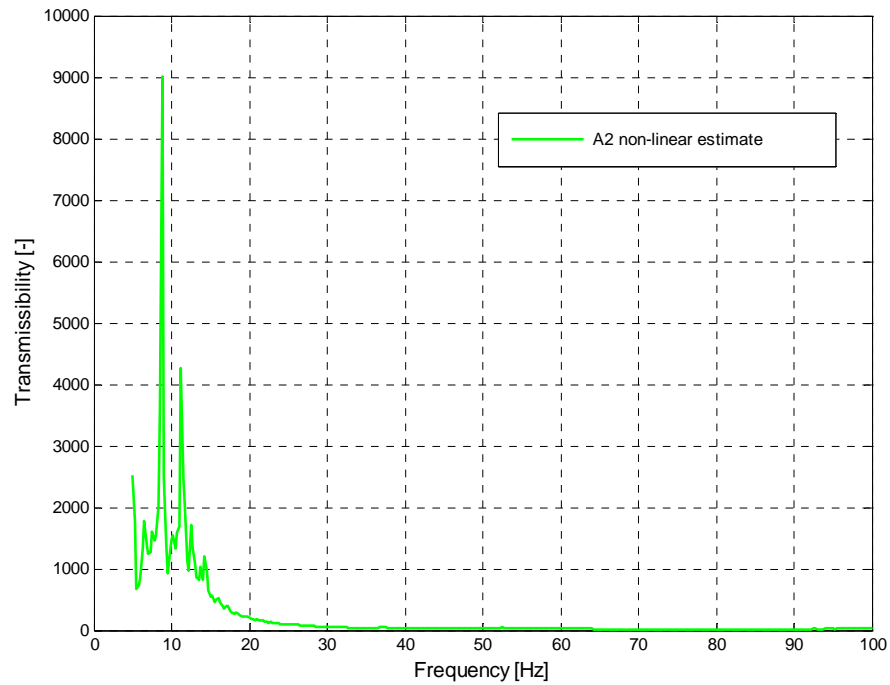


Figure 5-47 Nonlinear FRF estimate for eps grade sl @ 0.25g RMS

Figure 5-47 shows the R-MISO nonlinear frequency response estimate for the second input ($x \cdot \text{abs}(x)$). This is the magnitude plot of the nonlinear component of the system model and shows the contribution of the second term over the frequency range.

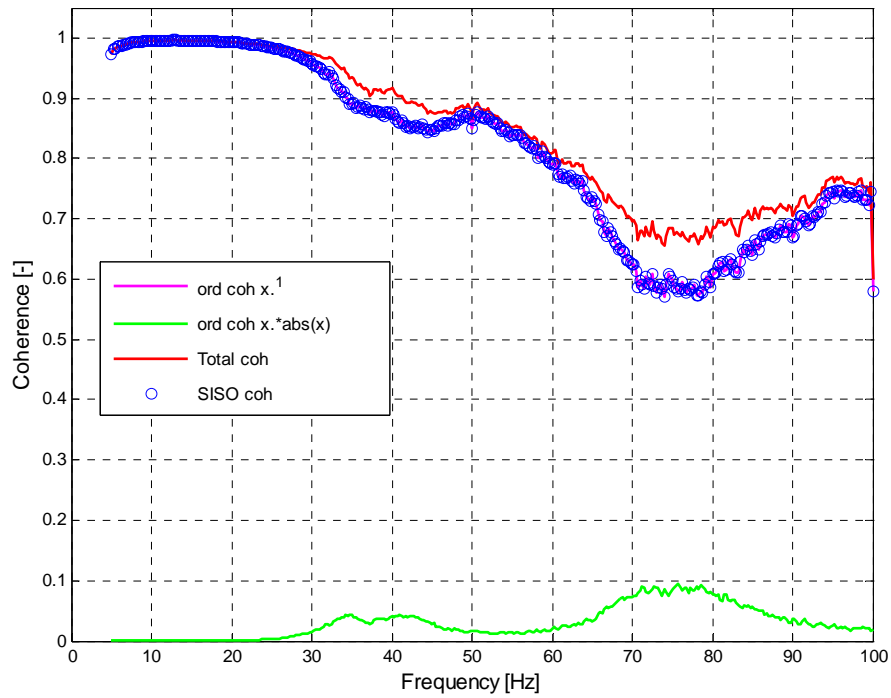


Figure 5-48 Coherence plot for eps grade sl @ 0.25g RMS

Figure 5-48 shows the R-MISO, ordinary and total coherence, and the SISO coherence for the system model. The contribution of the nonlinear term can be clearly seen. Note the slight improvement of the coherence in the region near the peak frequency and the continuous improvement in coherence at higher frequencies.

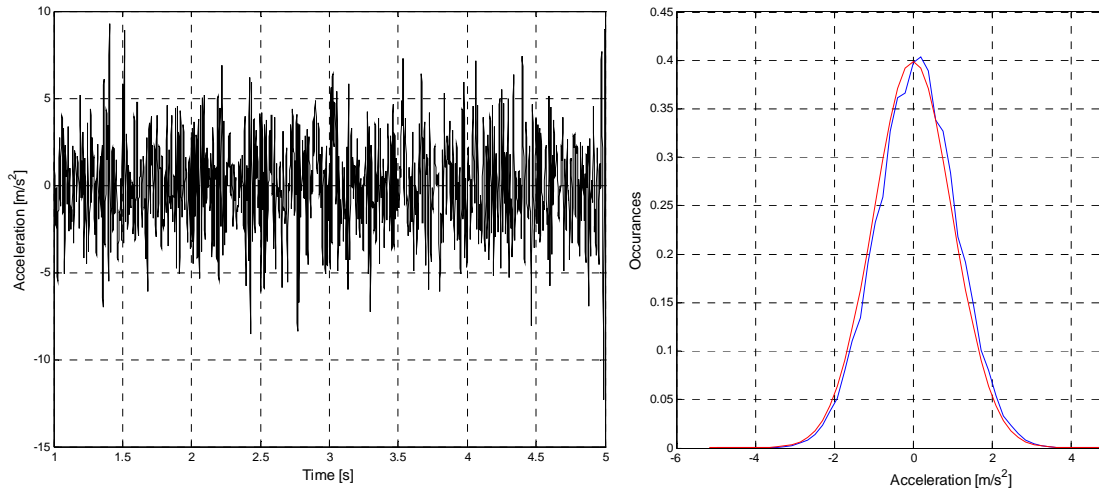


Figure 5-49 Excitation time history segment and histogram for eps grade sl

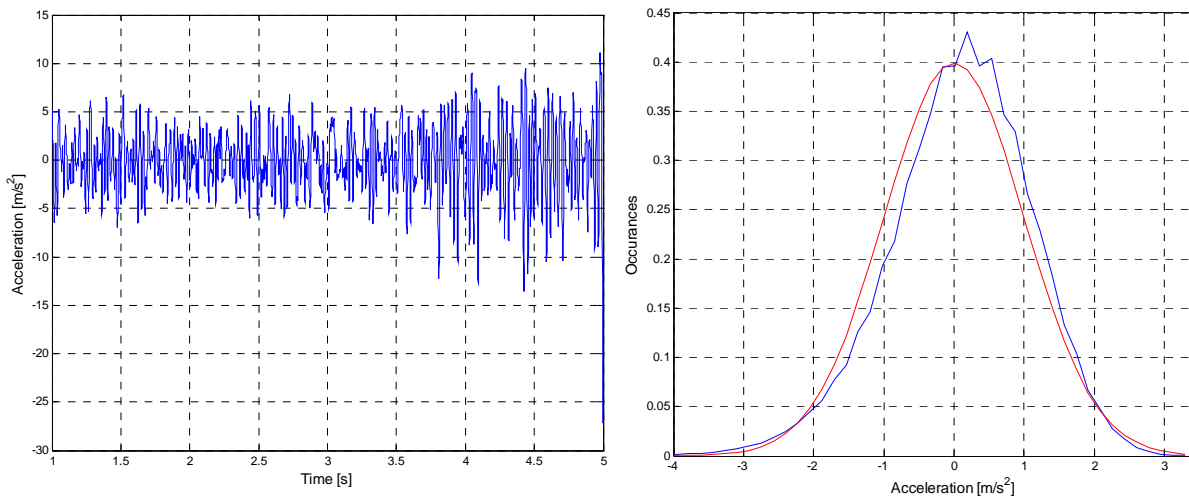


Figure 5-50 Response time history segment and histogram for eps grade sl

Figures 5-49 and 5-50 relate to the excitation and response of the system. Figure 5-49 shows a time history segment of the excitation and the corresponding normalised histogram. The normalised probability density function plot shows the close to Gaussian distribution of the excitation signal (normalised Gaussian distribution in red). Figure 5-50 is a time history segment of the system response and the corresponding normalised histogram (normalised Gaussian distribution in red).

Note the shift to the right of the response histogram compared to a Gaussian distribution. This non-Gaussian distribution clearly shows the nonlinearity of the response.

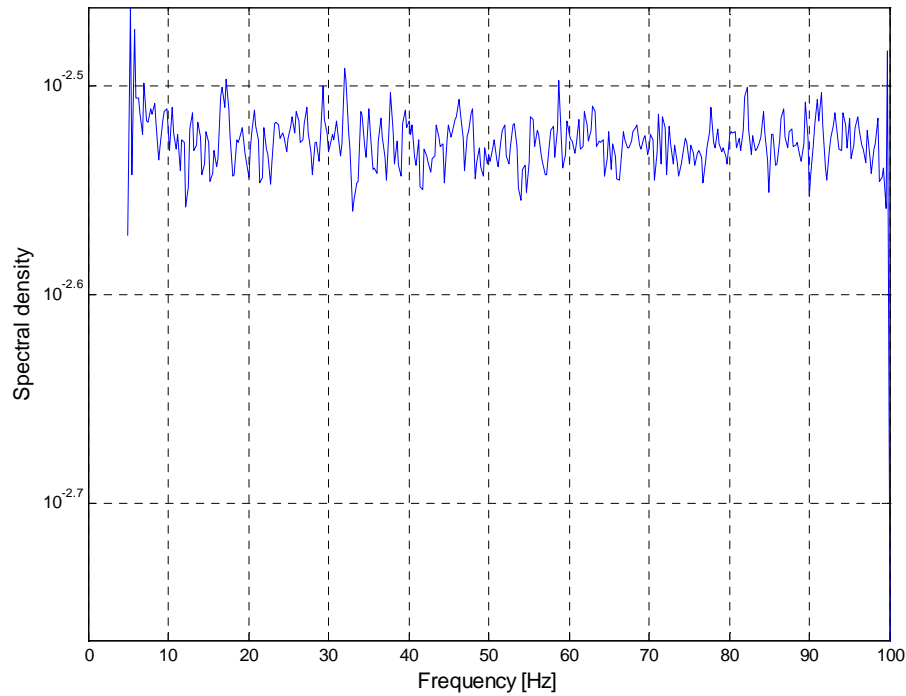


Figure 5-51 Excitation auto-spectrum @ 1125 averages for eps grade sl

Figure 5-51 shows the excitation auto-spectrum after 1125 averages and confirms the expected error of less than 3%. The expected error calculation is:

$$error = \frac{1}{\sqrt{N_d}}, \text{ where } N_d \text{ is the number of distinct averages.}$$

In this case, of 1125 averages, the calculated error equates to approximately 3%.

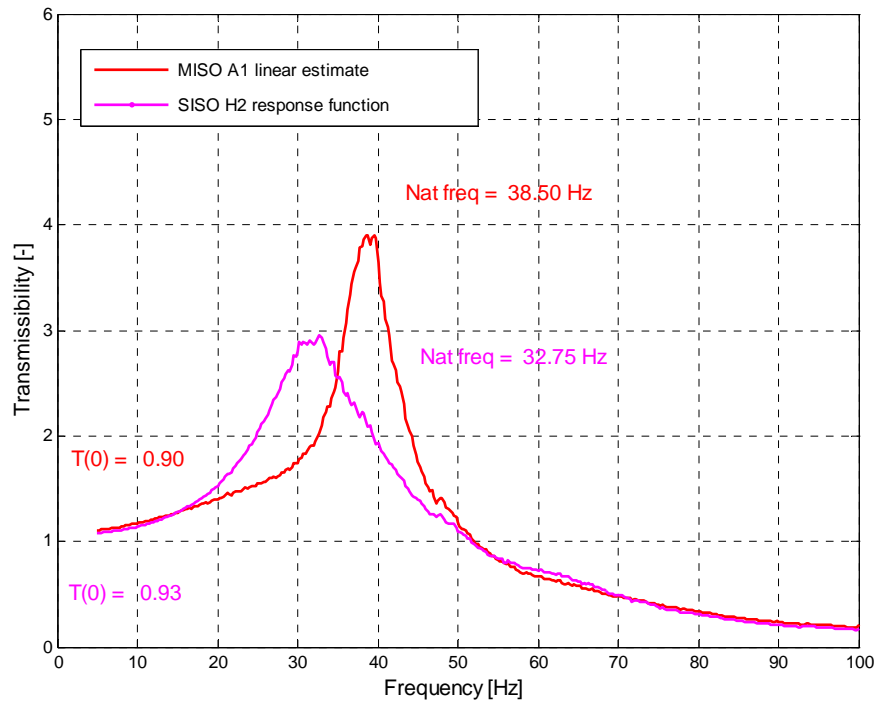


Figure 5-52 FRF estimate for eps grade sl @ 0.40g RMS

Figure 5-52 shows the R-MISO linear frequency response function estimate and the SISO frequency response function estimate. Also shown are the peak frequency estimates. The difference between the R-MISO and SISO, transmissibility magnitude and peak frequency, can be clearly seen.

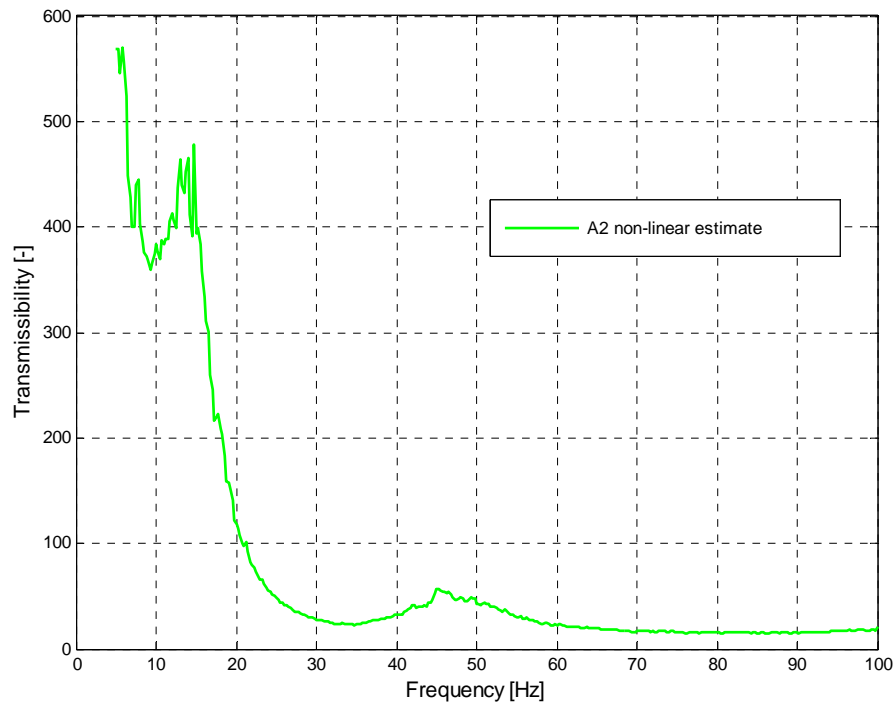


Figure 5-53 Nonlinear FRF estimate for eps grade sl @ 0.40g RMS

Figure 5-53 shows the R-MISO nonlinear frequency response estimate for the second input ($x \cdot \text{abs}(x)$). This is the magnitude plot of the nonlinear component of the system model and shows the contribution of the second term over the frequency range.

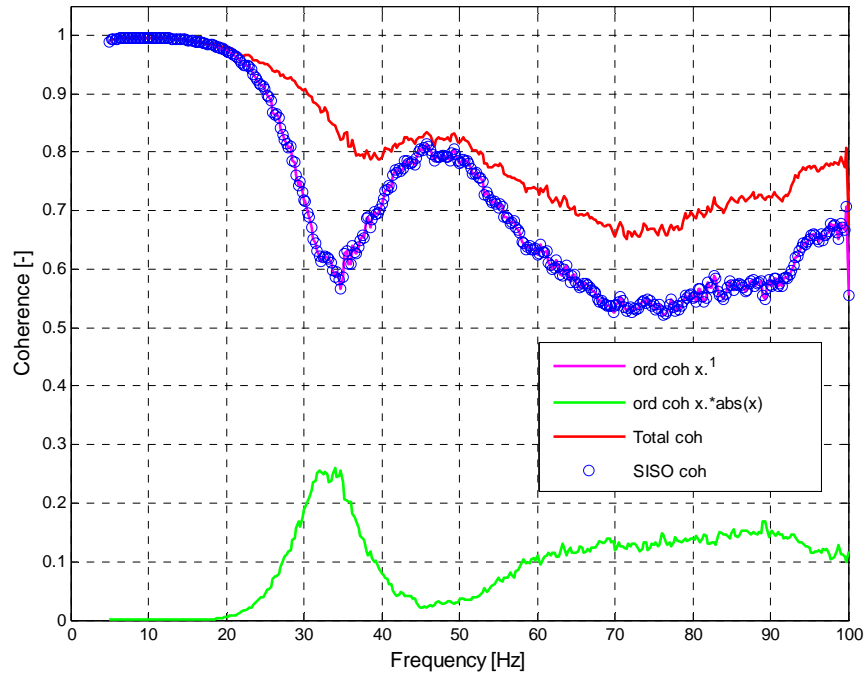


Figure 5-54 Coherence plot for eps grade sl @ 0.40g RMS

Figure 5-54 shows the R-MISO, ordinary and total coherence, and the SISO coherence for the system model. The contribution of the nonlinear term can be clearly seen. Note the particular improvement of the coherence in the region near the peak frequency and the continuous improvement in coherence at higher frequencies.

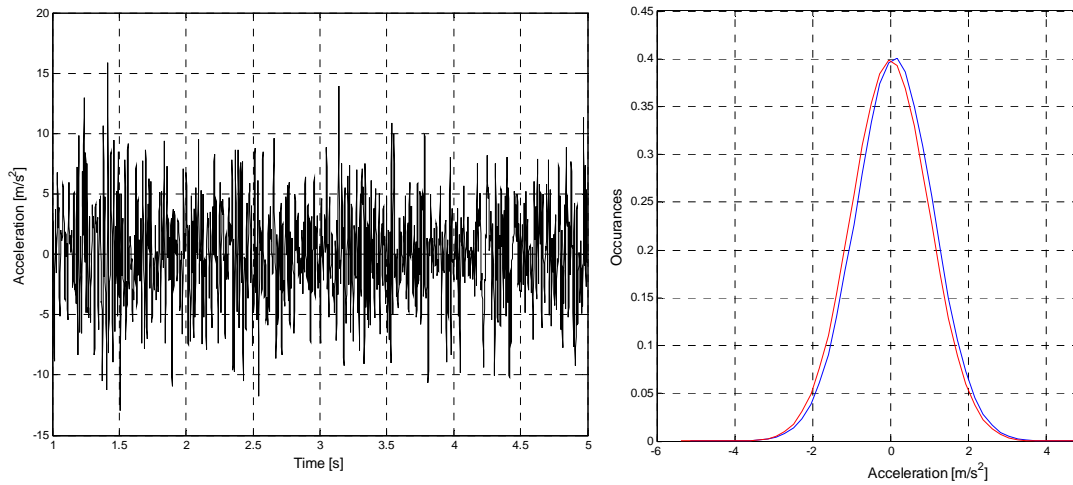


Figure 5-55 Excitation time history segment and histogram for eps grade sl

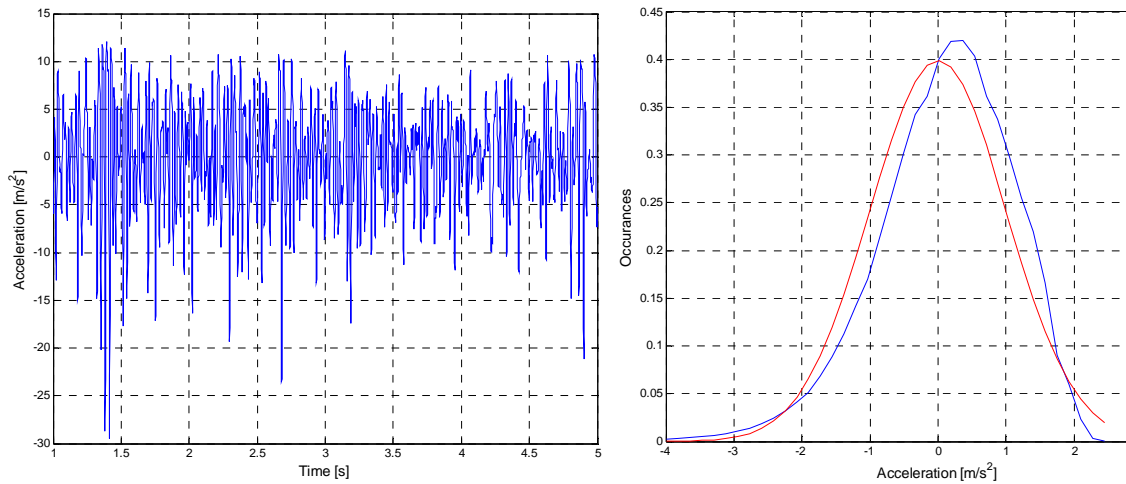


Figure 5-56 Response time history segment and histogram for eps grade sl

Figures 5-55 and 5-56 relate to the excitation and response of the system. Figure 5-55 shows a time history segment of the excitation and the corresponding normalised histogram. The normalised probability density function plot shows the close to Gaussian distribution of the excitation signal (normalised Gaussian distribution in red). Figure 5-56 is a time history segment of the system response and the corresponding normalised histogram (normalised Gaussian distribution in red).

Note the shift to the right of the response histogram compared to a Gaussian distribution. This non-Gaussian distribution clearly shows the nonlinearity of the response.

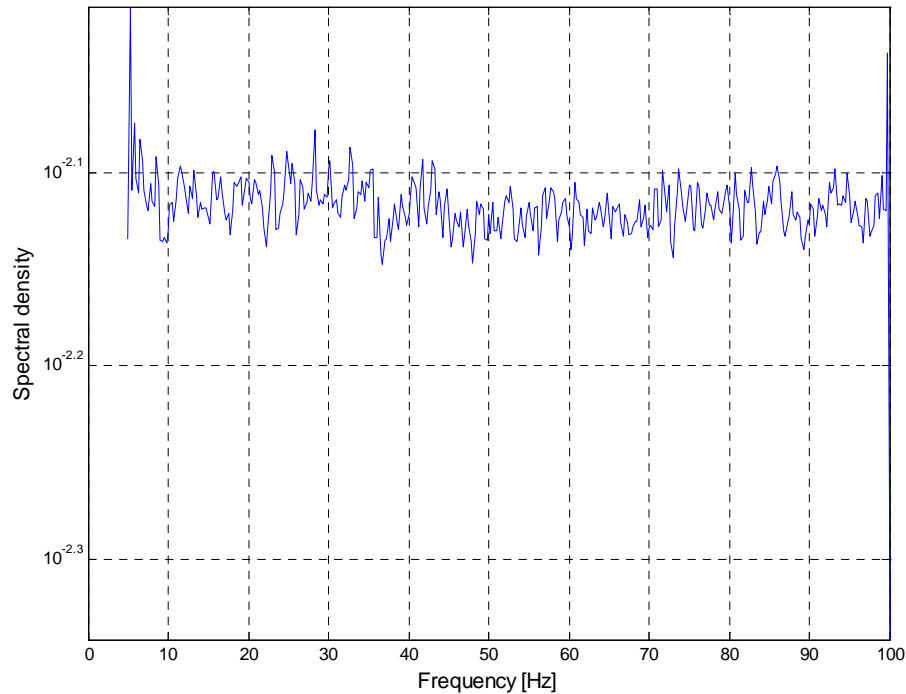


Figure 5-57 Excitation auto-spectrum @1125 averages for eps grade sl

Figure 5-57 shows the excitation auto-spectrum after 1125 averages and confirms the expected error of less than 3%. The expected error calculation is:

$$error = \frac{1}{\sqrt{N_d}}, \text{ where } N_d \text{ is the number of distinct averages}$$

In this case, of 1125 averages, the calculated error equates to approximately 3%.

5.5.3 Effect of increasing averages for EPS grade S

The following figures compare the effect of increasing the number of averages. Figures 5-58 and 5-59 show the linear estimate overlay and the coherence overlay respectively, for the material EPS grade S.

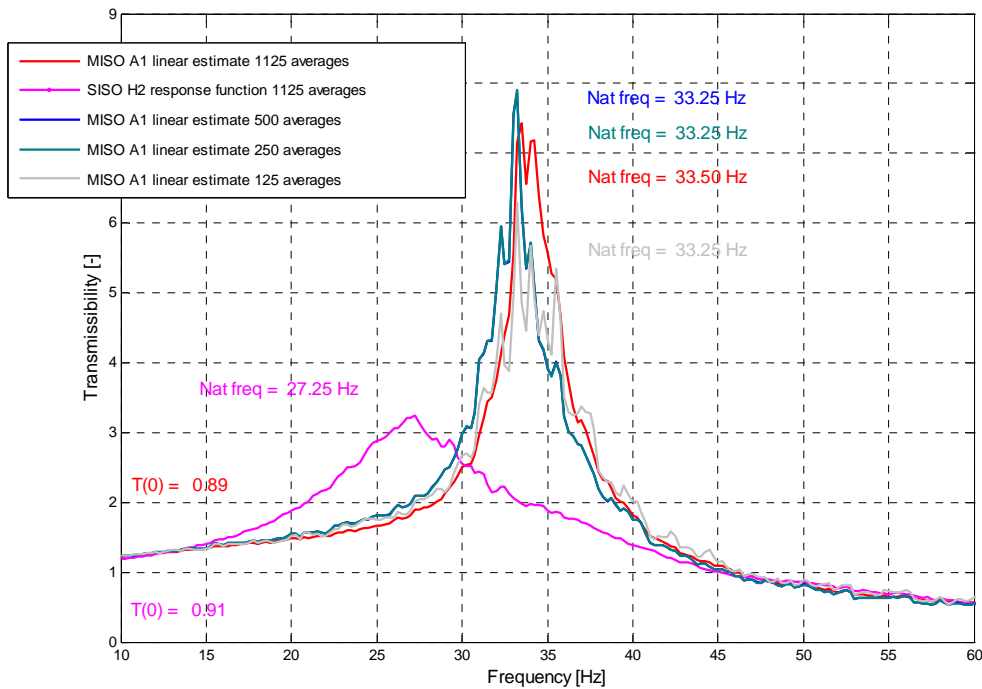


Figure 5-58 FRF overlay of increasing averages for eps grade s @ 0.40g RMS

Figure 5-58 shows the change in the linear FRF estimate for an increasing number of averages. The number of distinct averages was 125, 250, 500, and 1125. The peak transmissibility increases marginally and begins to settle at greater than 1000 distinct averages. The natural frequency estimate recovered by the R-MISO method also changes although the change is in the region of 2% over greater averaging.

The transmissibility estimated by the SISO differs by more than 150% at the estimated natural frequency at 1125 averages.

The SISO estimate of natural frequency varies by 25% from the R-MISO linear estimate.

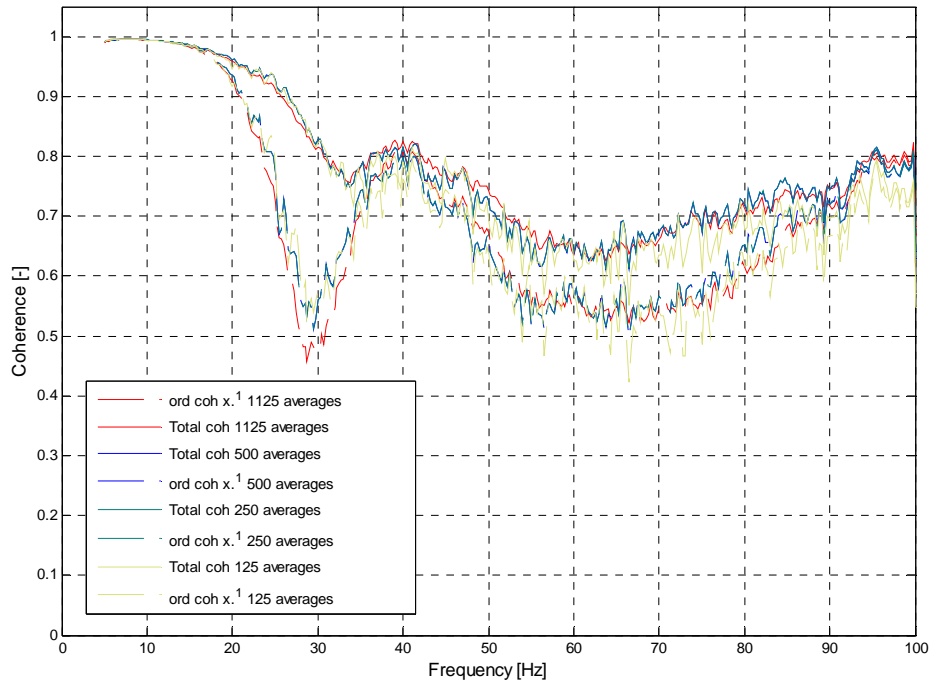


Figure 5-59 Coherence overlay of increasing averages for eps grade s @ 0.40g RMS

Figure 5-59 shows the change in the corresponding coherence plot for an increasing number of averages. The plot shows the effect of increasing the number of averages on both the SISO and R-MISO methods. The coherence plot settles at greater than 1000 distinct averages. In all cases the R-MISO total coherence is greater than the SISO coherence. The greatest improvement in the total coherence can be seen in the region around the R-MISO estimate of natural frequency.

5.5.4 Effect of increasing averages for EPS grade SL

Figures 5-60 and 5-61 show the linear estimate overlay and the coherence overlay respectively, for the material EPS grade SL.

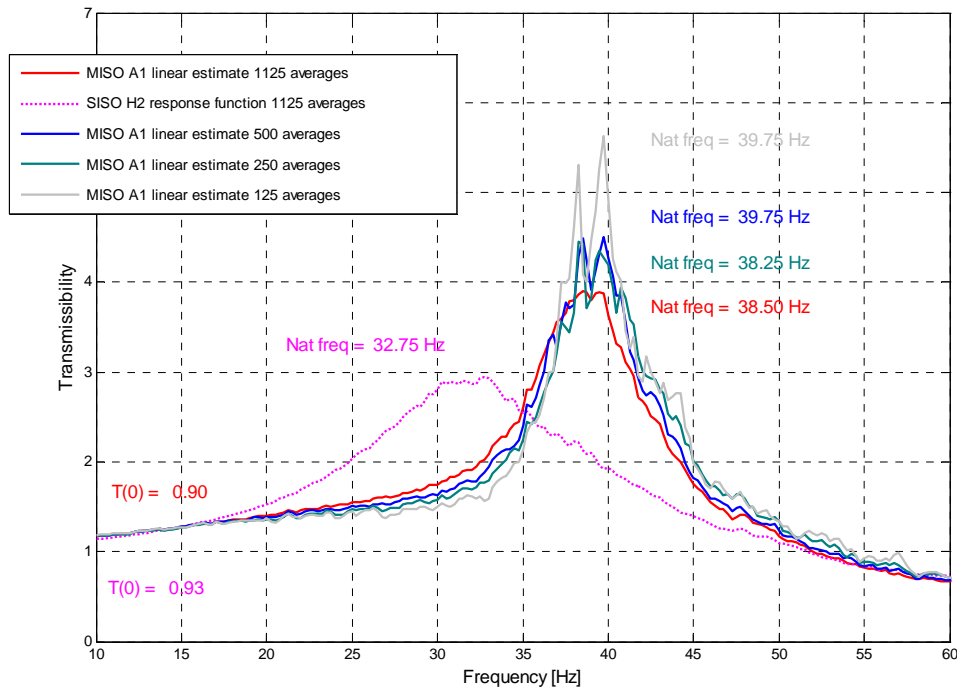


Figure 5-60 FRF overlay of increasing averages for eps grade sl @ 0.40g RMS

Figure 5-60 shows the change in the linear FRF estimate for an increasing number of averages. The number of distinct averages was 125, 250, 500, and 1125. The peak transmissibility reduces and begins to settle at greater than 1000 distinct averages. The natural frequency estimate recovered by the R-MISO method also changes although the change is in the region of 2% over greater averaging.

The transmissibility estimated by the SISO differs by more than 25% at the estimated natural frequency at 1125 averages.

The SISO estimate of natural frequency varies by 20% from the R-MISO recovered natural frequency estimate.

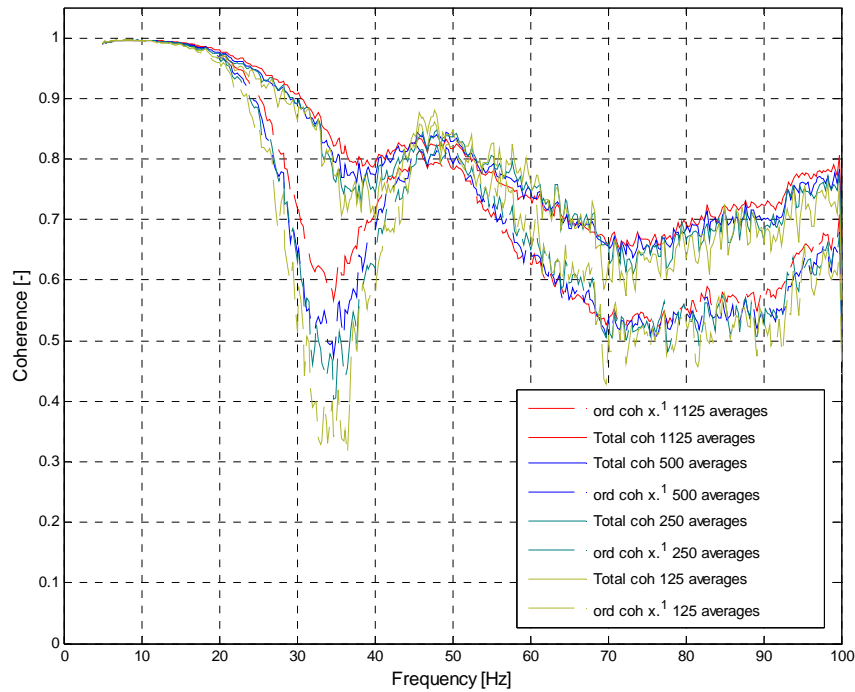


Figure 5-61 Coherence overlay of increasing averages for eps grade sl @ 0.40g RMS

Figure 5-61 shows the change in the corresponding coherence plot for an increasing number of averages on both the SISO and R-MISO methods. The coherence plot settles at greater than 1000 distinct averages. In all cases the R-MISO total coherence is greater than the SISO coherence. The greatest improvement in the total coherence can be seen in the region around the R-MISO estimate of natural frequency with continual improvement at higher frequencies.

Chapter 6

Conclusion

6 Conclusion

The R-MISO approach revealed a significant difference in the natural frequency estimate between the SISO linear assumption and the linear frequency response function estimate of the R-MISO approach. A considerable difference in the magnitude of the transmissibility at the estimated natural frequency was also shown. These differences were accompanied by an improvement in coherence.

The hypothesis has been shown to be correct. Yes, the description of a cushioning system with a Frequency Response Function accommodating some nonlinear effects will make a difference to the resulting characterisation. And the conclusions derived from the characterisation results will make a difference to the design of protective cushioning for a critical element.

A review of nonlinear analysis methods was presented along with a précis of the current approach to nonlinear SDOF systems. R-MISO is shown to have the ability to analyse a nonlinear system with a greater accuracy than an assumption of linearity.

R-MISO analysis allows, by definition, a number of inputs to model the system under investigation. The choice of inputs is one of trial and error, the coherence plot result will show if the chosen inputs are an improvement over a linear assumption. The inputs chosen for this research were x , the original response and $|x|^2$ the absolute of x squared. This retained the sign of the signal. By using coherence as the best guide for the “goodness of fit” of the proposed model, we can easily compare the SISO and R-MISO approaches. These inputs gave a much improved coherence result in all cases.

An improvement in coherence acknowledges the greater accuracy of the system model used. Such an improvement will facilitate more accurate predictions of the behavior of the system subjected to other excitations. Package designers rely upon the cushion characteristics, natural frequency, transmissibility etc in their calculations for the protection of a product.

R-MISO has shown a greater ability to more accurately characterise the cushion material. This greater accuracy will allow for the use of fewer materials with the benefits of cost and environmental savings.

This work adds to the knowledge of the package designer through the study of the significance of the nonlinear behavior of a common cushioning material using the Reverse Multiple Input-Single Output (R-MISO) method. This new approach to the vibration analysis of cushioning materials will allow the package designer to better assess the nonlinear behavior of a packaging material.

6.1 Further work

This study investigated the difference of the linear frequency response function estimates between the SISO linear assumption and the R-MISO approach. The effect of the nonlinearity on the system was studied using band limited white noise at two RMS levels. This revealed a significant difference, however further work should be done considering other excitations and excitation levels.

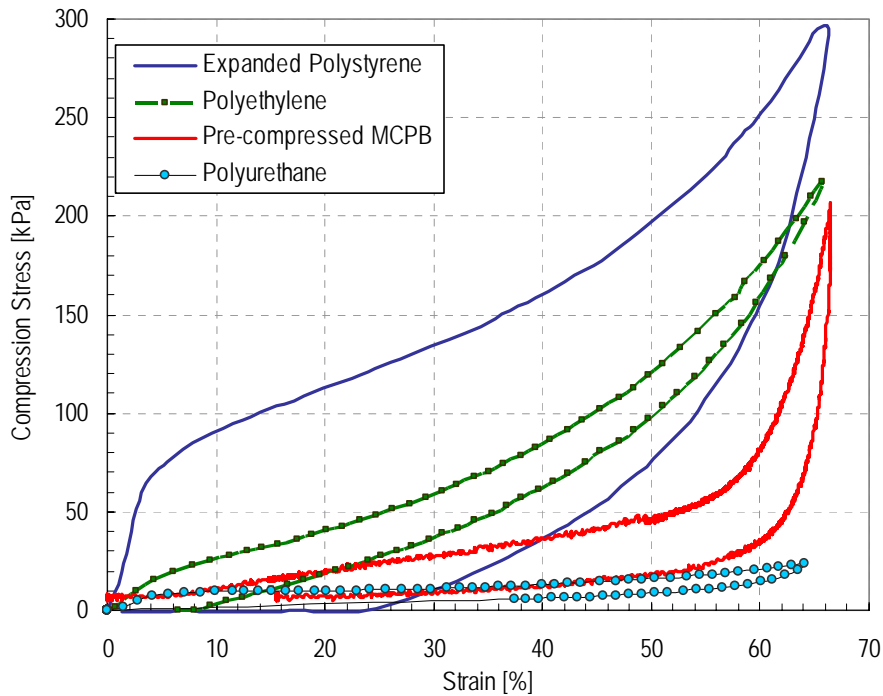


Figure 6-1 Typical compression curve of various cushion materials

Figure 6-1 clearly shows the highly nonlinear behaviour of various common cushioning materials. This research solely studied expanded polystyrene (EPS). However, EPS is very representative of such materials. Further work may be done on the characterisation of the behaviour of these materials.

Further improvements to the software could be made to choose inputs iteratively based on achieving the best coherence.

References

- Anon. "State of the Industry report". Flexible Packaging Association, 1996.
- Bendat, J.S, *Nonlinear system analysis and identification from random data*, New York, John Wiley & Sons, New York, 1990.
- Bendat, J.S, *Nonlinear systems techniques and applications*, New York, John Wiley & Sons, New York, 1998.
- Bendat, J.S, Piersol, A.G, Spectral analysis of nonlinear systems involving square law operations. *Journal of Sound and Vibration*, 81 (2), p199-213, 1982.
- Bendat, J.S, Piersol, A.G, Decomposition of wave forces into linear and non-linear components. *Journal of Sound and Vibration*, 106, (3), p. 391-408, 1986
- Bendat, J.S, Piersol, A.G, *Engineering applications of correlation and spectral analysis*. 2nd Edition, John Wiley & Sons, New York, 1993.
- Bruscella, B, Rouillard V. and Sek M.A, "Analysis of Road Profiles". ASCE *Journal of Transportation Engineering* Vol. 125 No. 1, p 55 – 59, 1999.
- Caldicott P.J, "Distribution testing – Sine or Random", *International Journal of Packaging Technology and Science*, 4, p 287 – 291, 1991.
- Eichstadt. T, Carius. A, Andreas Kraemer. R, Producer responsibility within policy networks: the case of German packaging policy, *Journal of Environmental Policy & Planning*, Routledge, part of the Taylor & Francis Group Issue: Volume 1, Number 2 / p 133 – 153, 1999.

European Commission, *European Transport Policy for 2010: time to decide*, Marco Polo paper, European Commission 2006 “Encouraging water and rail transport”, 2006.

European Commission, *European Transport Policy*, White Paper 2004, European Commission, 2006.

ENVIRONMENTAL CODE OF PRACTICE, Australian Industry Group, Beverage Industry Environment Council, Packaging Council of Australia, Plastics and Chemicals Industries Association, March 1997

Godshall, W.D, “*Frequency Response, Damping and Transmissibility Characteristics of Top Loaded Corrugated Cases*”. USDA Fed. Res. Paper FPL 160, 1971.

Gordon, G.A, Developing Better Vibration tests for Packages, *Journal of the Soc. of Environmental Engineers*, p 29-36, Dec 1980.

ISTA 4 Series: *Enhanced Simulation Performance Tests*, International Safe Transit Association

Kipp, W. I, *Vibration Testing Equivalence*. Proceedings of the International Safe Transit Association Conference, Orlando, Florida, 2000.

Liagre, P.F.B, *Investigation of nonlinear identification techniques*, 2002.

Mindlin, R.D, American Telephone and Telegraph Company, *The Bell System Technical Journal*, Dynamics of package cushioning Vol 24 3.4, American Telephone and Telegraph Company, Short Hills N.J, July/Oct 1945.

Mitchell L.D, Improved methods for the FFT calculation of the Frequency Response Function”, *Journal of Mechanical Design*, , Vol104, pp277-279, April 1982.

Narayanan, S, Yim, S.C.S, Palo, P.A, Nonlinear system identification of a moored structural system. *Proceedings of the 8th International Offshore and Polar Engineering Conference*, Montreal, Canada, 3,478-484, 1998.

National Packaging Covenant 15 July 2005 to 30 June 2010, *A commitment to the sustainable manufacture, use and recovery of packaging*, National Packaging Covenant Council, Australia, July 2005

Newton, P.W, *Australia State of the Environment Report*. CSIRO Publishing on behalf of the Department of the Environment and Heritage © Commonwealth of Australia, 2001.

O’Brien M. et. Al, “Causes of fruit bruising on transport trucks” *Hilgardia* 35(6), p 113 – 124, 1963.

Oestergaard S, *Packaging Goals in Transport Quality*, 7th IAPRI World Conference on Packaging, Utrecht, the Netherlands, 1991.

Panneer Selvam, R, Bhattacharyya, S.K, Parameter identification of a compliant nonlinear SDOF system in random ocean waves by reverse MISO method. *Journal of Ocean Engineering*, No28, p 1199-1223, 2001.

Panneer Selvam, R, Bhattacharyya, S.K., Parameter identification of a large floating body in random ocean waves by reverse MISO method. *Journal of Offshore Mechanics and Arctic Engineering* 125, p 81-86, 2003.

Parker A, Rouillard V. and Sek M, In *Proceedings of the 4th Australasian Congress on Applied Mechanics*, edited by M.Xie, Melbourne, Australia, p 739 – 744, 2005.

Parker A, Rouillard V. and Sek M, In *Proceedings of the Society for Experimental Mechanics Annual Conference on Experimental and Applied Mechanics*, Portland OR, p 46, 2005.

Koop G; Pesaran M.H; Potter S.M, Impulse response analysis in nonlinear multivariate models, *Journal of Econometrics*, Vol 74, Number 1, p 119-147(29), Elsevier, September 1996.

Queensland Transport Annual Report 2004-05, Vol 201-Annual Report-15 Environment © Commonwealth of Australia, 2005.

Rice, H.J, Fitzpatrick, J.A, A generalized technique for spectral analysis of nonlinear systems. *Mechanical Systems and Signal Processing* Vol 2 (2), p 195-207, 1988.

Rice, H.J, Fitzpatrick, J.A, A procedure for the identification of linear and nonlinear multi-degree-of-freedom systems. *Journal of Sound and Vibration* 149 (3), p 397-411, 1991.

Richards, C.M, Singh, R, Identification of multi-degree-of-freedom nonlinear systems under random excitations by the 'reverse path' spectral method. *Journal of Sound and Vibration* 213 (4), p 673-708, 1998.

Root, D, "Six-Step Method for Cushioned Package Development", Lansmont, 1997

Rouillard. V, "Monitoring, Control and Simulation of Distribution Hazards", *Proceedings of Research Seminar on Packaging Innovations*, Food Research and Development Centre, St Hyacinthe, Quebec, Canada, 2002.

Rouillard V. and Sek M.A. Simulation of Non-stationary vehicle Vibrations. *Proceedings of the Institution of Mechanical Engineers*. Vol 215, Part D, p 1069 – 1075, 2001.

Rouillard V. and Sek M.A. *A statistical model for longitudinal road topography*. Road and Transport Research, ARRB Vol 11, No.23 p 17 – 23, 2002.

Rugh W.J, *Nonlinear System Theory: The Volterra-Weiner Approach*, John Hopkins University Press, Baltimore, 1981.

Schetzen, M, *The Volterra & Weiner Theories of Nonlinear Systems*. Wiley-Interscience, New York, 1980.

Sek M.A, Minett M, Rouillard V, Bruscella B, “A New Method for the Determination of Cushion Curves”. *International Journal, Packaging Technology and Science*, 13 (6), p 249-255, 2000.

Sek M.A, “Optimisation of Packaging Design Through an Integrated Approach to the Measurement and Laboratory Simulation of Transportation Hazards”. *Proceedings of the 12th international Conference on Packaging, International Association of Packaging Research Institutes*, Warsaw, Poland, 2001.

Spanos, P.D, Lu, R, Nonlinear system identification in offshore reliability. *Journal of Offshore Mechanics and Arctic Engineering* 117 (3), p 171-177, 1995.

The Packaging Council of Australia., Issues paper 07, April 1994

Victorian Freight, Transport, *Distribution and Logistics Action Plan*, Victorian Government through the Department of Innovation, Industry and Regional development (DIIRD), © Commonwealth of Australia, 2001

Zell, G, *Vibration Testing of Resilient Package Cushioning Material*, Report PA-T-3610, Piccatinny Arsenal, Dover, N.J, 1969.

APPENDIX A: Common packaging standards

A widely accepted schedule is the American Society for Testing and Materials (ASTM). Of particular interest are:

ASTM D1596 “Standard Test Method for Shock Absorbing Characteristics of Package Cushioning Materials”

ASTM D3332 “Standard Test Methods for Mechanical Shock and Fragility of Products Using Shock Machines”,

ASTM D4169 “Standard Practice for Performance Testing of Shipping Containers and Systems”

ASTM D4168 “Standard Test Methods for Transmitted Shock Characteristics of Foam-in-Place Cushioning Materials”

ASTM D1596 covers a procedure for obtaining dynamic shock cushioning characteristics of packaging materials through acceleration-time data achieved from dropping a falling guided platen assembly onto a motionless sample. This test method does not address any effects or contributions of exterior packaging assemblies.

The data acquired may be used for a single point or for use in developing a dynamic cushion curve for the specific material being tested. Curves are used either to predict performance of materials under use conditions or for comparison among different materials at specific input conditions. Caution should be used when attempting to compare data from different methods or when using such data for predicting in-package performance. Depending upon the particular materials of concern, correlation of such data (from among differing procedures or for predicting in-package performance) may be highly variable.

ASTM D3332 covers a method for the determination of the shock fragility of products. This fragility information may be used in designing shipping containers for transporting the products. It may also be used to improve product ruggedness.

Unit or consumer packages, which are transported within an outer container, are considered to be the product for the purposes of these test methods. Two test methods are outlined, as follows:

1.1.1 Test Method A is used first, to determine the product's critical velocity.

1.1.2 Test Method B is used second, to determine the product's critical acceleration.

ASTM D4169 provides a uniform basis of evaluating, in a laboratory, the ability of shipping units to withstand the distribution environment. This is accomplished by subjecting them to a test plan consisting of a sequence of anticipated hazard elements encountered in various distribution cycles. This practice is not intended to supplant material specifications or existing pre-shipment test procedures.

1.2 The suitability of this practice for use with hazardous materials has not been determined.

ASTM D4168 provides test methods to determine the shock-absorbing characteristics of foam-in-place packaging materials.

1.2 Test Method A uses a free-fall package drop test apparatus.

1.3 Test Method B uses a shock-test apparatus.

ASTM D1185-98a Standard Test Methods for Pallets and Related Structures Employed in Materials Handling and Shipping

ASTM D1596-97 Standard Test Method for Dynamic Shock Cushioning Characteristics of Packaging Material

ASTM D3332-99 Standard Test Methods for Mechanical-Shock Fragility of Products, Using Shock Machines

ASTM D3580-95, Standard Test Methods for Vibration (Vertical Linear Motion) Test of Products

ASTM D4003-98 Standard Test Methods for Programmable Horizontal Impact Test for Shipping Containers and Systems

ASTM D4168-95 Standard Test Methods for Transmitted Shock Characteristics of Foam-in-Place Cushioning Materials

ASTM D4504-94 (2000) e1 Standard Specification for Molded Polyethylene Open-Head-Pails for Industrial Shipping of Non-hazardous Goods

ASTM D5277-92 (1997) Standard Test Method for Performing Programmed Horizontal Impacts Using an Inclined Impact Tester

ASTM D5487-98 Standard Test Method for Simulated Drop of Loaded Containers by Shock Machines

ASTM D6198-00 Standard Guide for Transport Packaging Design

ASTM D6537-00 Standard Practice for Instrumented Package Shock Testing for Determination of Package Performance

ASTM D999-96 Standard Methods for Vibration Testing of Shipping Containers

The International Safe Transit Association (ISTA) devised another commonly used package design and testing schedule. The ISTA standards marketed as “Just Right” Package Testing of particular interest are:

ISTA 1 Series: Non-Simulation Integrity Performance Tests. Challenge the strength and robustness of the product and package combination. Not designed to simulate environmental occurrences. These tests are useful as screening tests, particularly when used as a consistent benchmark over time.

ISTA 2 Series: Partial Simulation Performance Tests. Tests with at least one element of a, 3 Series type general simulation performance test, such as atmospheric conditioning or mode-shaped random vibration and at least one element of a, 1 Series type non-simulation integrity test.

ISTA 3 Series: General Simulation Performance Tests, designed to provide a laboratory simulation, of the damage-producing forces and conditions, of transport environments. These tests are applicable across broad sets of circumstances, such as a variety of vehicle types and routes, or a varying number of handling exposures. Characteristics will include simple shaped random vibration, different drop heights

applied to the sample package, and/or atmospheric conditioning such as tropical wet or winter/frozen.

ISTA 4 Series: Enhanced Simulation Performance Tests. General Simulation test with at least one element of focused simulation, such as test sequence or condition linked to actual known distribution pattern.

ISTA 5 Series: Focused Simulation Performance Tests. Designed to provide a laboratory simulation based on actual field-measured hazards and levels. Measured hazards will typically include complex shaped random vibration, multi-tiered drop height distribution, temperature and humidity extremes and/or cycling, and dynamic or static compressive loads.

ISTA 7 Series: Development Tests. These tests are used in the development of transport packages. They can be used to compare relative performance of two or more container designs, but are not intended to evaluate the protection afforded packaged-products.

AS 2400.10-1991 PACKAGING - Protection against Shock and Vibration (Cushioning) is the Australian Standard of interest. This standard provides guidance on the protection of packaged goods against shock and vibration. The ways in which protection can be provided are defined, and the more commonly used materials and methods are described.

APPENDIX B: Equipment used during experimentation

Electro-magnetic shaker by Vibration Test Systems Ohio

Model VTS-500

- Stroke 1” peak to peak
- Velocity 45” per second
- Acceleration 111 g @ 0.3 lb test load
- Resonance frequency 3430 Hz @ 0.3 lb test load

Various accelerometers

- Bruel & Kjaer Type 4370

APPENDIX C: Compression curves of expanded polystyrene samples

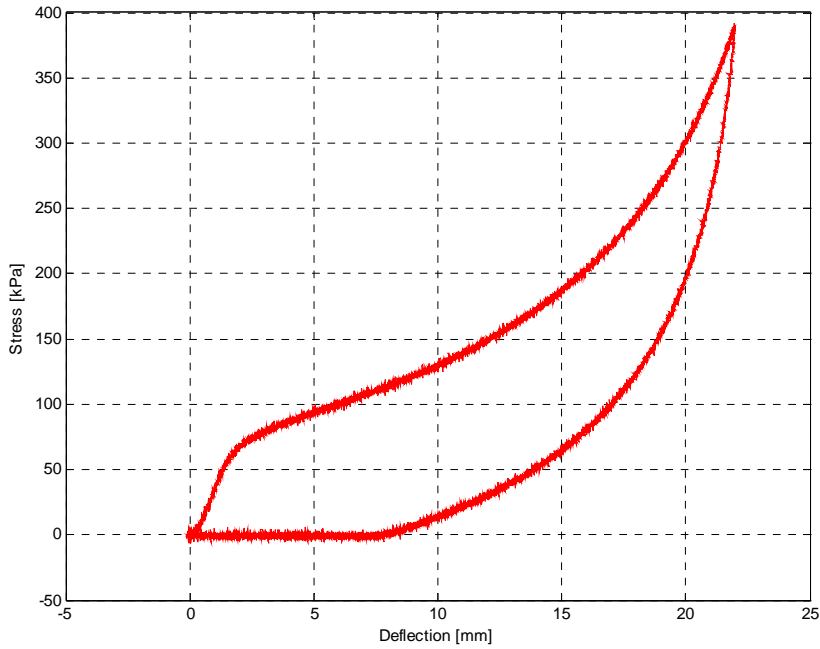


Figure 1 Raw compression data for EPS grade sl

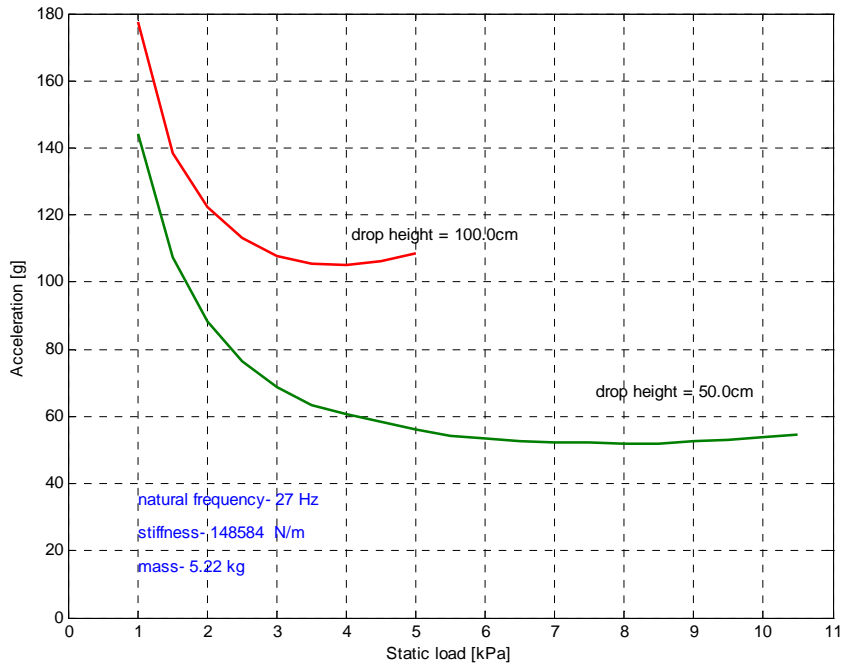


Figure 2 Cushion curve for EPS grade sl

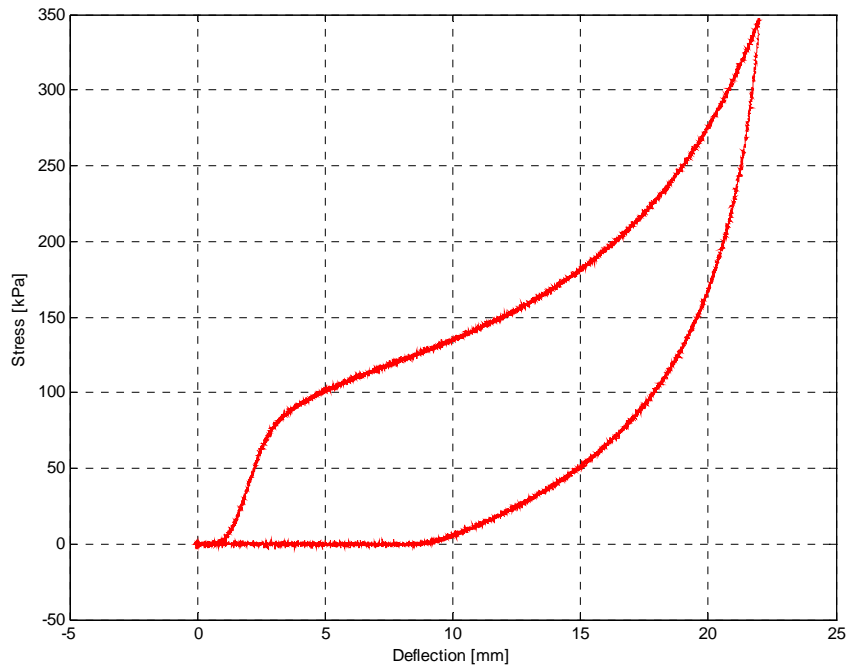


Figure 3 Raw compression data for EPS grade s

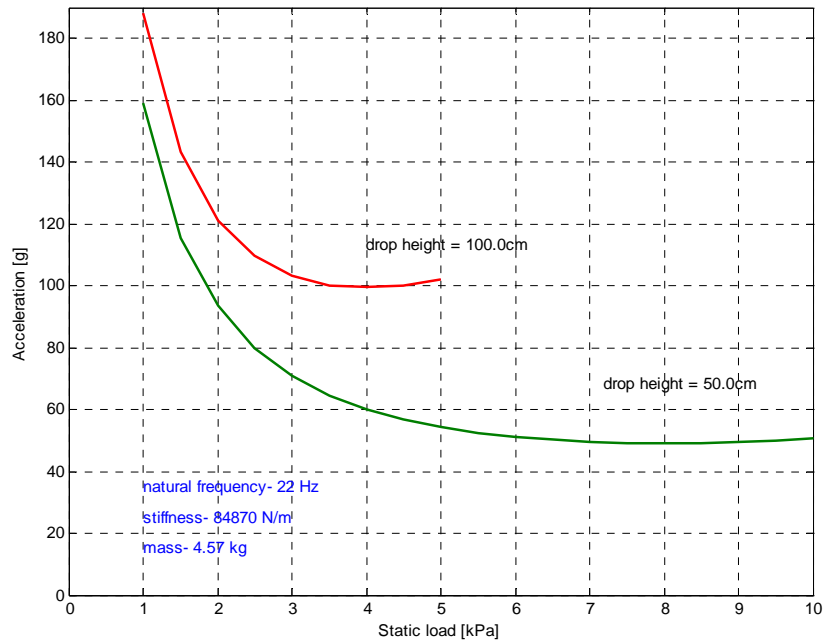


Figure 4 Cushion curve for EPS grade s

APPENDIX D: Summary of the natural frequency estimate

Table 1 Natural frequency (Hz) estimate, recovered parameter, by both the SISO and R-MISO methods

EPS grade	SISO	R-MISO	SISO	R-MISO	SISO	R-MISO	SISO	R-MISO
0.25g RMS	125 av	125 av	250 av	250 av	500 av	500 av	1125 av	1125 av
S	29.00	35.00	30.00	35.00	30.00	35.00	30.00	34.75
SL	31.00	36.25	29.25	34.00	28.75	33.25	28.50	33.00
H	55.00	67.25	55.00	67.25	55.25	67.25	54.00	67.50
L	31.00	36.25	29.25	34.00	28.75	33.25	28.50	33.00
VH	54.75	74.50	54.00	69.75	53.75	69.75	53.75	72.25
X	37.25	37.50	37.25	58.00	55.25	57.75	50.50	56.75
EPS grade	SISO	R-MISO	SISO	R-MISO	SISO	R-MISO	SISO	R-MISO
0.40g RMS	125 av	125 av	250 av	250 av	500 av	500 av	1125 av	1125 av
S	27.50	33.25	27.25	33.25	27.25	33.25	27.25	33.50
SL	36.25	40.50	24.00	32.00	25.50	31.75	25.75	30.75
H	40.25	50.25	40.25	51.25	50.50	53.50	42.50	53.50
L	36.25	40.50	24.00	32.00	25.50	31.75	25.75	30.75
VH	49.50	64.25	49.50	62.50	49.50	62.75	48.75	62.00
X	36.00	52.50	36.00	52.50	39.25	58.50	39.25	58.50

APPENDIX E: Summary of the MATLAB files created

Ccurve2

Generates 'cushion' curve data
Usage: [curvedata] = ccurve2(x,f,carea,h,sl, labelFlag,cfile)
curvedata - sl(Pa) in 1st column, gmax - in remaining columns (g)
x - deflection vector
f - compression force vector / or Pa
carea - compression area
h - vector of drop heights
sl - vector of static loads
labelFlag = 1 , (default 1) enables/suppresses text labeling of drop height
labelFlag = 2, plots the line on yellow for ppt.
cfile name of file opened

cushionCurve

Usage: The file reads Instron ASCII data files saved with the HPVEE program where the 1st column is deflection in mm, the 2nd column is Force in kN in ASCII and modifies it to ensure that yc is monotonic
Then it generates a cushion curve
It also stores the results in a *.mat file with the same name

compressionplot

Usage: Will open experimental data from an HPVEE file and plot the compression data based on sample size 80x80 mm²

Gpredic2

Usage: [gi,fmax,xfmax,xmax,ep,e] = gpredic2(x,f,carea,h,sl, pptFlag)
Function returns predicted peak 'g' from compression data for the static load and the drop height h:
x(:) - deflection in m
f(:) - force in N
returns:
gi - peak 'g' from impact
max force and location
max deflection and potential energy there
vector of energy points for reference
When nargout = 0, results are plotted
gi = 0 when sl exceeds the range of compression data

HPVEEfile

Usage: opens a HP VEE file of experimental data

Halfspec

Usage: returns magnitude and phase frequency vectors for a fft

Inputcontrol

Usage input file pro-former for, input2, input3, and input4
default = {'x.^1','abs(x).*x',x.^3'};

MISOcontrol

Usage: MISO program that will run the simulink model
"generalsysmodel.mdl" in the fwd directions and saves the input and output
as a .dat file.
The choice of simulation or experimental, "filename".dat will be opened and
run by analyserexpdata/analyserwnmodel/analyserzmodel,
The figures saved in the folder "Figure files".
These figure files and data therein can be opened by "figdataopen.m"
Uses the following files:

generalsysmodel.mdl	choice of model
SIMULfile	open a simulation data file
HPVEEfile	open a experimental data file
input2	choose the inputs
input3	
input4	
input5	
Halfspec	FFT spectrum
modeldetails	natural freq etc
Simrun	simulation details
analyserexpdata, analyserwnmodel, analyserzmodel	
RMISOanalyser	RMISO frequency analysis
Tdomainplot	graphs of the time base signals

RMISOanalyser1

Usage: R-MISO1 analyser code to open files and continue averaging till
there are no more files, requires MISOcontrol

SIMULfile

Usage: opens the simulink model data file
duffbase: non-parameterised equation (k, c, and k3)
duffbase1: parameterised equation (wn and zeta)
duffbase2: non-parameterised equation (k, c, and k3 and using derivative
block)

SignalGen

Usage: Signal Generator
This program generates sinusoidal, random and impulse accelerations and
saves the corresponding velocity and displacement data as 'ss.mat' for input
as base excitation in simulink

Simrun

Usage: Program to run the chosen simulink model and save input and output data as a 'filename'.dat file.

Tdomainplot

Usage: will plot the excitation and response in the time domain, and save as a figure file.

These figure files and data therein can be opened by "figdataopen.m"

analyserexpdata1

Usage: Natural freq as the vector

This program uses the data generated by "RMISOanalyser1" ie 'short'.dat files then plots the frequency response functions of the, chosen duffing and vandepol systems.

Using the fwd SISO and reverse MI/SO technique, from input and output data

analyserwnmodel

Usage: Natural freq as the vector

This program uses the data generated by "RMISOanalyser1" ie 'short'.dat files then plots the frequency response functions of the, chosen duffing and vandepol systems.

Using the fwd SISO and reverse MI/SO technique, from input and output data

analyserzmodel

Usage: Critical damping as the vector

This program uses the data generated by "RMISOanalyser1" ie 'short'.dat files then plots the frequency response functions of the, chosen duffing and vandepol systems.

Using the fwd SISO and reverse MI/SO technique, from input and output data

averagingfunction

function newAverage = averaging(lastEnsamble, oldAverage, counter, method)

progressing averagaing

method 'c' - complex averaging ie magnitude as the geometric average and phase as arithmetic, lastEnsamble and old Average are complex

method 'a' - arithmetic averaging

for complex numbers it's a vector averaging ie mean of reals and mean of imaginaries

crossSpectra

function [inputXspectra, inputOutputXspectra] = crossSpectra(a,b>window)

Cross and autospectra of signals- window='hanning' or 'rectangular'

figcharacterchange

Usage: checks figure files and then changes characteristics as determined by the following:
logarithmic: plot to linear
SISO dashed line to none on Coherence plot
if Spectral density leave y axis limits
then save the figure file
see also figlinestylechange.m

figdataopen

Usage: Will open 'UserData' from a figure file (created in analyserwnmodel.m etc) (particular to the "Linear Frequency Response" figure(1) file
eg..."filename_Linear.fig"

figlinestylechange

Usage: checks figure files and then changes characteristics as determined by the following:
LineWidth change to 1
LineStyle to none etc then save the figure file_a.fig
see also figcharacterchange.m

figuredataimbed

Usage: will imbed data in a figure file in UserData partner file is figuredataout

figuredataout

Usage: Will open 'UserData' from a figure file partner file is figuredataimbed

figuredatarecall

Usage: opens a figure file and recalls lines (from xData) and text (from String) within the graph

filedatasave

Usage: creates a .dat or .txt file and saves text and data

Hpveefileappend

Usage file to open HP VEE data file ending in a,b,c,d,e,f,g,h and append to a binary single precision file.

Opening_surf_data

Usage: creates a surf plot from the .dat or .txt file data from Saving_surf_data.m

Saving_Opening_surf_data

Usage: creates a .dat or .txt file and saves text and data

Nomenclature

$A(f)$	Frequency response function “after” nonlinear function
$b []$	Bias of []
B	Cyclic frequency bandwidth (Hz)
c	Damping coefficient, propagation velocity
$C_{xx}(\tau)$	Auto covariance function
$C_{xy}(\tau)$	Covariance function
$C_{xx}(f)$	Coincident spectral density function (one sided)
D	Distance
$E []$	Expected value of []
f	Cyclical frequency (Hz)
$X(f)$	Fourier transform of $x(t)$
Δf	Bandwidth resolution (Hz)
$g(\mathbf{x})$	Zero memory nonlinear function of $\mathbf{x}=\mathbf{x}(t)$
$G_{xx}(f)$	Auto-spectral density function (one-sided)
$G_{xy}(f)$	Cross-spectral density function (one-sided)
$G_{yy.x}(f)$	Conditioned auto-spectral density function (one-sided)
$G_{x_i y_j}(f)$	Conditioned cross-spectral density function (one-sided)
$G_{xx}(f,t)$	Instantaneous auto-spectral density function (one-sided)
$H(f)$	Frequency response function
$ H(f) $	System gain factor
i	index
j	$\sqrt{-1}$, index
k	Spring constant, index
$L(f)$	Frequency response function for conditioned inputs
m	Mass
n_d	Number of records, number of averages
N	Number of points per record, sample size
$p(\mathbf{x})$	Probability density function
$P(\mathbf{x})$	Probability distribution function
q	Number of inputs
r	Number of outputs
$R_{xx}(\tau)$	Autocorrelation function
$R_{xy}(\tau)$	Cross-correlation function
$R_{xx}(\tau,t)$	Instantaneous autocorrelation function
$S_{xx}(f)$	Auto spectral density function (two-sided)
$S_{xy}(f)$	Cross-spectral density function (two- sided)
$S_{xx}(f,t)$	Instantaneous spectral density function(two-sided)
t	Time variable
Δt	Sampling interval
T	Record length, period
$\text{Var} []$	Variance

$x(t), y(t)$	Time history records
$X(f)$	Fourier transform of $x(t)$
$X(f, t)$	Finite fourier transform of $x(t)$
$w(t)$	Window function, time history record
$[*]$	Complex conjugate of []
$[\wedge]$	Estimate of []
$ \gamma_{xy}(f) $	Positive square root of $\gamma_{xy}^2(f)$
$\gamma_{xy}^2(f)$	Ordinary coherence function
$\gamma_{x:y}^2(f)$	Multiple coherence function
$\gamma_{xiv:x}^2(f)$	Partial coherence function
$\delta()$	Delta function
ε	Normalised error
ζ	Damping ratio
$\theta_{xy}(f)$	Phase angle of $G_{xy}(f)$
μ	Mean value
ρ	Correlation coefficient
$\rho_{xy}(\tau)$	Correlation coefficient function
σ	Standard deviation
σ^2	Variance
τ	Time delay
$\phi(f)$	System phase factor
ψ	Root mean square value
ψ^2	Mean square value